SKB

TECHNICAL REPORT 92-45

Mechanical integrity of canisters

Compiled by Fred Nilsson

Royal Institute of Technology

December 1992

SVENSK KÄRNBRÄNSLEHANTERING AB
SWEDISH NUCLEAR FUEL AND WASTE MANAGEMENT CO
BOX 5864 S-102 48 STOCKHOLM
TEL 08-665 28 00 TELEX 13108 SKB S
TELEFAX 08-661 57 19

MECHANICAL INTEGRITY OF CANISTERS

compiled by Fred Nilsson

Royal Institute of Technology

December 1992

Mechanical Integrity of Canisters

compiled by
Fred Nilsson
Royal Institute of Technology

December 1992

ABSTRACT

English

This document constitutes the final report from "SKB's Reference Group for Mechanical Integrity of Canisters for Spent Nuclear Fuel". A complete list of all reports initiated by the Reference Group can be found in the Summary Report in this document. The main task of the Reference Group has been to advice SKB regarding the choice (ranking of alternatives) of canister type for different types of storage. The choice should be based on requirements of impermeability for a given time period and identification of possible limiting mechanisms.

The main conclusions from the work were:

From mechanical point of view, low phosphorous oxygen free copper (Cu-OFP) is a preferred canisters material. It exhibits satisfactory ductility both during tensile and creep testing. The residual stresses in the canisters are of such a magnitude that the estimated time to creep rupture with the data obtained for the Cu-OFP material is essentially infinite. Based on the present knowledge of stress corrosion cracking of copper there appears to be a small risk for such to occur in the projected environment. This risk needs some further study. Rock shear movements of the size of 10 cm should pose no direct threat to the integrity of the canisters. Considering mechanical integrity, the composite copper/steel canister is an advantageous alternative.

The recommendations for further research included continued studies of the creep properties of copper and of stress corrosion cracking. However, the studies should focus more directly on the design and fabrication aspects of the canister.

Swedish

Detta dokument utgör slutrapporten from "SKBs referensgrupp för mekanisk integritet hos kapslar för använt kärnbränsle". En fullständig lista över de rapporter, som initierats genom referensgruppen finns i Summary Report-delen av detta dokument. Referensgruppen huvuduppgift har varit att ge SKB råd i valet av kapseltyp för olika förvarsutformningar. Detta val baseras dels på kravet att kapseln skall vara tät under en given tidsperiod och på identifieringen av möjliga brottmekanismer.

De viktigaste slutsatserna av arbetet har varit:

Från mekanisk synpunkt är syrefri koppar med låg fosforhalt (Cu-OFP) att föredra. Den har tillfredsställande duktilitet både vid dragprovning och krypprovning. Restspänningarna i kapslarna är av sådan storlek att den tiden till krypbrott, som uppskattas utifrån erhållna data för Cu-OFP materialet, i princip är oändlig. Utifrån den nuvarande kunskapen om spänningskorrosionssprickning i koppar är risken för att detta skall inträffa i förvarsmiljön liten. Den bör dock studeras ytterligare. Bergrörelser på 10 cm utgör inget direkt hot mot kapseln integritet. Ur mekanisk synpunkt är kompositkapseln av koppar/stål ett fördelaktigt alternativ.

Rekommendationerna för fortsatt forskning och utveckling innefattade ytterligare krypprovning och studier av koppars känslighet för spänningskorrosionssprickning. Tonvikten bör dock läggas på konstruktions och tillverkningsfrågor.

Contents:

The following technical reports are appended to this summary report

[A] M. Fryklund and B. Larsson, *"Residual stresses in hot iso-statically pressed copper-canister for spent nuclear fuel"*, ABB Corporate Research, SKB Technical Report, in preparation (1992) , Appendix I, This Report.

[B] L. Josefson, L. Karlsson, L.-E. Lindgren and M. Jonsson, *"Thermo-mechanical FE-analysis of butt-welding of canister for spent nuclear fuel"*, SKB Technical Report 92-27 (1992), to be presented at the Twelfth International Conference in Reactor Technology (SMIRT12), Stuttgart, August 1993.

[C] L. Josefson, L. Karlsson, and H.-Å. Häggblad, *"Stress redistribution and void growth in butt-welded canister for spent nuclear fuel"*, SKB Technical Report, in preparation, 1992.

[D] K. Pettersson, *"Creep and creep fracture of copper canisters for nuclear waste"*, Division of Mechanical Metallurgy, Royal Institute of Technology (1992), Appendix II, This Report.

[E] L. Börgesson, *"Interaction between rock, bentonite buffer and canister. FEM calculations of some mechanical effects on the canister in different disposal concepts"*, SKB Technical report 92-30 (1992).

[F] P. J. Henderson, J.-O. Österberg and B. Ivarsson,*"Low temperature creep of copper intended for nuclear waste containers"*, SKB Technical Report 92-04 (1992).

[G] J. Lindblom, P. J. Henderson and F. Sietisleam, *"Creep, stress relaxation and tensile testing of oxygen free phosphorus copper (Cu-OFP) intended for nuclear waste containment"*, The Swedish Institute for Metals Research, Report (1992), Appendix III, This Report.

[H] L. Josefson,"Creep deformation and void growth in copper canisters for spent nuclear fuel" (1992), Appendix IV, This Report.

SUMMARY REPORT

Mechanical Integrity of Canisters

compiled by
Fred Nilsson
Royal Institute of Technology

Background and introduction

Questions about the mechanical integrity of the canisters have always been of some concern in connection with the storage of spent nuclear fuel. Although the canister is only one of several barriers against undesired release and migration of nucleids, it is obviously of great benefit to the total safety of the storage system if the integrity of the containers can be upheld during a large part of the intended design life. Activities to increase the amount of knowledge in this area have been under way for a considerable time. In order to further advance the collection of knowledge SKB has formed a reference group which met for the first time on Oct 10, 1990. This group has consisted of experts in different areas of the problem complex. At its first meeting the group formulated its task as:

The main task of the reference group is to advice SKB regarding the choice (ranking of alternatives) of canister type for different types of storage. The choice should be based on requirements of impermeability for a given time period and identification of possible limiting mechanisms. In addition leakage modes for the different canister types should be identified.

The members of the group have been:

Dr. Lennart Josefson, Chalmers University of Technology (CTH), Gothenburg
Dr. Bertil Larsson, ABB Corporate Research, Västerås
Prof. Fred Nilsson, Royal Institute of Technology (KTH), Stockholm, chairman
Prof. Kjell Pettersson, Royal Institute of Technology (KTH), Stockholm
Prof. Roland Pusch, Clay Technology AB, Lund (meetings 1 and 2)
Dr. Lennart Börgesson, Clay Technology AB, Lund
Dr. Lars Werme, SKB, secretary and project leader

In addition the Swedish Nuclear Power Inspectorate has been invited to participate through an observer which has been Dr. Gert Hedner until April 1992 and Dr. Karen Gott since then.

The group has been working by suggesting various research tasks to be performed. The topics considered to be relevant were arrived at through discussions with all group members present. In many cases the individual members of the group have undertaken the research activities.

Storage and canister types

A number of different storage concepts have been subject to discussion and the different types are displayed in Table 1 where also the various types of canisters have been indicated. The abbreviation used in the following for the different types is shown in the rightmost column. The emphasis of the group's work has, however, been on the three different KBS-3 alternatives, especially since SKB during the spring 1992 has decided not to further consider the VLH and VDH alternatives. This decision was based on other considerations than those within the present group's area of interest. It should also be pointed out that the group has so far not considered the details of the design of the canister but has rather been concerned with overall questions about the viability of the concepts.

Type of storage	containment requirements	types of canister	Abbreviation
KBS-3	> 100 000 years	welded lead filled copper canister	CC
		hot iso-statically pressed (HIP) copper canister	HIP
		Copper/steel (Cu/Fe) canister	CompC
Long horizontal bore-holes (VLH)	> 100 000 years	Copper/steel canister with hemispherical heads	CompC(h)
		Copper canister with hemispherical heads	CC(h)
Very deep bore-holes (VDH)	containment upheld during at least 2 years, subsequently limited leakage	Titanium canister, self-supporting or concrete filled	TiC
		Copper canister, self-supporting or HIPped	CC(d) HIP(d)

Table 1. The different storage types and canister concepts.

Problem structuring

A number of different mechanisms that can be potentially dangerous to mechanical integrity of the canister exist. The following mechanisms (listed in the left column of Table 2) have been identified as being potentially detrimental to the canister integrity. Factors affecting the integrity connected to the particular mechanism are indicated in the right column.

During the work of the group a selection of mechanisms were chosen for further study. This choice was based on the judged importance of the mechanisms for the canister integrity and is outlined in the subsequent discussion. Other mechanisms were either judged to be of secondary importance or of such a nature that the group did not find the time ripe for a treatment. Among the latter ones are those connected with details of the fabrication process and how the canister is to be handled. Many of the circumstances around this are so far not specified.

All of the considered mechanisms must be driven by mechanical loads in some form. The loads (stresses) can be classified into

Mechanisms	*Factors*
fabrication defects	welding HIP quality assurance material faults
handling damage	handling loads quality control
general corrosion	chemical conditions material behaviour temperature
stress corrosion	material behaviour material defects chemical conditions loads
plastic or creep collapse	material behaviour external loads
creep rupture	material behaviour material defects loads

Table 2. Integrity threatening mechanisms.

a) *External loads*

1) Normal loads, hydrostatic pressure and swelling of bentonite
2) Tectonic loads

b) *Internal loads*

Pressure from helium production.

c) *Residual stresses*

1) Welding residual stresses
2) Shrinkage stresses in the HIP process
3) Stresses from bolting

Creep properties of copper

A fairly extensive experimental program has been undertaken in order to determine the mechanical behaviour of different types of copper. The main emphasis has been on creep testing in order to determine the creep deformation and rupture properties [F]. In addition tensile testing at different temperatures and creep relaxation testing have been performed [G]. Five different types of copper were considered in [F]. We will here limit the discussion to oxygen-free high purity copper (Cu-OFHC) and oxygen-free phosphorous copper (Cu-OFP). It was found during the testing that the Cu-OFHC material exhibits creep and creep rupture properties that are much inferior than the corresponding properties of the Cu-OFP material. The poor ductile and creep fracture elongations were attributed to grain boundary segregations of sulphur. The Cu-OFP material did not display this behaviour and followingly the ductility and creep properties were much more favourable. This was also true for oxygen-free silver copper.

The possible creep deformation of a canister occurs in two considerably different time regimes. Due to the high temperature in the canister, initially about 150°C in the copper part, a fairly rapid relaxation process of the residual stresses occurs after the manufacturing process (welding or HIP). This initial relaxation is essentially finished after say 100 hours and seems mainly to be of the dislocation glide mechanism. In long time regime creep deformation due to external pressure may occur. It was judged that at the temperatures and stress levels of interest the deformation mechanism for the Cu-OFP material should be of the volume diffusion type. Mathematical expressions for the creep deformation and the damage accumulation rates were adjusted to experimental observations. The creep deformation rate $\dot{\varepsilon}_{ij}^{c}$ is assumed to be of the secondary (Norton-Bailey) creep form

$$\dot{\varepsilon}_{ij}^{c} = B_0 e^{-(Q_c/RT)} \sigma_{eff}^{n-1} s_{ij} \qquad (1)$$

where B_0 is a constant, T the absolute temperature, Q_c the activation energy, R the gas constant, σ_{eff} the effective stress and s_{ij} the stress deviator. It turned out that a description of the deformation over the entire time range by a single equation of the type (1) was not possible. Instead for the material of interest, *i.e.* Cu-OFP, two different fits were utilized. The one applicable in the short time regime was determined by adjustment of the parameters in (1) to the relaxation experiments [G]. For the long time range a value of the exponent n=5 was assumed as typical for the assumed mechanism. The remaining parameters were determined by a fit to experimental observations of the creep rate at 215°C. Using the units hours for time and MPa for stress, the constants B_0, Q_c and n for the two different materials are given in Table 3.

Material	B_0	Q_c/kJ mol^{-1}	n
Cu-OFHC, long time regime	$2.14 \cdot 10^{7}$	205	5.32
Cu-OFP, short time regime	$8.58 \cdot 10^{-25}$	117	20.0
Cu-OFP, long time regime	$6.77 \cdot 10^{-4}$	117	5

Table 3. Material constants for creep deformation and failure.

The large difference in creep deformation rates between the Cu-OFHC material and the the Cu-OFP material is seen from Table 3.

Residual stress distribution in copper canisters

The residual stresses in the canisters that remain after manufacture are among the factors that can affect the different detrimental mechanisms. The distribution of residual stress is in general very dependent of the details of the fabrication process (for instance welding) and the prediction of these necessitates complex numerical analysis. Such computations have been performed for the CompC canister [B] and the HIP canister [A].

In the CompC canister the residual stresses emanate from the welding of the lid to the remaining structure. It is intended that this welding should be performed by the electron beam welding technique. In this canister the waste is contained in an inner container of steel. This container is in turn placed into a copper cylinder which is sealed by welding a lid to cylinder. It turns out that the clearing between the steel and copper cylinder is crucial for the residual stress distribution. If the gap is sufficiently small contact will occur between the cylinders, at the inner vertical surface of the backing ring, during the welding process. If the gap is large this will not happen and the residual stress pattern will be significantly different for the two cases. The calculations were performed for two different gap sizes, 0.2 mm and 2.0 mm, respectively. It should be pointed out that it might become very difficult to place the inner cylinder into the outer one if the gap is too small. In [B] first the thermal problem associated with the welding process was analysed by aid of the finite element program TOPAZ2D [3]. The subsequent mechanical analysis was performed using the program NIKE2D [4]. The calculated residual stress levels in the weld vicinity are of the order 60 MPa. At the lower right corner of the backing ring a concentration of the hoop stresses appears and the local stress is up to 140 MPa. By adjusting the design of the backing ring this stress concentration should be possible to reduce considerably. The accumulated effective plastic strain in the vicinity of the weld after cooling after welding was calculated to be about 5 %, which is much lower than the ductility of this copper alloy.

In the HIP canister the residual stresses develop after the final pressurized sintering because of the different thermal properties of the spent fuel and the surrounding copper material. Such stresses have been previously estimated [5] in an analysis where the influence of the end regions was neglected. In the present analysis [A] the effects of the geometrically complicated end regions are taken into account in the finite element computations which were performed with aid of the program system SOLVIA [6]. The maximum effective stress was around 70 MPa and occurred in the corner of the top cover and the boxes of spent fuel. The maximum stress on the surface of the canisters was estimated to around 50 MPa. Thus, the residual stress levels in CompC and the HIP canister, respectively are of the same order although it should be remembered that in the CompC the stressed regions are much more local.

Relaxation of residual stresses

As discussed above the main relaxation of the residual stresses occurs very rapidly and when the canister is deposited this process could be considered to be essentially finished. A mathematical description of the relaxation process on basis of the experimentally observed results is difficult. With the assumptions for the relaxation behaviour described above FEM element calculations of the relaxation process have been conducted [C]. These calculations are performed only for the gap 2 mm since this clearance is believed to be needed for the assembly of the canister. It was found that, during the first 100 hours after welding, the copper end will contract axially and eventually come into contact with the steel end. This leads to a radial increase of the copper cylinder at the location of the weld. the axial stresses at the weld will be redistributed without reducing the maximum magnitudes. The very high hoop stresses in the backing ring are both redistributed and reduced (the maximum hoop stress is reduced from 140 MPa to 70 MPa). The loading situation present when the canister is placed in the storage is simulated by subjecting the canister to a linearly increasing external pressure which reaches the peak value 10 MPa after 10 years. The long time creep parameters of Table 3 are then employed. During this time period stresses are reduced roughly without changing the distribution. The total accumulation of plastic strain (plastic+creep) was found to be less than the 5 % accumulated during the welding process.

Possibilities of creep rupture

The two variants of high purity copper on which most of the testing has been performed display a surprisingly large difference in creep fracture behaviour. The type of creep fracture of concern in the present context is the low ductility intergranular creep fracture, since any creep deformation would mainly be in the form of stress relaxation, a loading case where the creep deformation is the same order as the stress divided by the elastic modulus, *i.e.* about 0.1 %. This fracture mode has been observed in the creep tests of Cu-OFHC but not in the Cu-OFP tests. It is difficult to understand the large difference in creep fracture behaviour between these two variants of pure copper, but it has been speculated that the phosphorous in the latter material in some way prevents the sulphur access to the grain boundaries where sulphur otherwise would have an embrittling effect.

The intergranular creep fracture has been analyzed [D] on the basis of a model developed by Cocks and Ashby [1]. Even if this model is not necessarily perfect in detail, it is physically reasonable and can be expected to have approximately the correct dependence of the various parameters and constants of importance to creep fracture like stress, diffusion coefficient, surface energy etc. If literature values of these constants are used the model over predicts the creep fracture failure times of the Cu-OFHC material by a factor of 10^6. The constants were then adjusted so that they would correctly predict observed failure times of the Cu-OFHC. Based on the new values creep fracture life times were then calculated for stresses of interest for the waste canister. At a service temperature of 100°C and a stress of 60 MPa the creep life of the inferior Cu-OFHC material under these assumptions would be 84 000 years. The Cu-OFP material is much less sensitive to creep fracture even under creep tests (*i.e.* constant stress). Under the deformation controlled conditions typical for the canister the possibility of a creep type fracture in the Cu-OFP material must be extremely remote. In [H] void growth during relaxation was studied numerically based on growth relations proposed in [1] (and supported by Reference [B1] in [G]) for the actual temperatures and stress levels in Cu-OFP copper. It is seen that growth of voids will be extremely low resulting in an infinite life for this type of failure.

Stress corrosion cracking

A very limited selection of literature on the problem of stress corrosion cracking (SCC) in copper has been the base for the considerations below. This includes the reports [7]-[10]. The work by Parkins *et al.* [7]-[8] shows that all copper qualities considered for the waste canisters are sensitive to SCC in nitrite solutions. In typical 50-150 hours constant extension rate tests (CERT) SCC is observed even at the free corrosion potential, while in deareated solutions it is necessary to apply a higher potential to get SCC. In simulated ground water no SCC is observed, but there seems to be a slight effect of the environment on the tensile properties. These results together with the information in the report by Taxén [9] about the possible environment *inside* the canisters raise some concern about SCC. The fact found in [7]-[8] that lowering the potential and using less concentrated solutions reduce the SCC sensitivity should not be too encouraging in view of the long exposure time for the canisters. It seems necessary that a more quantitative way of showing that no SCC occurs should be found. One possible approach is to use fracture mechanics type specimens and study the crack growth rate under environmental conditions for the waste storage.

One reason for concern about the environment outside the capsule is the recent discovery by Sieradzki and Kim [10] of an apparently new SCC mechanism in pure metals, which they observed in single crystals of copper. This mechanism is thought to work in alloys where one component is selectively dissolved. This results in a microporous film which cracks easily. By pure inertia a crack in the film can continue as a short cleavage crack into the base metal where corrosion can start again and the process repeats itself. What happens in the pure copper under active dissolution conditions is that the metal is selectively dissolved where dislocations emerge on the surface. The idea is that the selective attack on the dislocations results in a porous structure which under certain circumstances can lead to film-induced cleavage. In order for the SCC promoting porosity to occur a fine balance between dissolution rate and strain rate must prevail. This is taken as the reason why this phenomenon is only observed in a particular strain rate range. For the canister both dissolution and strain rates are very small.

The net reaction used in experiments on copper single crystals is reduction of Cu^{2+}-ions and oxidation of Cu to Cu^{+}, via the formation of complexes with ammonia. This certainly seems to be possible inside the capsule according to [9]. This situation could be remedied by drying the capsule properly before sealing. Outside the canister the situation is different. If there is some dissolution, however small, there is a chance that the film-induced cleavage mechanism might become active. If the radiation level is sufficiently high there is also a chance that Cu^{+} might be oxidized to Cu^{2+} which might increase the dissolution rate. These questions need further studies.

There is some concern that stress corrosion cracking of the inner steel canister might occur under unfortunate circumstances. There are however two actions which will contribute to a minimisation of the risk of stress corrosion cracking in the steel. One action is to have a proper drying procedure for the steel canister and if possible also fill it with inert gas before it is sealed. The other action would be to use very low carbon steel. Such a steel would still have a sufficient mechanical resistance to serve its structural purpose.

Tectonic movements

Should tectonic movements occur the most dangerous threat to the canister integrity seems to be a rock shear somewhere along the canister and perpendicular to its axis. In the report [E] stresses and strains in some of the different canisters have been calculated for a movement of the surrounding rock of 10 cm. To what extent this particular value is relevant or not is outside the competence of the present group, so that a correct interpretation would rather be that a damage tolerance analysis for the assigned value of shear has been performed. In [E] the HIP and the

CompC canisters are analysed as well as the VLH concept. The latter has as mentioned above been abandoned by SKB and will not be further commented upon.

In the HIP canister residual stresses of the order 50 MPa according to the previous discussion occur all along the cylindrical surface. These have been included as initial conditions for the tectonic calculations. In [E] the modelling of the bentonite and the copper are described in detail. The behaviour of the bentonite is very complex. The plastic part of the bentonite deformation is described by a Drucker-Prager model while the elastic part is described by a model that includes porous elasticity. The constitutive equation for the copper is taken as that of von Mises material with a hardening according to the tensile data. The calculations resulted in the following main conclusions.

- The effect of the rock shear depends strongly on the density of the bentonite.

- 10 cm rock shear applied asymmetrically (at 1/4 distance from one the canister ends) is estimated to give a maximum plastic strain in the copper of 1,5 % at a bentonite density of 2.05 t/m^3.

We can thus conclude that such a rock shear is of little consequence for the integrity of the canister in view of the large ductility of the copper.

Corresponding calculations were also performed for the CompC canister. In this case no residual stresses were modelled, since these are very localized to the weld region and are not expected to greatly affect the behaviour due to a rock movement. Also in this case the plastic strains in the copper remain moderate. A maximum strain of 2.5 % occurs at the cylindrical surface for the asymmetric shearing, while the the corresponding number for a symmetric shearing is lower (1.2%).

An attempt to include further creep deformation of the copper and bentonite after a rock shearing was also made. Due to very time-consuming calculations the FEM runs could not be continued beyond 30 years after the shear event. A conservative extrapolation indicated that such deformation during a period of 10^5 years could lead to strains of the order 6 % on the cylindrical surface and 36 % for the lid. It thus appears that creep deformation under sustained rock shear can be a potentially detrimental mechanism for the canister. Which importance that should attached to this fact is uncertain since the probability is very low that the canister has to survive 10^5 years after such an unlikely event such as a rock shear.

Pressure loading due to production of He-gas

One particular potential problem for the integrity of the canisters is the helium production from the spent fuel. A conservative estimate of the stresses due the gas pressure can be obtained by assuming that the internal volume of the canister does not change *i.e.* that the volume change due to deformation can be neglected. It also turns out that with creep data according to the previous discussion the deformation that can occur during the time period of interest is negligible in this respect. n Fig. 3 the internal pressure due to helium production assuming constant values for the void volume.

It can be seen that even for the conservative case with a void of 1 % it takes one million years until the internal pressure is equal to the external design pressure of 16 MPa. We thus immediately conclude that the helium production is not of any concern for the mechanical integrity during the time period of interest. For longer time periods this conclusion may not be valid.

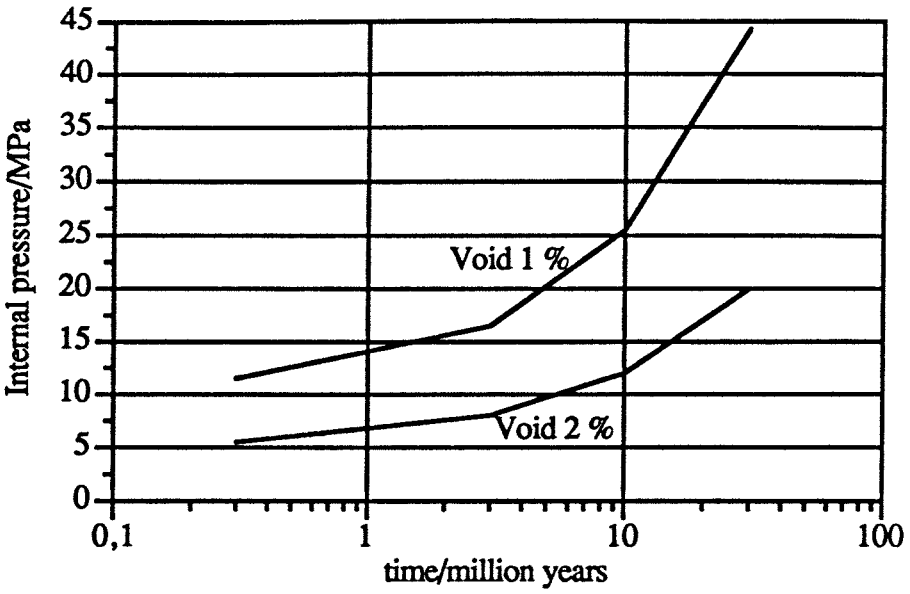

Fig. 3. Pressure for an initial void of a) 2%, b) 1%.

Conclusions

- The oxygen free high conductivity copper (Cu-OFHC) is quite unsuitable as canister material because of its low creep ductility. In contrast, phosphorous de-oxidised copper (Cu-OFP) exhibits satisfactory ductility both during tensile and creep testing.

- The residual stress level in the CompC canister will not exceed around 60 MPa (dependent on the radial gap between the steel and copper cylinders and excepting the stress concentration). For the HIP canister.a corresponding figure is around 70 MPa. In the HIP canister a residual stress state of about 50 MPa is present along the entire canister surface immediately after the completion of the sintering, while for the CompC canister the stresses are concentrated to the weld region. In both cases a substantial part of the stress is rapidly relaxed by creep deformation. No residual stress calculations have been performed for the CC canister, but it can be expected that similar levels (but possibly differently distributed) will be obtained.

- The stresses in the canisters are such magnitude that the estimated time to creep rupture with the data obtained for the Cu-OFP material is essentially infinite for all three alternatives (CC, CompC, HIP).

- Based on the present knowledge about stress-corrosion cracking of copper there appears to be a small risk for such to occur in the projected environment. This risk needs some further study. The HIP canister is from this view-point the most unfavourable one because of the tensile stress state at the canister surface. The composite canister poses some further questions regarding the risk for stress-corrosion from the inside.

- Helium production is of no concern for the time period of interest.

- According to the tectonic calculations a rock shear of the considered size (10 cm during 30 days) should pose no direct threat to the integrity of the canisters. Continued creep defor-

mation during a long period after such an event could be detrimental. It is however uncertain whether such considerations should be among the design requirements.

- Considering only mechanical integrity (not production) aspects the CompC canister seems to be an advantageous alternative.

Recommendations for future research

In general the research during the next three-year period will focus more directly on design and fabrication aspects of the canister. These questions have so far not been very thoroughly considered because much of the possible canister design still remains open. Questions that are likely to achieve attention are:

- Optimization of welding techniques with particular emphasis on weld defects and residual stresses.

- Non-destructive testing of welds in copper.

- Assessment of handling and transportation loads.

- Quality assurance aspects.

Some of activities initiated during the present period need to be continued during the next three year period.

- Continuation of creep and relaxation testing to further verify the the material properties.

- The question of possible stress corrosion cracking needs some further consideration.

References

[1] A. C. F. Cocks and M. F. Ashby, "On creep fracture by void growth", *Progress in Materials Science,* **27**, 189-244, 1982.

[2] H. E. Evans, "*Mechanisms of creep fracture*", Elsevier, 1984.

[3] A. B. Shapiro, *"TOPAZ2D-A two dimensional finite element code for heat analysis, electrostatic, and magnetostatic problems"*, UCID-20824, Lawrence Livermore National Laboratory.

[4] J. O. Hallquist, *"NIKE2D-A vectorized implicit, finite deformation finite element code for analyzing the static and dynamic response of 2-D solids with interactive rezoning and graphics"*, UCID-119677, Rev.1, Lawrence Livermore National Laboratory.

[5] *"Beräkning av restspänningar i kopparkapsel efter HIP"*, ASEA Technical Report, TR KYBA 82-105,1982.

[6] SOLVIA-PRE90, User's Manual for Stress Analysis, Report 90-1, SOLVIA Engineering, Västerås, Sweden, 1990.

[7] L. A. Benjamin, D. Hardie and R. N. Parkins, *"Investigations of the stress corrosion cracking of pure copper"*, KBS TR 83-06, 1983.

[8] R. N. Parkins, *"Investigations of the stress corrosion cracking of sintered copper in sodium nitrite solutions"*, Report from University of Newcastle upon Tyne, Department of Metallurgy and Engineering Materials, March 1988.

[9] C. Taxén, *"Förutsättningar för spänningskorrosionssprickning av kolstål eller koppar i en kapsel för utbränt kärnbränsle"*, Korrosionsinstitutet, 1991-10-30.

[10] K. Sieradzki and J. S. Kim, "Etch pitting and stress corrosion cracking of copper", *Acta Metall. Mater.*, **40**, 625-635, 1992.

Appendix I

Residual Stresses in Hot Iso-Statically Pressed Copper Canisters for Spent Nuclear Fuel

Mikael Fryklund and Bertil Larsson
ABB Corporate Research

Residual Stresses in Hot Iso-Statically Pressed Copper Canisters for Spent Nuclear Fuel

Mikael Fryklund and Bertil Larsson
ABB Corporate Research
a division of Asea Brown Boveri AB

Summary

In one current proposal for the final disposal of spent nuclear fuel, the copper canisters will be sealed by using hot isostatic pressing (HIP). Residual stresses will occur in the material due to different thermal properties of fuel elements and solid copper. A finite element analysis has been performed to determine the residual stress state in the copper canister after the HIP process.

The analysis has been done using a thermoelastic-plastic material model for the copper. Before cooling of the canister after the HIP process, the material is supposed to be stress free. The cooling is slow and therefore no transient effects are taken into account.

Maximum calculated residual stress after cooling is σ_{eff}=71 MPa. On the outer surface of the canister, the corresponding maximum value is σ_{eff}=48 MPa.

CONTENTS

LIST OF APPENDICES

1. INTRODUCTION

In one current proposal for final disposal of spent nuclear fuel, copper canisters will be used and sealed by hot isostatic pressing (HIP).

The copper canister with fuel boxes (see appendix A-1 and A-2) is filled up with copper powder and fitted with a lid. By applying a high external hydrostatic pressure at increased temperature, the canister, the copper powder and the lid solidifies and becomes a solid, homogeneous body. After that, the canister is cooled to room temperature. Due to different thermal properties of fuel elements and copper, residual stresses will occur in the copper canister.

In the present report an analysis of the residual stress state in the copper canister is presented.

2. GEOMETRY AND FEM-MODEL

The geometry and FEM-model is shown in appendix A.

By using symmetry of the canister with fuel elements, only 1/8 of the cross section of the canister needs to be modelled. The length of the model is chosen in such a way that all end effects are taken into account. That means that the model is cut off where the stress state has become independent of the axial coordinate. The results show that this condition is fulfilled.

The material model for the copper is thermoelastic-plastic and for the uranium-dioxide+copper thermoelastic. The anisotropic properties of UO_2+Cu is judged to have only minor influence on the results, and is therefore not taken into account in the model. Material properties are taken from [2] and [3] and are shown in appendix A-5

The finite element program SOLVIA [1] is used for the calculations. The model is built up of 20-node 3D-solid elements.

3. CALCULATIONS

At the end of the HIP process, the temperature is high. The yield limit for the material is low and relaxation of internal stresses in the copper material occurs very easy. Based on this, it is assumed that no stresses exist in the canister at the temperature 500 deg C. This condition is used as an initial condition in the analysis.

It has been shown earlier [3] that after cooling of the canister from the outer surface, the residual stresses depends on the cooling rate. Cooling by forced convection, for example by water spraying, decreases the residual stresses. Slow cooling is therefore judged to be a "worst case" with respect to residual stresses.

In the present analysis the temperature is decreased homogeneously (very slow cooling) from 500 deg C to room temperature.

4. RESULTS

The resulting residual stresses are shown in appendix B as deformation plots, isostress plots and also line plots on the outer surface.

The largest residual stresses at 20 deg C is obtained in the corner of the top-cover and the boxes of spent fuel. The maximum values are:

σ_{eff}	= 71 MPa	(von Mises effective stress)
EPACC	= 2.0 %	(effective plastic strain)

This maximum residual stress σ_{eff} appears only in a very small material volume and depends on the exact shape of the end of the fuel boxes.

On the outer surface of the copper canister the following maximum values are obtained:

σ_{eff}	= 48 MPa	(von Mises effective stress)
EPACC	= 0.3 %	(effective plastic strain)
SPMAX	= 43 MPa	(max principal stress)

5. REFERENCES

1. SOLVIA-PRE90
User's Manual for Stress Analysis

2. Journal of Engineering for Industry
November 1989, vol. 111/343

3. Beräkning av restspänningar i kopparkapsel efter HIP (In Swedish). ASEA Technical Report, TR KYBA 82-105, 1982.

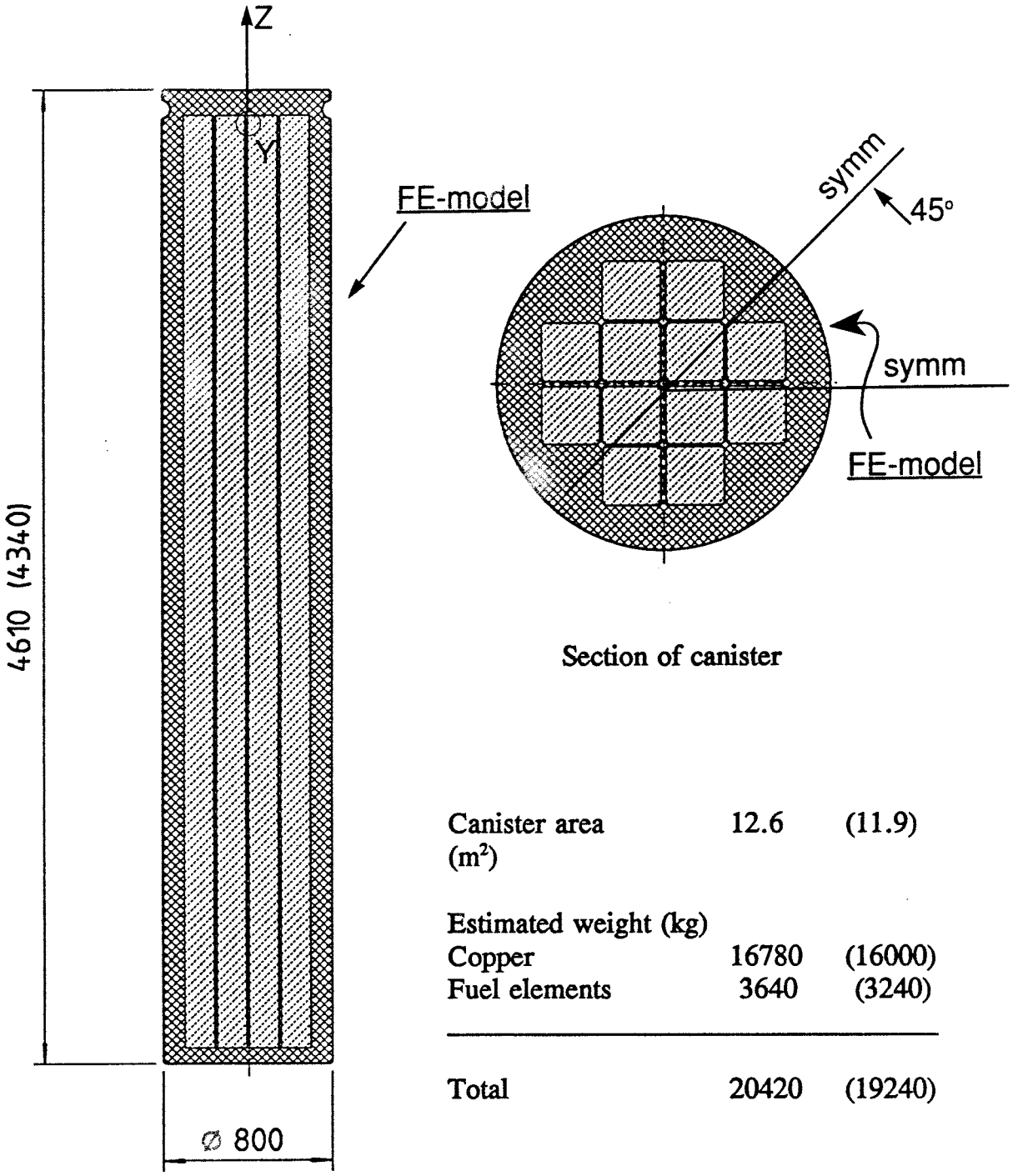

Section of canister

Canister area (m^2)	12.6	(11.9)
Estimated weight (kg)		
Copper	16780	(16000)
Fuel elements	3640	(3240)
Total	20420	(19240)

Measures and weight in parenthesis apply to canister BWR elements without fuel channel

HIP canister
BWR type with fuel channels

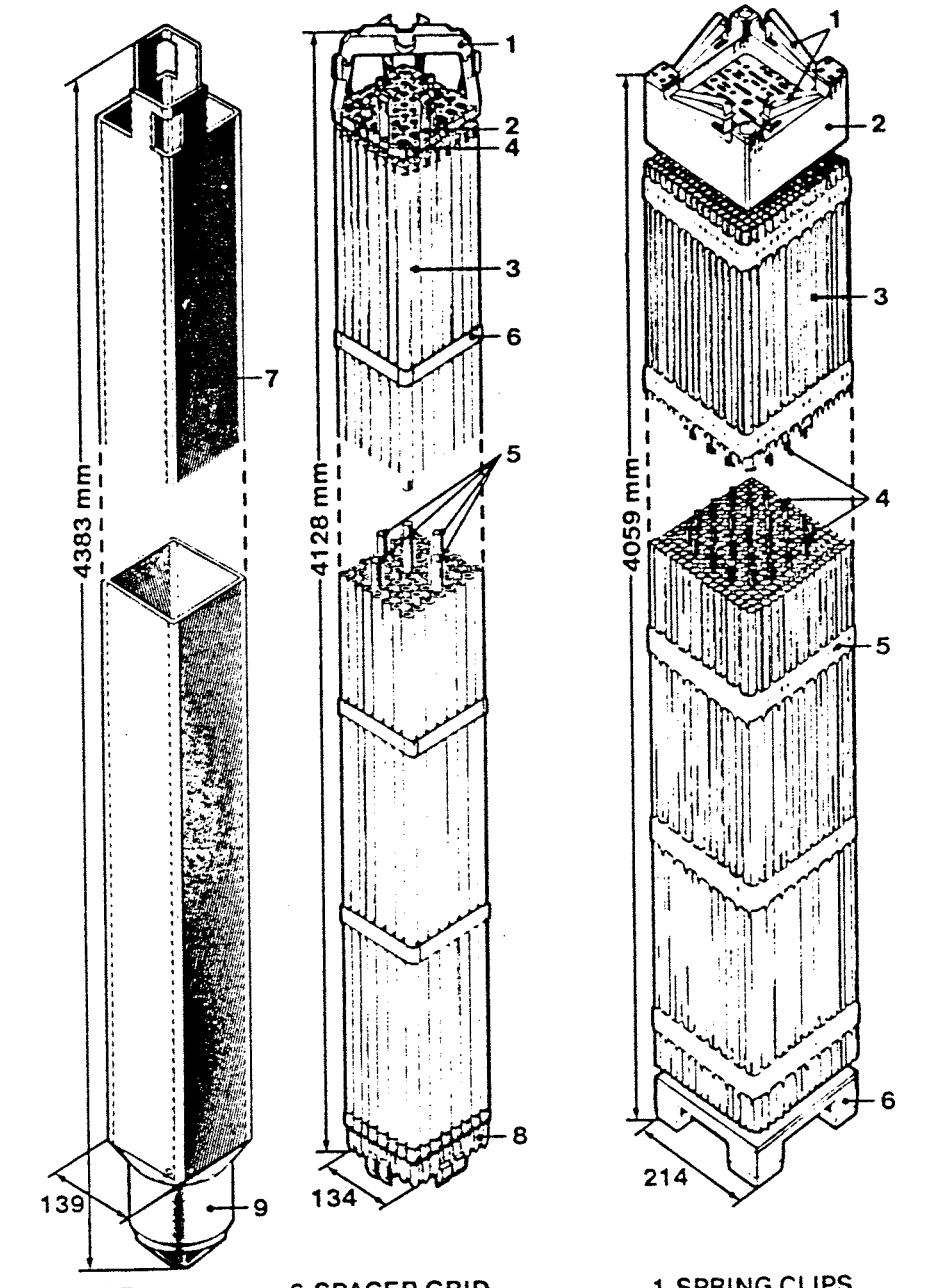

BWR fuel.

PWR fuel.

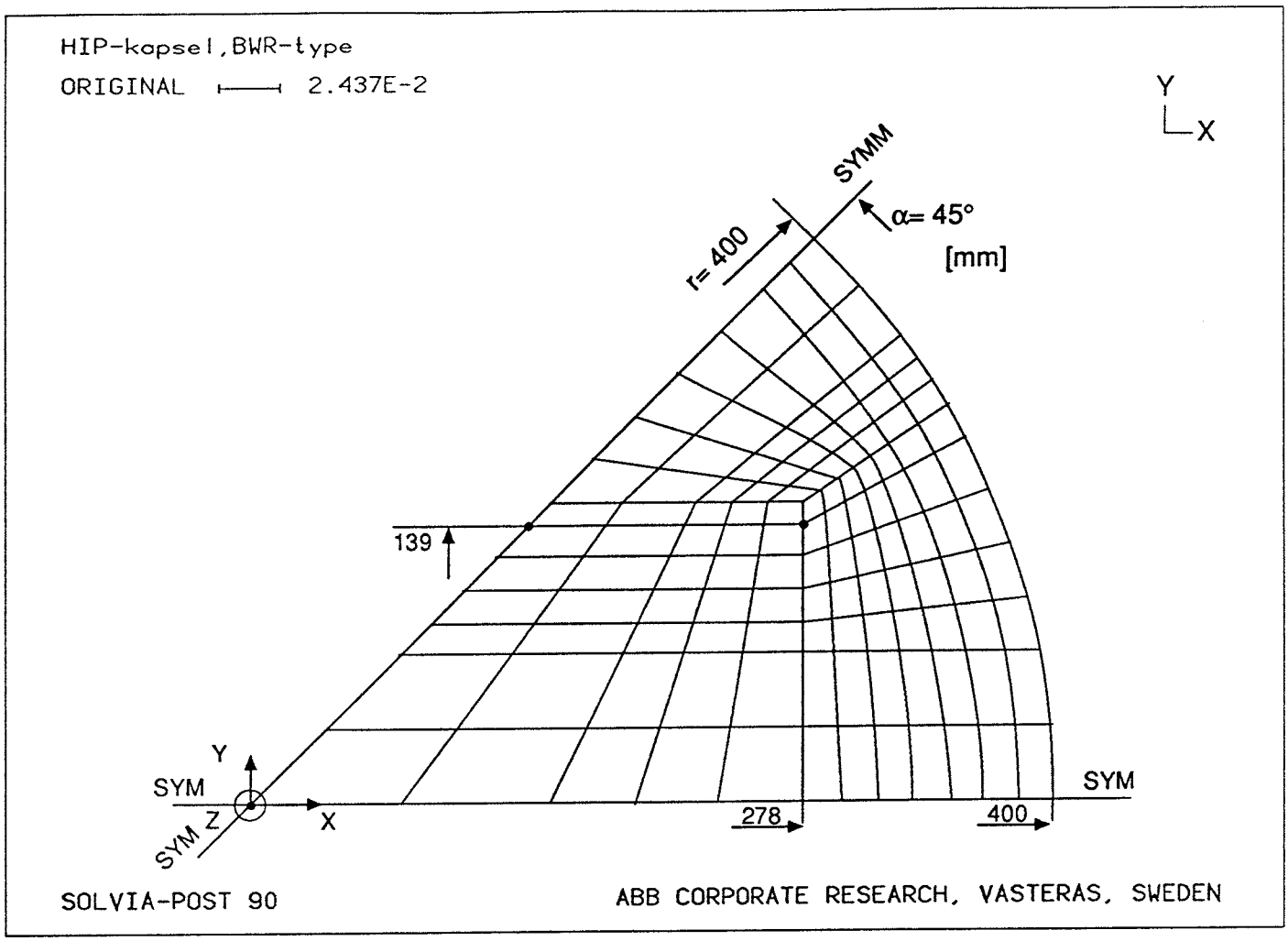

Finite Element Model Data

Number of nodes	7351
Number of elements	1547 (20-node, 3D solid elements)
Number of DOF	20537

HIP-kapsel,BWR-type
ORIGINAL ⟷ 7.125E-2 FEM-MODEL.

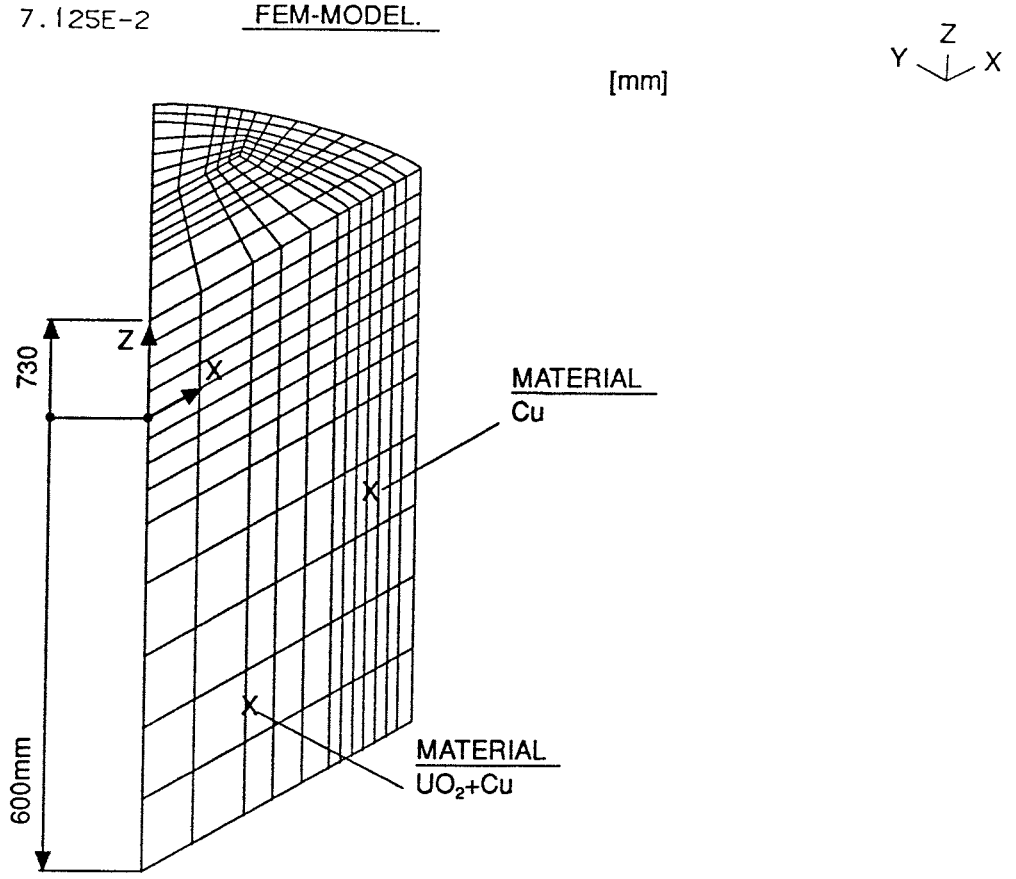

SOLVIA-POST 90 ABB CORPORATE RESEARCH, VASTERAS, SWEDEN

HIP-kapsel,BWR-type
DEFORMED ⟷ 6.781E-2
TIME 3600.

THE COPPER PART OF THE MODEL.

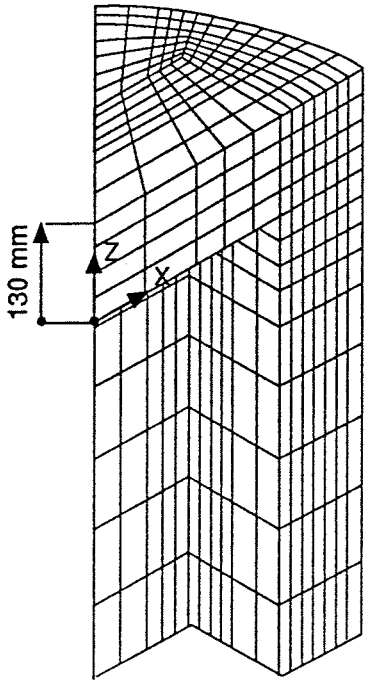

SOLVIA-POST 90 ABB CORPORATE RESEARCH, VASTERAS, SWEDEN

Material properties (taken from ref 2 and 3)

Cu
Solid copper after HIP

Temp deg C	E MPa	ν	σ_Y MPa	E_T MPa	α 10^{-6} C^{-1}
-50	117650	0.33	44	1220	16.8
20	117650	0.33	44	1220	16.8
100	115380	0.33	42	868	17.2
200	96550	0.33	37	625	18.0
300	80650	0.33	32	313	18.7
500	50000	0.33	21	36	19.9
550	40000	0.33	16	36	19.9

UO_2 + Cu
Fuel elements filled with Cu powder and HIPed

Temp deg C	E MPa	ν	α 10^{-6} C^{-1}
-50	153680	0.32	12.3
50	153680	0.32	12.3
150	141030	0.32	12.9
250	126230	0.32	13.5
350	111130	0.32	13.7
450	93070	0.32	14.6
550	75000	0.32	14.6

HIP-kapsel,BWR-type
ORIGINAL ⊢ ⊣ 6.961E-2
DEFORMED ⊢——⊣ 1.633E-2
TIME 3600.

DEFORMATION AT T=20°C

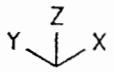

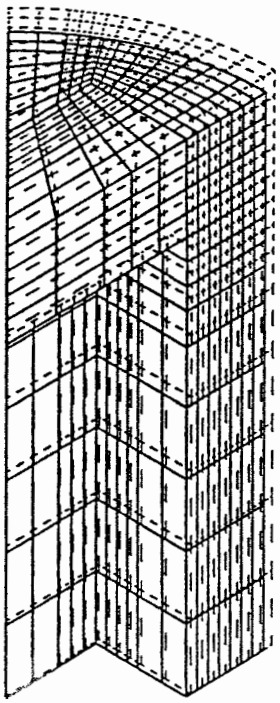

NOTE
Deformation is enlarged.

SOLVIA-POST 90 ABB CORPORATE RESEARCH, VASTERAS, SWEDEN

HIP-kapsel,BWR-type
ORIGINAL ⊢ ⊣ 7.122E-2
DEFORMED ⊢——⊣ 1.391E-2
TIME 3600.

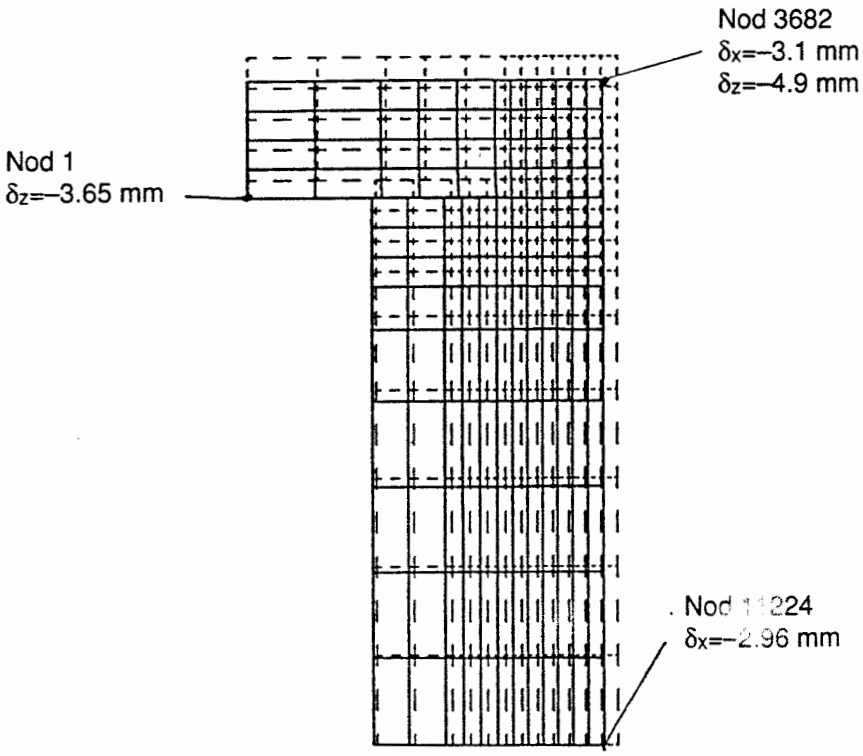

SOLVIA-POST 90 ABB CORPORATE RESEARCH, VASTERAS, SWEDEN

HIP-kapsel,BWR-type
DEFORMED ⟷ 6.781E-2
TIME 3600.

Z
Y X

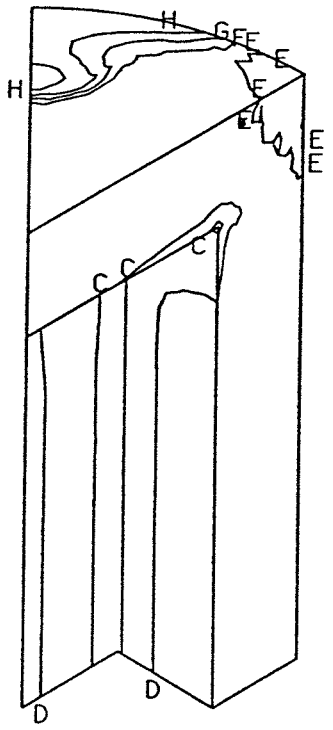

B4

EFF. STRESS
BASED ON ZONE
MAX 7.119E7 [N/m²]

A 6.813E7
B 6.202E7
C 5.590E7
D 4.978E7
E 4.367E7
F 3.755E7
G 3.143E7
H 2.531E7

MIN 2.226E7

SOLVIA-POST 90 ABB CORPORATE RESEARCH, VASTERAS, SWEDEN

HIP-kapsel,BWR-type
DEFORMED ⟷ 6.781E-2
TIME 3600.

Z
Y X

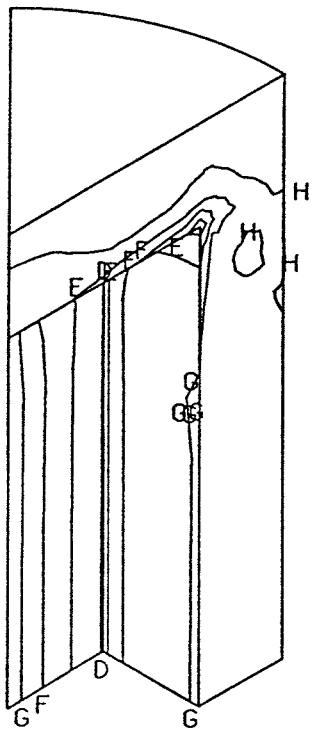

B2

EPACC
BASED ON ZONE
MAX 2.027E-2

A 1.900E-2
B 1.646E-2
C 1.391E-2
D 1.137E-2
E 8.827E-3
F 6.284E-3
G 3.741E-3
H 1.197E-3

MIN -7.438E-5

SOLVIA-POST 90 ABB CORPORATE RESEARCH, VASTERAS, SWEDEN

HIP-kapsel,BWR-type
DEFORMED ⟷ 6.781E-2
TIME 3600.

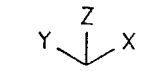

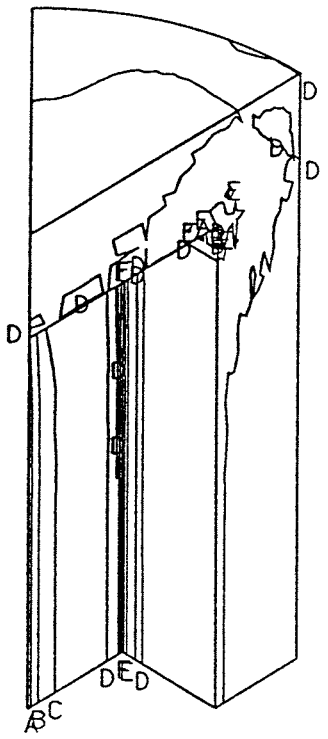

PRINCIPAL
STRESS MAX.
BASED ON ZONE
MAX 1.694E8 [N/m²]

A 1.513E8
B 1.153E8
C 7.919E7
D 4.312E7
E 7.050E6
F –2.902E7
G –6.509E7
H –1.012E8

MIN –1.192E8

SOLVIA-POST 90 ABB CORPORATE RESEARCH, VASTERAS, SWEDEN

HIP-kapsel,BWR-type
DEFORMED ⟷ 6.781E-2
TIME 3600.

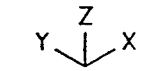

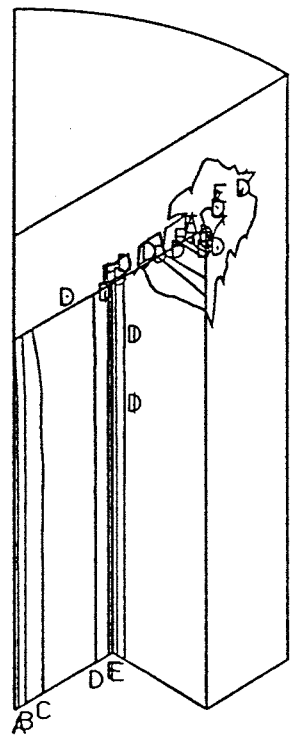

PRINCIPAL
STRESS MIN.
BASED ON ZONE
MAX 1.19E8 [N/m²]

A 9.89E7
B 5.94E7
C 1.98E7
D –1.97E7
E –5.92E7
F –9.87E7
G –1.38E8
H –1.78E8

MIN –1.98E8

SOLVIA-POST 90 ABB CORPORATE RESEARCH, VASTERAS, SWEDEN

HIP-kapsel,BWR-type
DEFORMED ⟷ 7.851E-2
TIME 3600.

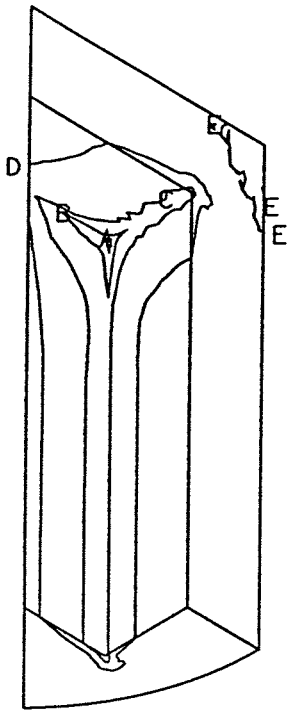

EFF. STRESS
BASED ON ZONE
MAX 7.119E7 [N/m²]

A 6.813E7
B 6.202E7
C 5.590E7
D 4.978E7
E 4.367E7
F 3.755E7
G 3.143E7
H 2.531E7

MIN 2.226E7

SOLVIA-POST 90 ABB CORPORATE RESEARCH, VASTERAS, SWEDEN

HIP-kapsel,BWR-type
DEFORMED ⟷ 7.851E-2
TIME 3600.

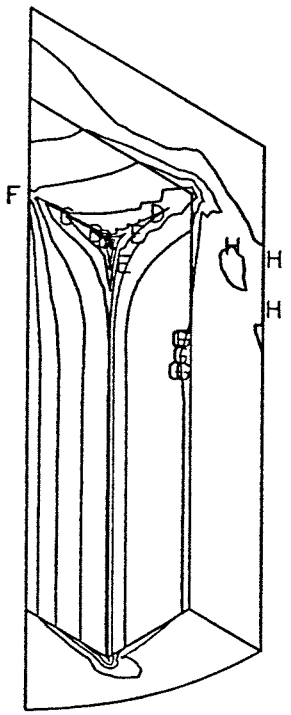

EPACC
BASED ON ZONE
MAX 2.027E-2

A 1.900E-2
B 1.646E-2
C 1.391E-2
D 1.137E-2
E 8.827E-3
F 6.284E-3
G 3.741E-3
H 1.197E-3

MIN -7.438E-5

SOLVIA-POST 90 ABB CORPORATE RESEARCH, VASTERAS, SWEDEN

HIP-kapsel,BWR-type

DEFORMED ⟷ 7.851E-2
TIME 3600.

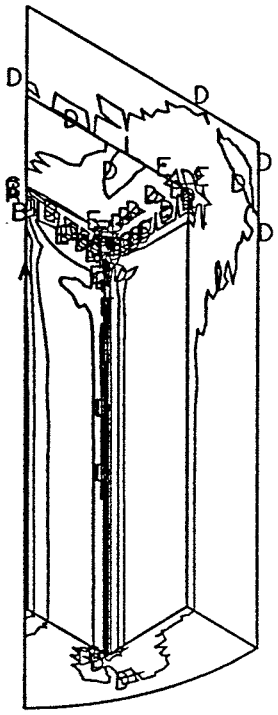

PRINCIPAL
STRESS MAX.
BASED ON ZONE
MAX 1.694E8 [N/m²]

A 1.513E8
B 1.153E8
C 7.919E7
D 4.312E7
E 7.050E6
F –2.902E7
G –6.509E7
H –1.012E8

MIN –1.192E8

SOLVIA-POST 90

ABB CORPORATE RESEARCH, VASTERAS, SWEDEN

HIP-kapsel,BWR-type

DEFORMED ⟷ 7.851E-2
TIME 3600.

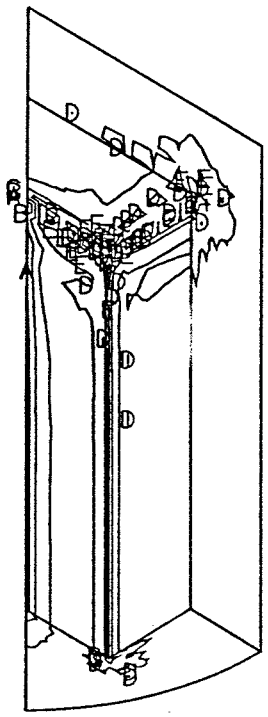

PRINCIPAL
STRESS MIN.
BASED ON ZONE
MAX 1.19E8 [N/m²]

A 9.89E7
B 5.94E7
C 1.98E7
D –1.97E7
E –5.92E7
F –9.87E7
G –1.38E8
H –1.78E8

MIN –1.98E8

SOLVIA-POST 90

ABB CORPORATE RESEARCH, VASTERAS, SWEDEN

HIP-kapsel,BWR-type
DEFORMED ⟷ 7.851E-2
TIME 3600.

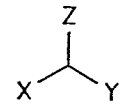

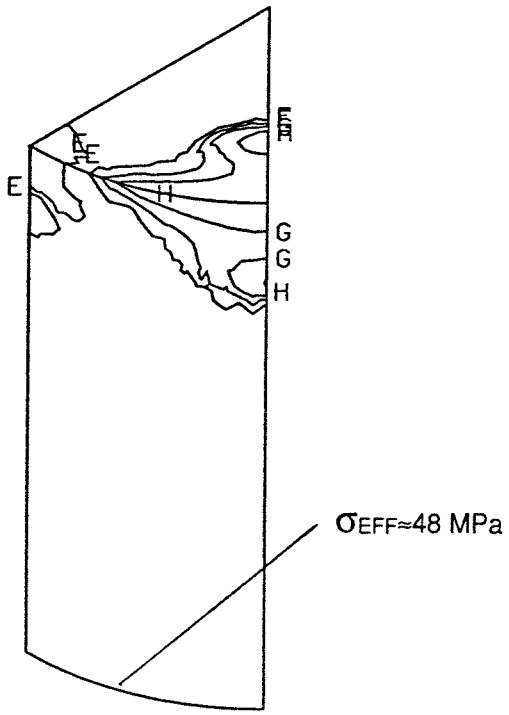

EFF. STRESS
BASED ON ZONE
MAX 7.119E7 [N/m²]

A 6.813E7
B 6.202E7
C 5.590E7
D 4.978E7
E 4.367E7
F 3.755E7
G 3.143E7
H 2.531E7

MIN 2.226E7

SOLVIA-POST 90 ABB CORPORATE RESEARCH, VASTERAS, SWEDEN

HIP-kapsel,BWR-type
DEFORMED ⟷ 7.851E-2
TIME 3600.

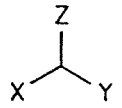

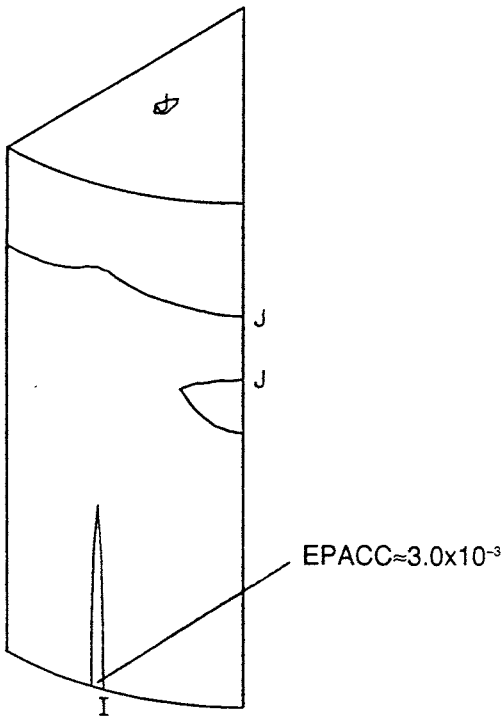

EPACC
BASED ON ZONE
MAX 2.027E-2

A 1.925E-2
B 1.722E-2
C 1.519E-2
D 1.315E-2
E 1.112E-2
F 9.082E-3
G 7.047E-3
H 5.012E-3
I 2.978E-3
J 9.430E-4

MIN -7.438E-5

SOLVIA-POST 90 ABB CORPORATE RESEARCH, VASTERAS, SWEDEN

HIP-kapsel,BWR-type
DEFORMED ⟵⟶ 7.851E-2
TIME 3600.

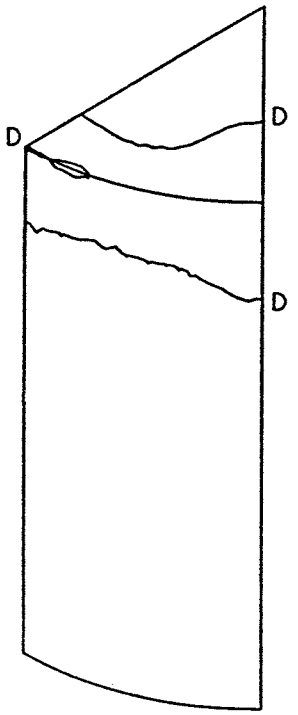

PRINCIPAL STRESS MIN.
SPMIN=0

PRINCIPAL
STRESS MAX.
BASED ON ZONE
MAX 1.694E8 [N/m²]

A 1.513E8
B 1.153E8
C 7.919E7
D 4.312E7
E 7.050E6
F −2.902E7
G −6.509E7
H −1.012E8

MIN −1.192E8

SOLVIA-POST 90

ABB CORPORATE RESEARCH, VASTERAS, SWEDEN

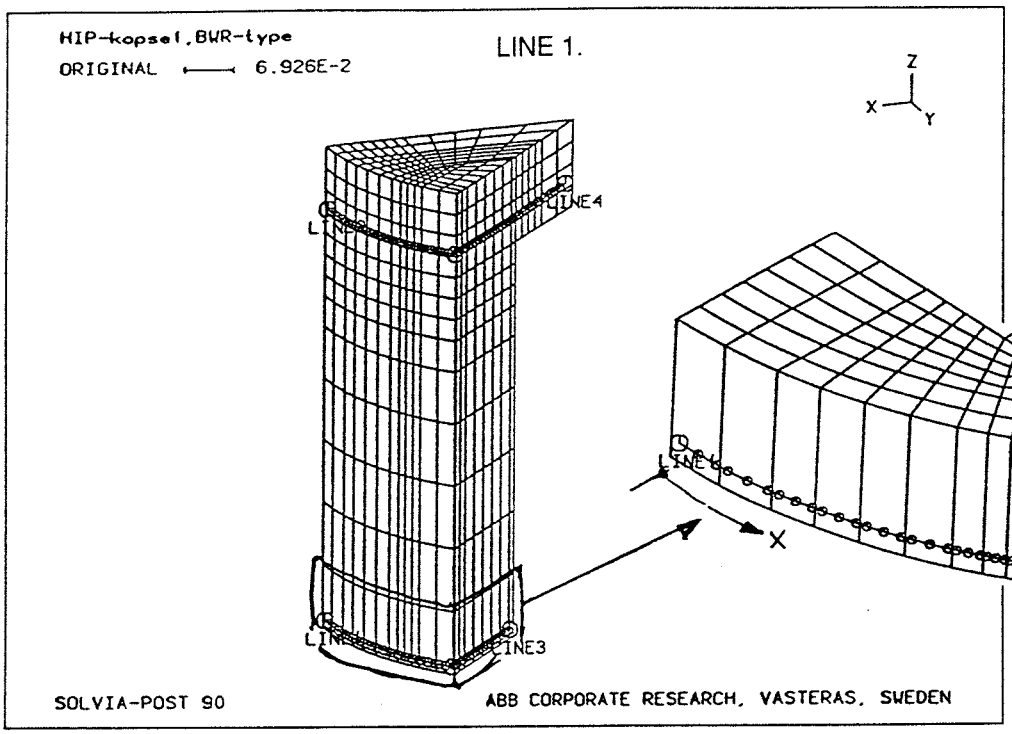
HIP-kopsel,BWR-type
ORIGINAL 6.926E-2
LINE 1.
Z
X
Y
LINE4
LINE1
LINE2
LINE3
SOLVIA-POST 90
ABB CORPORATE RESEARCH, VASTERAS, SWEDEN

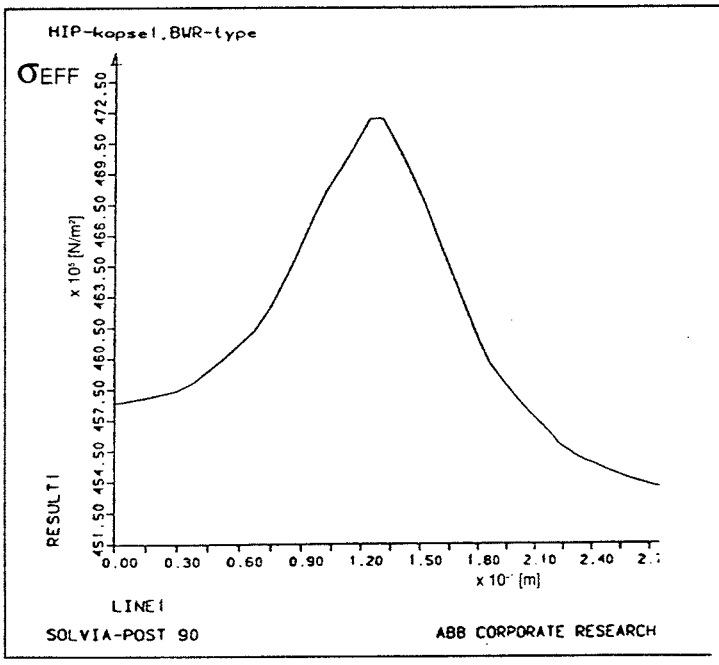
HIP-kopsel,BWR-type
TIME 3600.
σEFF
RESULT
x 10⁶ [N/m²]
451.50 454.50 457.50 460.50 463.50 466.50 469.50 472.50
0.00 0.30 0.60 0.90 1.20 1.50 1.80 2.10 2.40
x 10⁻¹ [m]
LINE1
SOLVIA-POST 90
ABB CORPORATE RESEARCH

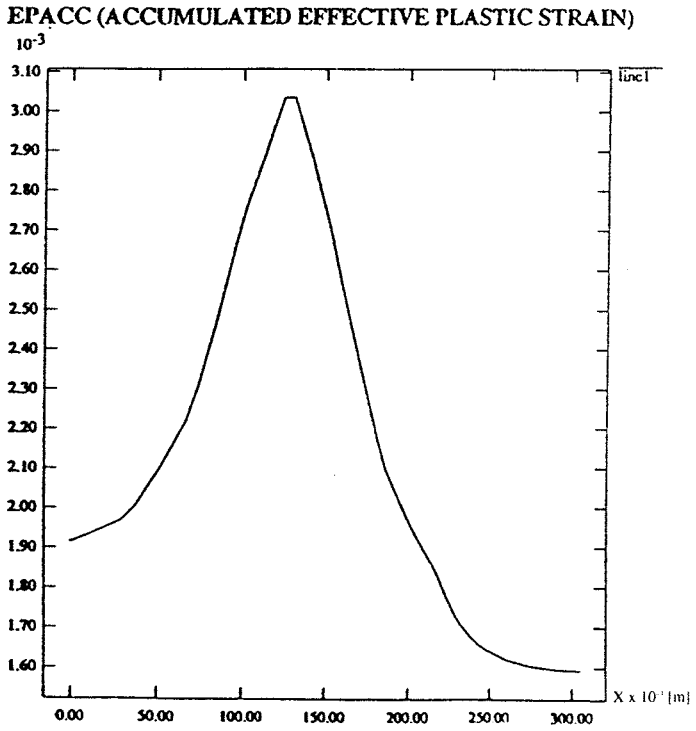
EPACC (ACCUMULATED EFFECTIVE PLASTIC STRAIN)
10⁻³
3.10
3.00
2.90
2.80
2.70
2.60
2.50
2.40
2.30
2.20
2.10
2.00
1.90
1.80
1.70
1.60
line1
0.00 50.00 100.00 150.00 200.00 250.00 300.00
X x 10⁻¹ [m]

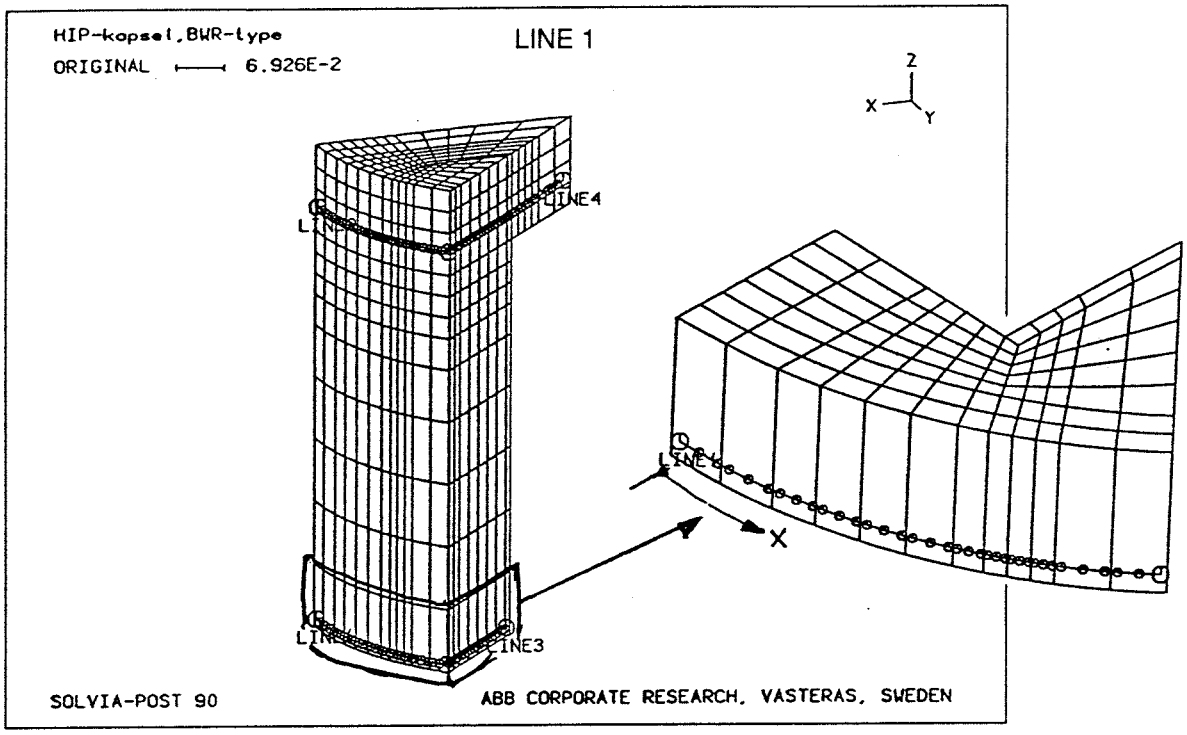

SPMAX (MAX.PRINCIPALSTRESS)

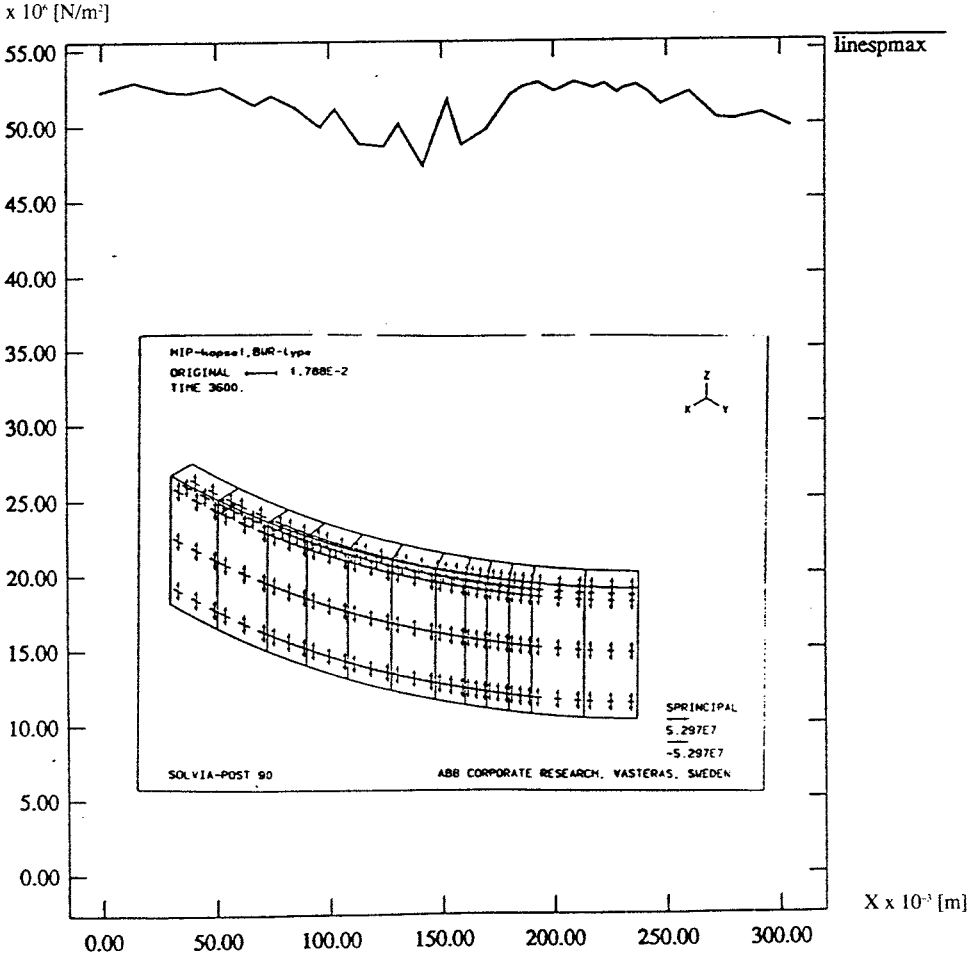

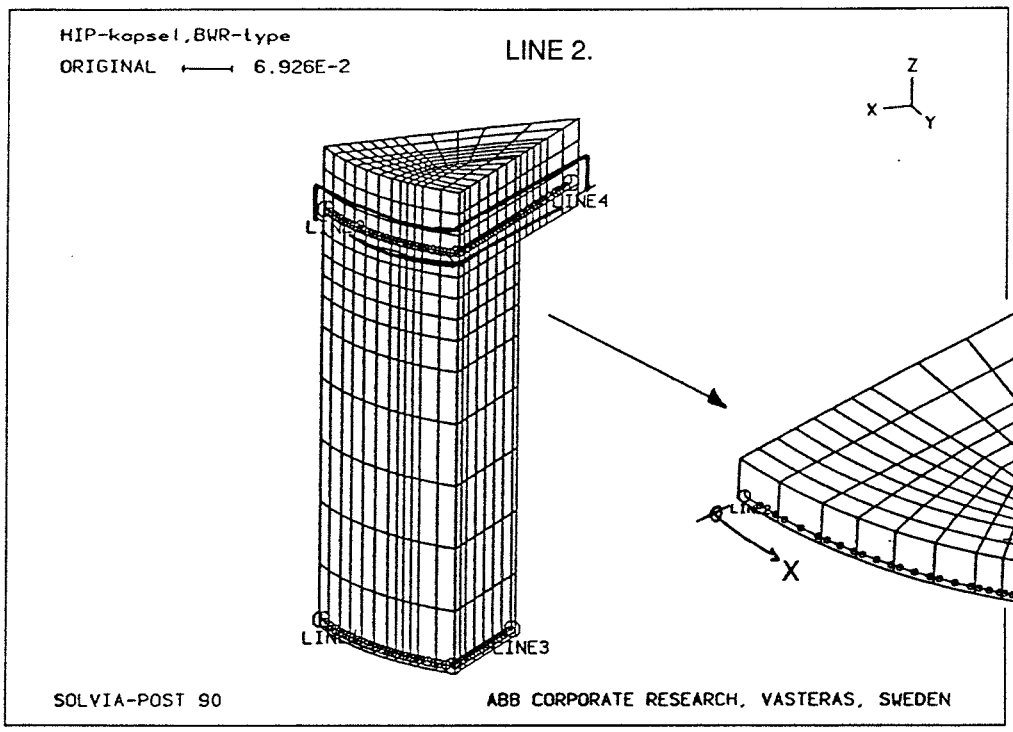

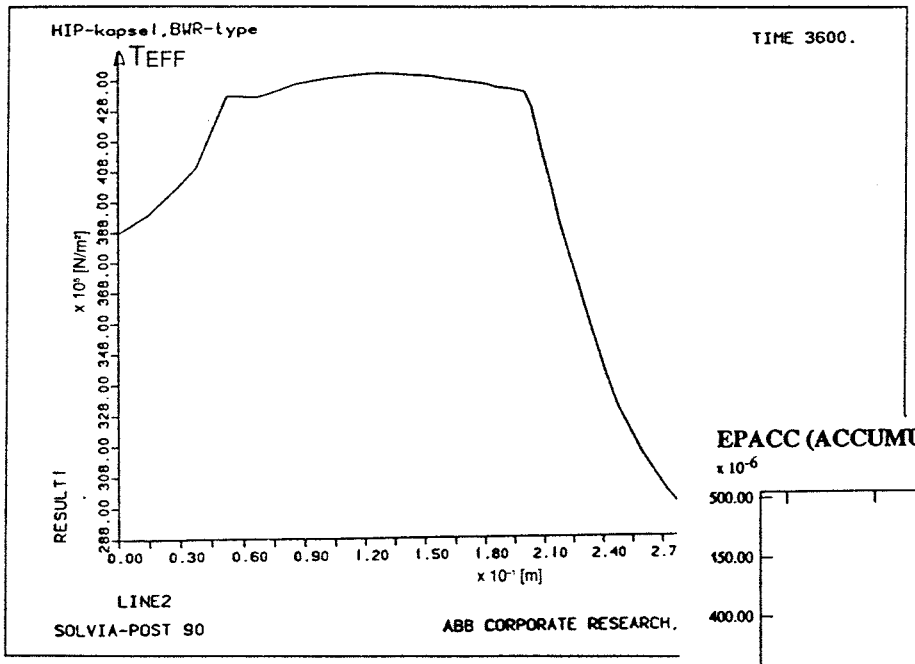

EPACC (ACCUMULATED EFFECTIVE PLASTIC STRAIN)

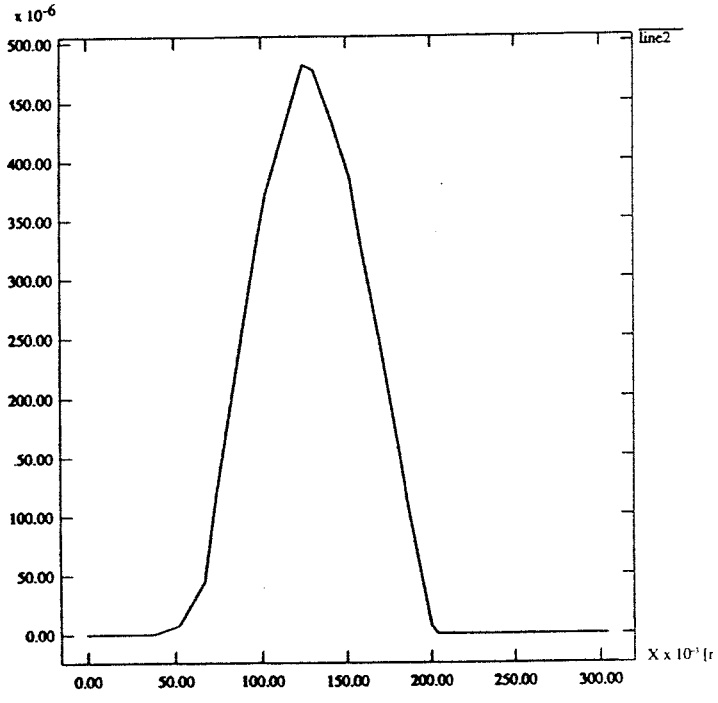

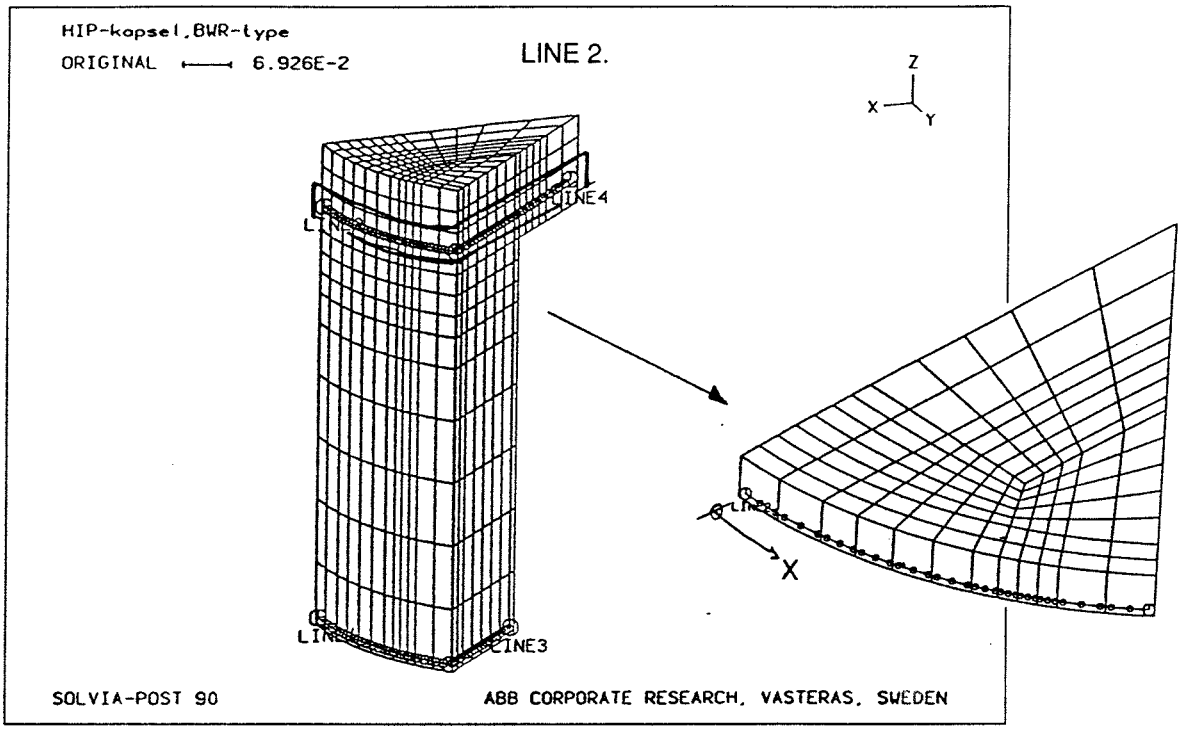

SPMAX (MAX.PRINCIPALSTRESS)

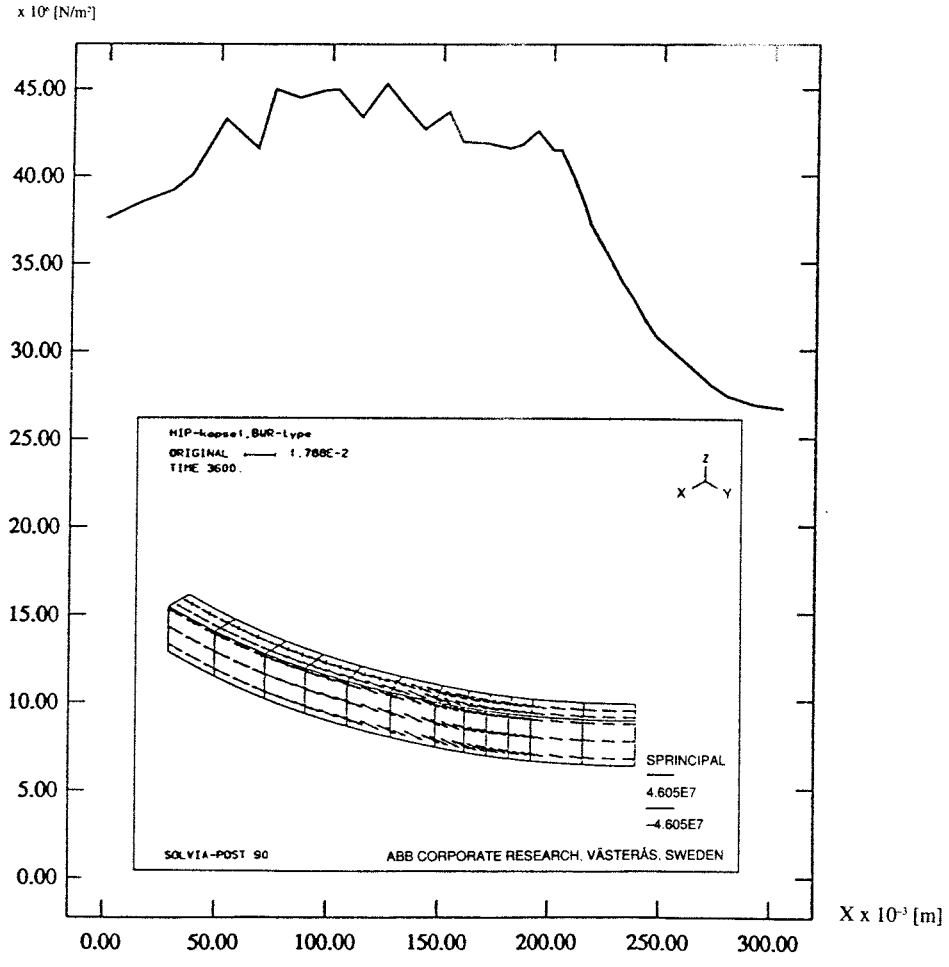

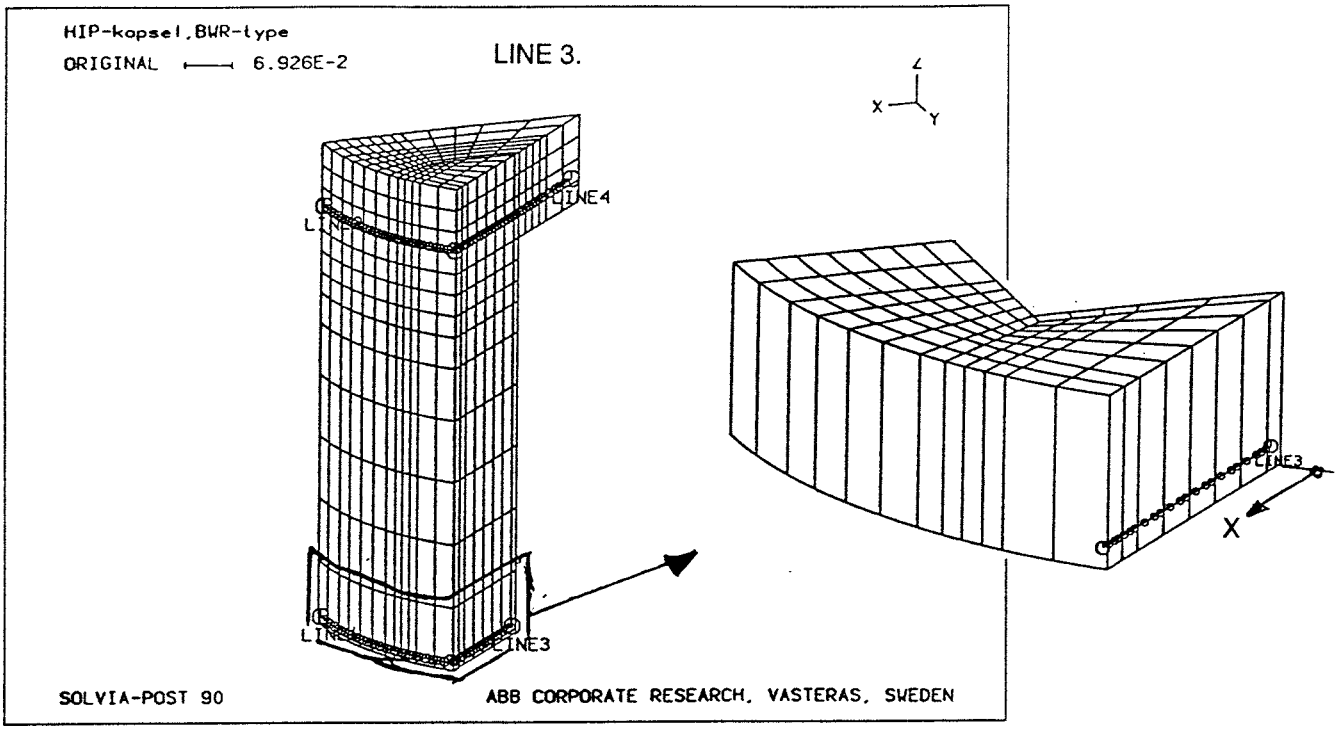

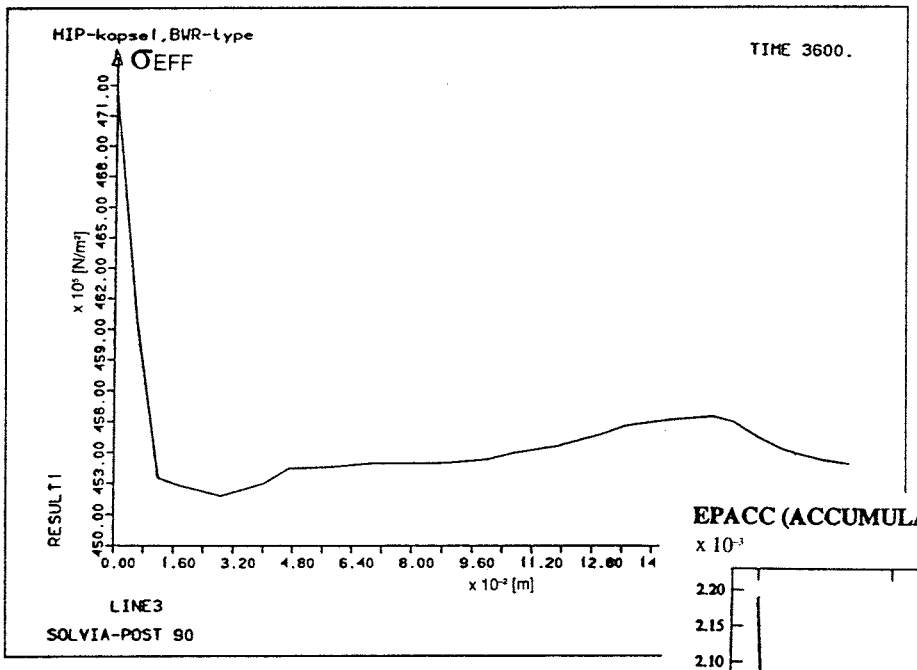

EPACC (ACCUMULATED EFFECTIVE PLASTIC STRAIN)

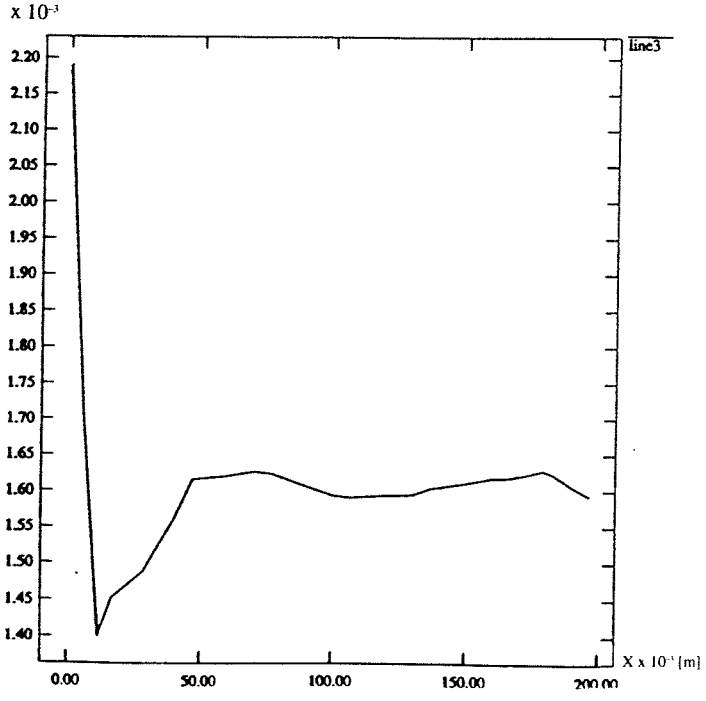

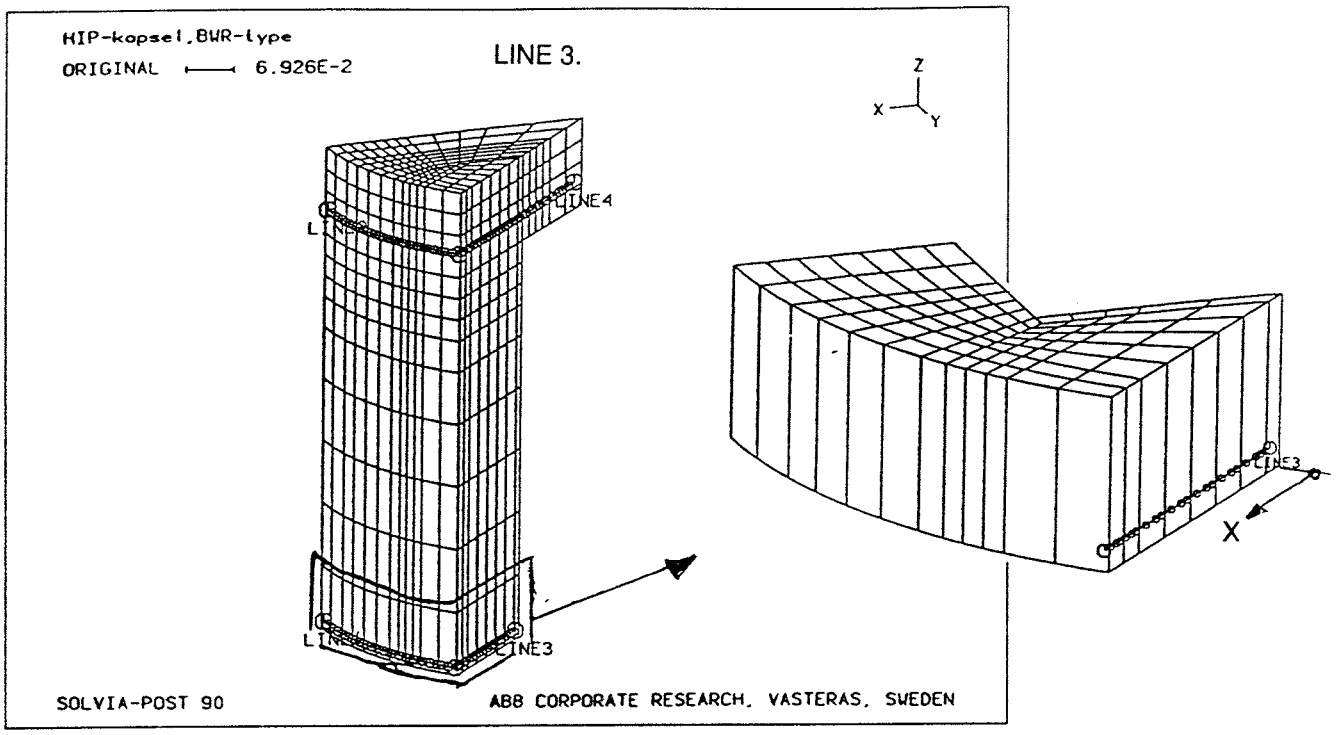

SPMAX (MAX.PRINCIPALSTRESS)

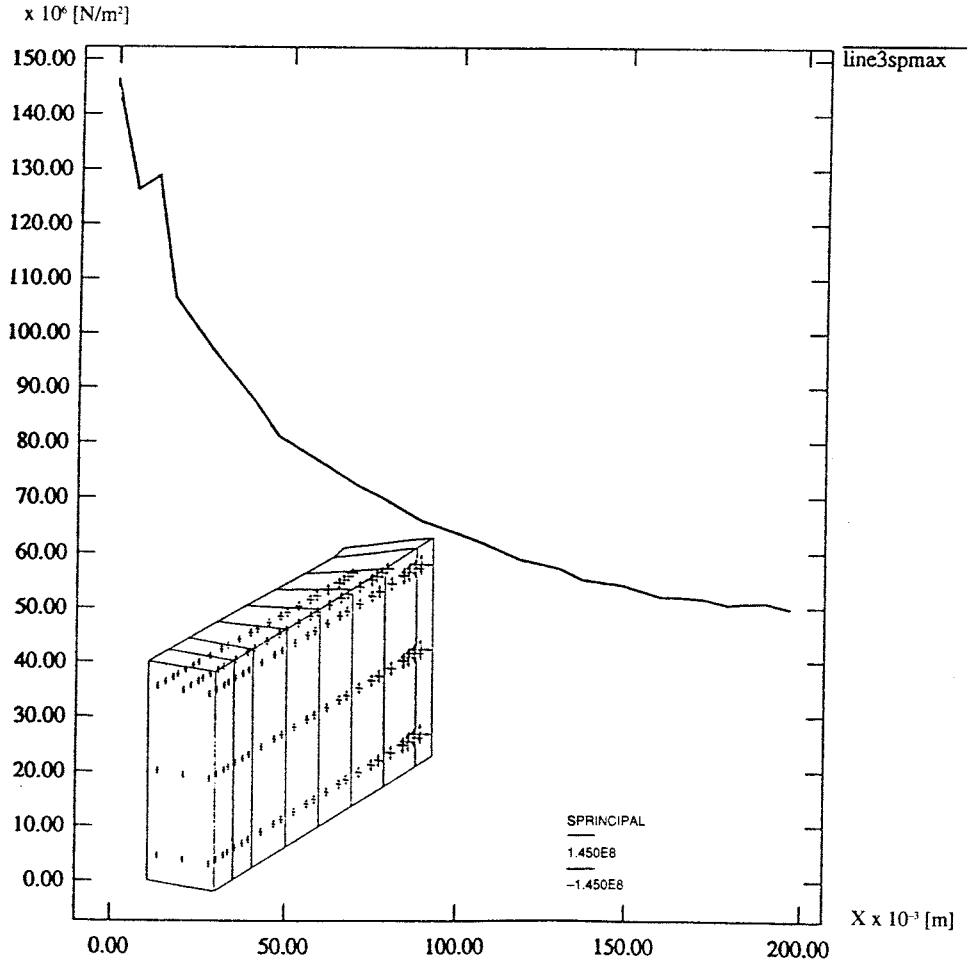

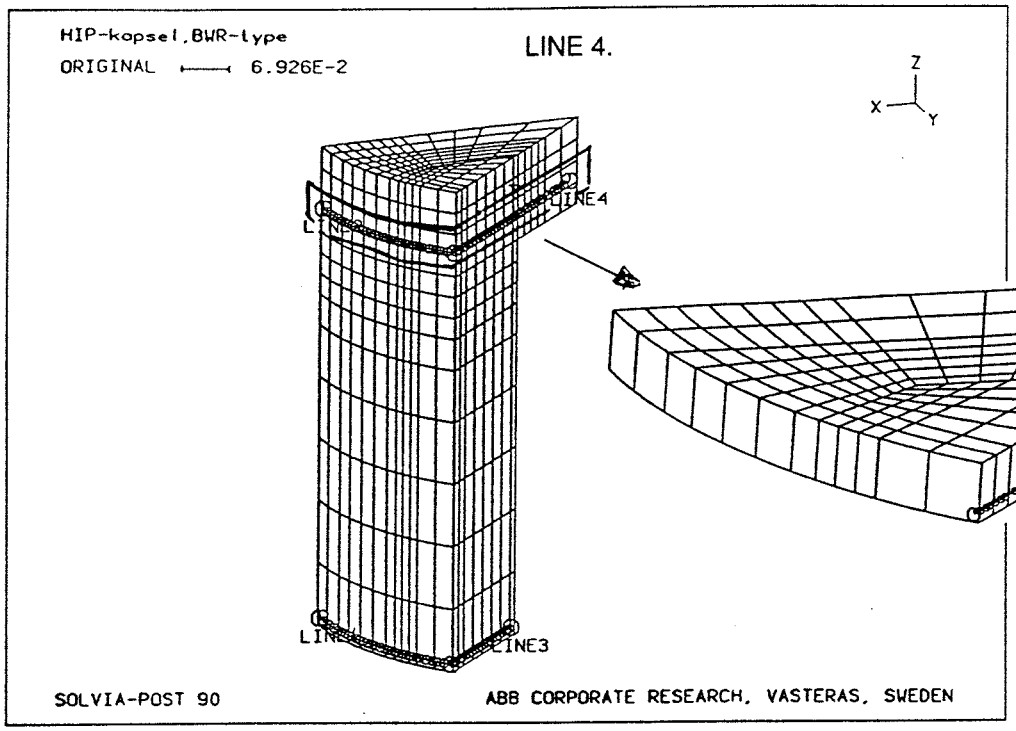

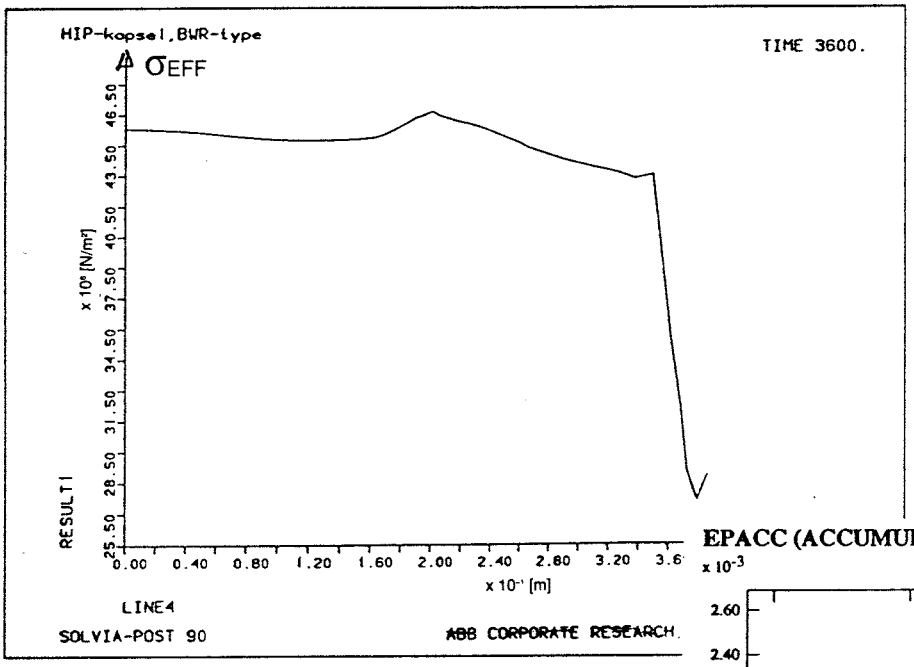

EPACC (ACCUMULATED EFFECTIVE PLASTIC STRAIN)

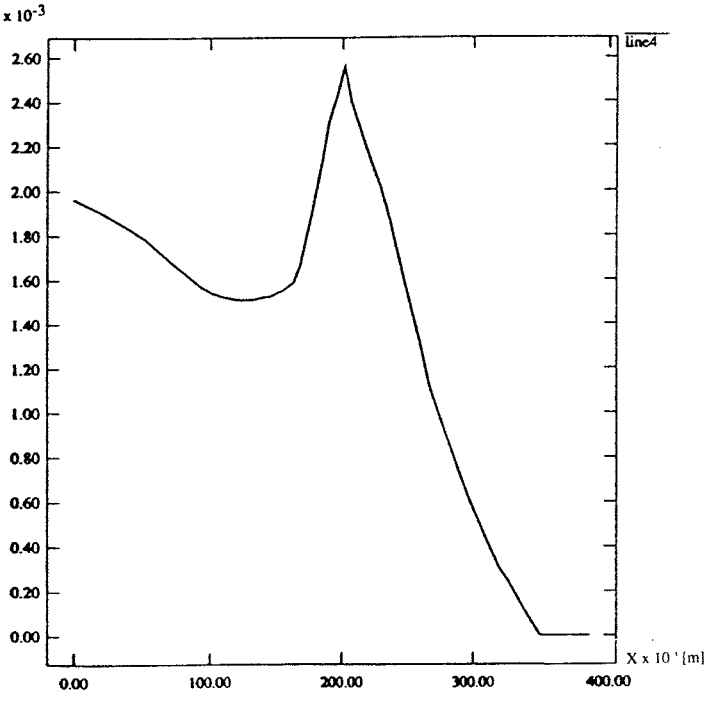

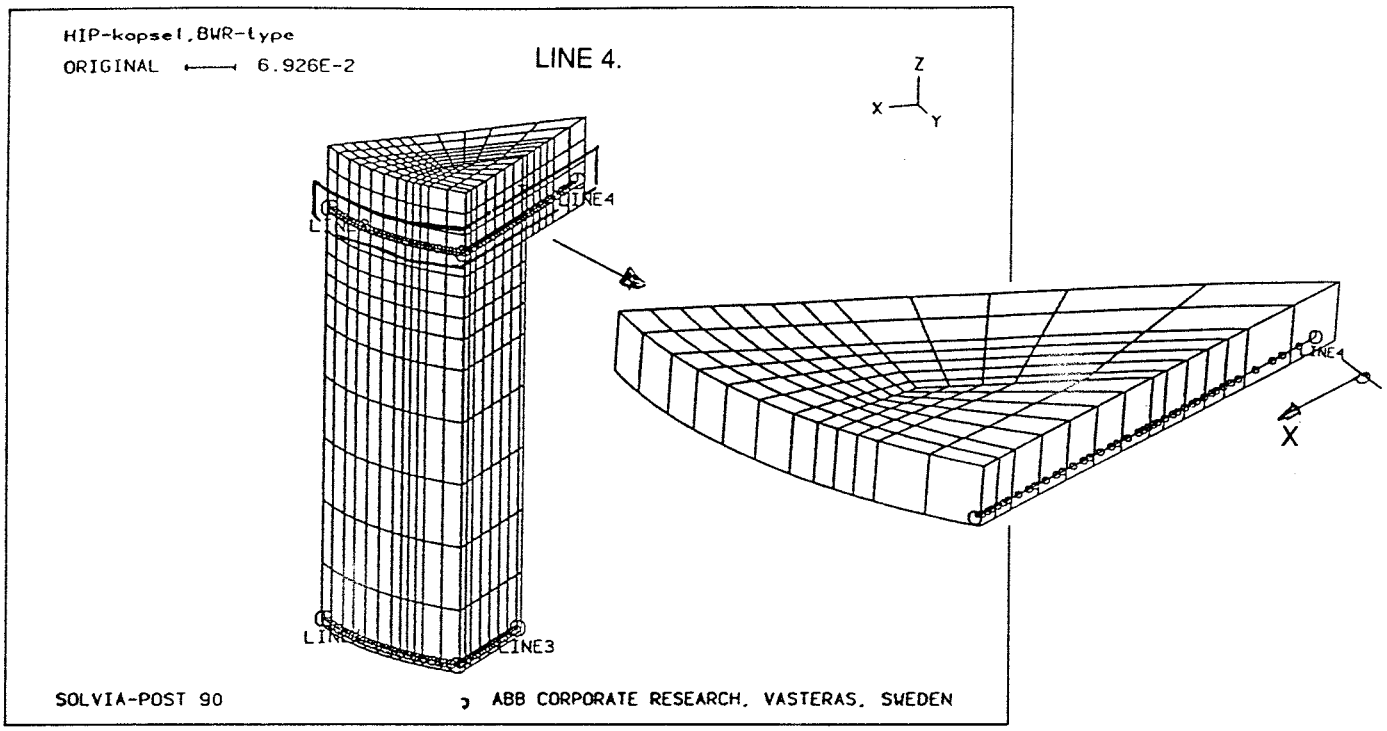

SPMAX (MAX.PRINCIPALSTRESS)

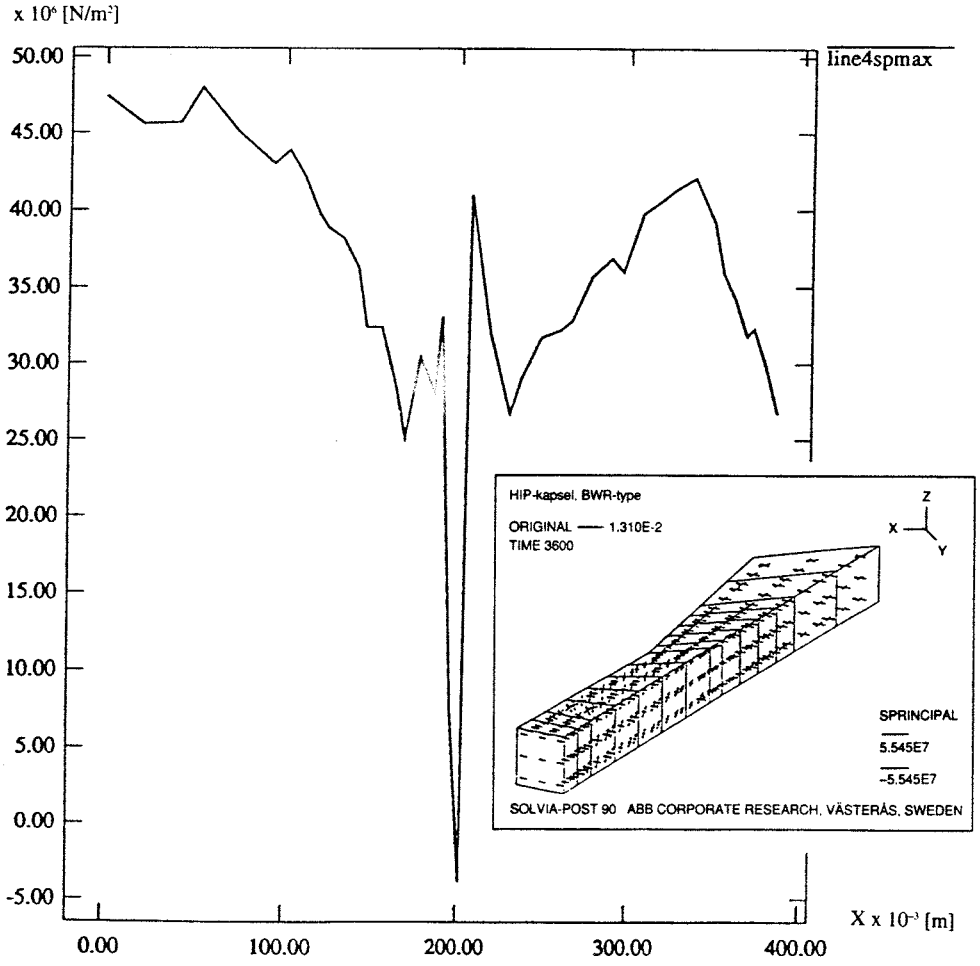

Appendix II

Creep and Creep Fracture of Copper Canisters Nuclear Fuel Waste

Kjell Pettersson
Royal Institute of Technology

Division of Mechanical
Metallurgy, KTH

1992-04-23

Creep and creep fracture of copper canisters for nuclear waste

Kjell Pettersson

Division of Mechanical Metallurgy, Royal Institute of Technology

The following discussion is based primarily on a review paper on creep fracture by void growth by Cocks and Ashby (1). That paper has also been consulted by Josefson in a previous discussion on creep fracture in copper (2). However in the present note the problem will be discussed from a slightly different perspective. There is also a more comprehensive treatise on creep fracture by Evans available (3). Evans treats the complete problem of creep fracture while the paper by Cocks and Ashby is limited to the modelling of void growth under different conditions of stress and temperature. They therefore bypass the most difficult problem of creep fracture: the nucleation of the voids in the grain boundary. But in order to demonstrate the integrity of a waste canister with regard to creep fracture it is sufficient to prove that the growth of voids will not lead to fracture during the life time of the capsule. In this note I will try to demonstrate that the models proposed by Cocks and Ashby leads to life predictions which exceeds the desired life time of a waste canister.

Cocks and Ashby identify three mechanisms which lead to void growth, Figure 1. These mechanisms dominate at different temperatures and stresses. They can thus, in analogy with deformation mechanisms and fracture mechanisms, be displayed in void growth maps. One such map is shown in Figure 2. The region of interest for nuclear waste approximately 0.2 - 0.3 T_M and 10^{-4} - 10^{-3} E. Void growth is therefore controlled by surface diffusion with some influence of power law creep growth as indicated by the

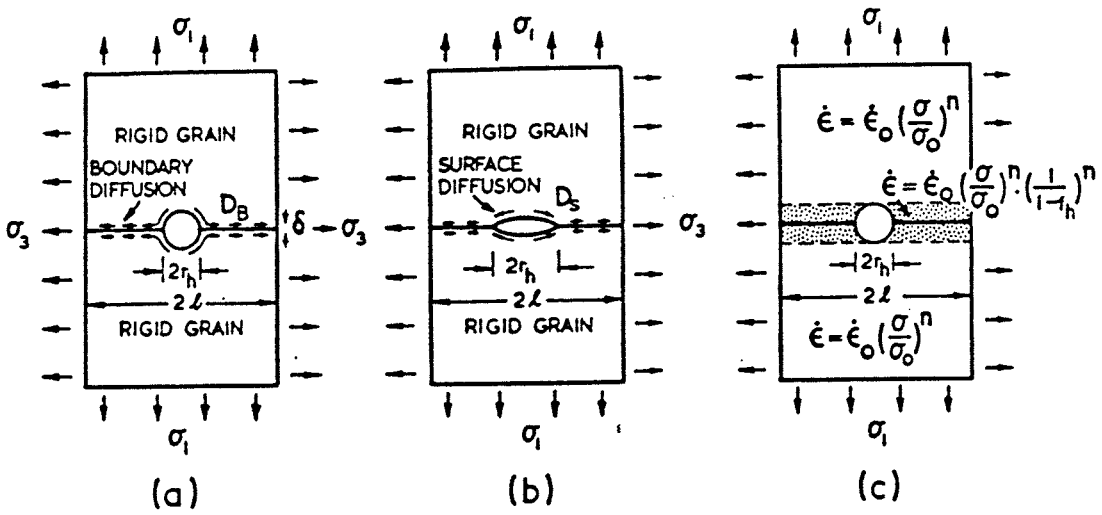

Figure 1. The three simple mechanisms which limit void growth

shading on the void growth map. Power law creep growth is additional to the surface diffusion creep growth. It is thus non-conservative to disregard it. However in this preliminary analysis it shall, for simplicity, be disregarded from.

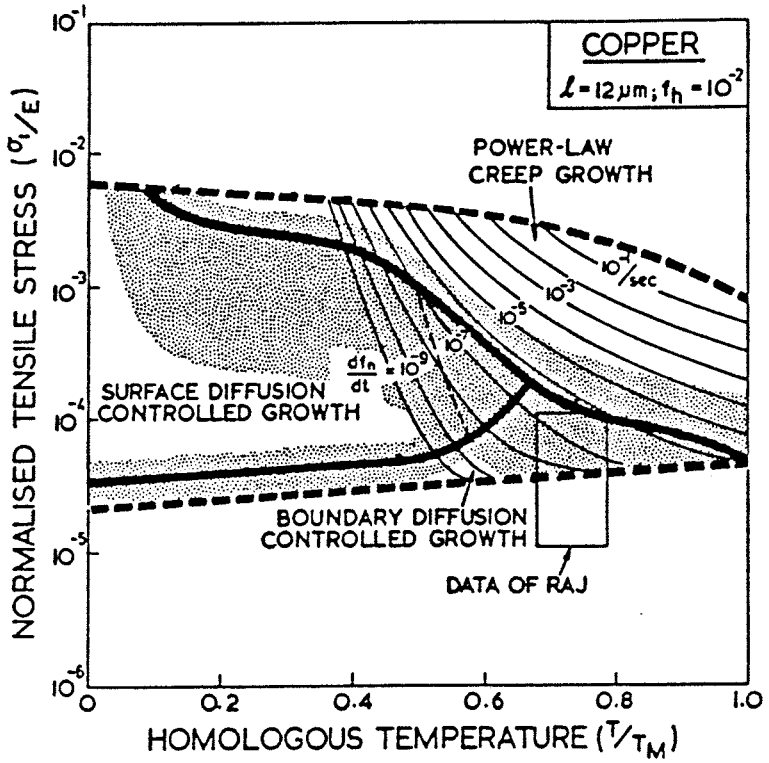

Figure 2. A void growth map for copper

As indicated in Figure 1 the shape of the void is relatively flat under surface diffusion

control while it is spherical under the other modes. This means that the growth of voids under surface diffusion control makes little contribution to the strain while the growth of voids contribute a strain of the order of $0.2 \cdot l/d$ at fracture with the other mechanisms at work (l is the void spacing and d the grain size). This is significant for the canisters since a main concern for these is that creep cracks will grow due to residual stresses. Thus with any other mechanism than surface diffusion there would not be enough stored elastic strain to grow a crack to failure (with reasonable values of l and d).

The void growth map can be correlated with the results reported by Henderson et. al (4). In that work the test series 000 and 100 resulted in low ductile creep failure for specimens tested at stresses between 40 and 100 MPa and at temperatures between 180 and 250°C. Both SEM and light optical microscopy showed that the fractures were intergranular with heavily voided grain facets. The void spacing seems to be about 7 μm. From the appearance of the voids on SEM pictures they were relatively spherical. This can perhaps be a result of general plastic deformation just before failure. Auger electron spectroscopy of voids on grain boundary facets showed that the surfaces of the voids were covered with sulphur. It is possible but by no means proved that the sulphur has played a role in the creep fracture.

The time to failure under surface diffusion control can approximately be written as

$$t_f = \frac{\sqrt{2}\, kT\, l\, \gamma_s^2}{D_s\delta_s\, \Omega\, \sigma^3} \qquad (1)$$

where

l = void spacing

γ_s = surface energy

$D_s\delta_s$ = surface diffusion constant

Ω = atomic volume

Other symbols have their usual or obvious meaning. The various constants can be taken from Table 1 reproduced from ref. 1. If the constants from Table 1 are used failure times for series 000 and 100 in ref. 4 are overestimated by factors of up to $6.4 \cdot 10^6$. It is

Table 1

	Copper	Silver
n	4.8	5.3
A	2.1×10^{-9}	2.1×10^{-9}
D_{0V} ($m^3 s^{-1}$)	6.2×10^{-5}	4.4×10^{-5}
Q_V (KJ $mole^{-1}$)	207	185
b (m)	2.56×10^{-10}	2.89×10^{-10}
μ_0 ($MN m^{-2}$)	4.21×10^4	2.64×10^4
T_m (K)	1356	1234
$\Delta\mu_T$ (K^{-1})	3.97×10^{-4}	4.36×10^{-4}
Ω (m^3)	1.18×10^{-29}	1.71×10^{-29}
$D_{0B}\delta_B$ ($m^3 s^{-1}$)	5.12×10^{-15}	6.94×10^{-15}
Q_B (KJ $mole^{-1}$)	105	89.8
γ_s ($J m^{-2}$)	1.72	1.12
$D_{0s}\delta_s$ ($m^3 s^{-1}$)	6×10^{-10}	6×10^{-10}†
Q_s (kJ $mole^{-1}$)	205	186†
σ_0 ($MN m^{-2}$)	39.0	61.0

†The values of $D_{0s}\delta_s$ and Q_s for silver were calculated by averaging over a number of f.c.c. metals (Neumann and Neumann, 1972).

possible that the diffusion constant is wrong by a factor of 10. It is also possible, but perhaps unlikely, that the presence of sulphur on the void surface can account for the rest of the difference between theory and experiment. Let us thus assume that the diffusion constant is $6.4 \cdot 10^6$ times larger than according to Table 1 and see what life times can be expected for a copper canister. Table 2 gives a selection of life times under different conditions according to the theory of Cocks and Ashby.

The results presented in Table 2 show clearly that there is no risk of creep fracture through void growth if the temperature is below 80°C for most of the time. In should be noted that the calculation was performed with the constants adjusted to fit the OFHC copper with bad creep fracture properties. It is reasonable to assume that the life times of the phosphorus containing copper will be much longer.

Table 2: Predicted creep life according to the theory of Cocks and Ashby.

Temperature (°C)	Stress (MPa)	Creep life (years)
120	80	384
120	60	910
120	40	3074
100	80	10500
100	60	25000
100	40	84000
80	80	420000
80	60	1000000
80	40	3400000

An attractive feature of the Cocks-Ashby model is that it should in principle be easy to use it with variable stress and temperature. The important parameter is the fraction of voids on the grain boundary, f_h. f_h can be regarded as a measure of creep damage. In the equation for t_f above it was assumed that the failure criterion was $f_h = 0.25$. The equation for the development of f_h is:

$$\frac{df_h}{dt} = \frac{f_h^{1/2} D_s \delta_s \Omega \sigma^3}{(1-f_h)^3 \sqrt{2}\, kT\, l\, \gamma_s^2} \qquad (2)$$

This equation could be used for integrating damage with a variable stress-temperature history. It is necessary to assume that there is an initial damage. It would not seem unreasonable to assume that the initial value is at most 0.01. Especially in a stress relaxation situation it must be resonable to assume that the growth of voids have very little effect on the stresses in general. Thus there is no interaction between void growth and the development of the stresses with time. This justifies the use of equation 2 independently of the stress calculation for a judgement on the possibility of creep fracture.

Is there a need for validation of the Cocks-Ashby model?

It is very difficult to visualize any other mechanism by which the copper canister can suffer creep fracture. The Cocks-Ashby model is physically reasonable and it only suffers from the uncertainty in the diffusion constant. A few other parameters of the model have some uncertainty but this is in no case so large that the results can be orders of magnitude wrong. The same argument applies to the geometrical simplifications inherent in the model. Thus my conclusion is that in the present state of the science of materials we can use the model to predict the creep life of a canister and we should be able to rely on the result. What now needs to be done is to find more data on creep failure in a range where there is surface diffusion control and check these against the model. There is also a need for an analysis of whether or not it was justified or at least conservative to neglect the other two modes of void growth.

References

1. Cocks, A.C.F. and Ashby, M.F. *"On creep fracture by void growth"*, Progress in Materials Science, vol. 27, pp. 189-244

2 Josefson, L. *"Creep deformation and void growth in copper canisters for spent nuclear fuel"* (1992), Appendix IV, This Report.

3. Evans, H. E., *"Mechanisms of creep fracture"*, Elsevier Applied Science Publishers, 1984

4. Henderson, P. J., Österberg, J-O., and Ivarsson, B. G., *"Low temperature creep of copper intended for nuclear waste containers"*, SKB Technical Report 92-04 (1992)

Appendix III

Creep, Stress Relaxation and Tensile Testing of Oxygen Free Phosphorous Copper (Cu-OFP) Intended for Nuclear Waste Containment

Joakim Lindblom, Pamela Henderson
and Facredin Seitisleam
Swedish Institute for Metals Research

CREEP, STRESS RELAXATION AND TENSILE TESTING OF OXYGEN FREE PHOSPHORUS COPPER (Cu-OFP) INTENDED FOR NUCLEAR WASTE CONTAINMENT

Joakim Lindblom, Pamela Henderson and Facredin Seitisleam
Institutet för Metallforskning
Drottning Kristinas väg 48
114 28 Stockholm, Sweden

Key words : Copper, creep, stress relaxation, tensile strength, ductility.

ABSTRACT

Creep and stress relaxation tests have been performed on Cu-OFP under similar conditions of stress and temperature to provide data for modelling the deformation behaviour of copper canisters during long-term service. The initial conditions are about 100 °C and 100 MPa; these values will gradually decrease during service. This means that the canisters are expected to deform by *power-law creep*, a deformation mechanism which is diffusion-controlled. The stress to elastic modulus ratios (σ/E) associated with power-law creep are values of less than 1.26×10^{-3}. The tests were carried out at appropriate temperatures, but some of the stresses were marginally too high resulting in σ/E values greater than 1.26×10^{-3}. Lower σ/E values at suitable temperatures would result in creep tests too long to be accommodated in a research project. For future creep testing it would be better to select a σ/E value appropriate to service conditions rather than a suitable temperature. The steady-state creep rate at 100 MPa /100°C was estimated to be 5×10^{-10} per hour.

Stress relaxation tests at 75 to 150 °C showed that the initial stress relaxation rate is rapid; the stress falls by at least 30% within the first 200 hours.

Tensile tests have been performed at various strain rates at temperatures up to 600°C. Unlike oxygen-free high purity copper (Cu-OF), no reduction in ductility was seen with decreasing strain rate or increasing temperature. This makes Cu-OFP the better canister material in terms of mechanical integrity.

1. INTRODUCTION

Spent nuclear fuel in Sweden is to be disposed of by being placed in cylindrical canisters made entirely or partly of copper. The canisters are to be buried in granite, surrounded bentonite clay and will experience an initial maximum stress of 100 MPa and maximum temperature of 100 °C. They must remain intact for more than 100,000 years. Results of a previous investigation [B1] indicated that poor ductility can result from a large grain size and/or lack of control of the sulphur content in oxygen-free copper. Specimens of Cu-OFP appeared to be more tolerant of impurities like S and exhibited a large creep elongation (about 40%) when tested at temperatures above 200 °C. Cu-OFP therefore seemed to be the more suitable canister material. However, no creep tests had been performed on Cu-OFP below 200 °C and there was no information on stress relaxation at the service temperature or the elevated temperature tensile properties. The results of these tests are reported here.

This progress report is divided into four parts as specified by SKB in contract number 912560, dated 91-11-21.

Part A Creep of Cu-OFP above 200 °C

Part B Creep of Cu-OFP below 200 °C

Part C Stress relaxation below 200 °C

Part D Tensile testing up to 600 °C

The chemical analysis of the Cu-OFP investigated is given below in grammes per tonne.
P 50, Ag 12, Al 2, As 2, Bi <1,Cd <1, Co <10, Cr <3, Fe 7, H <0.10, Hg <1, Mn <1, Ni 4, O 0.9, Pb <1, S 6, Sb 4, Se 2, Si <1, Sn <3, Te <3, Zn <1, Zr <3.
The grain size was 45 μm. The Cu-OFP was manufactured by Outokumpu Poricopper Oy, Finland and supplied in the form of 10 mm diameter bars which had been hot extruded at 800 °C.

Part A
Continuation of creep tests above 200 °C

Experimental

Creep tests were performed under constant load in air in uniaxial tension on cylindrical specimens with a 5 mm diameter and a 50 mm gauge length. Deformation was measured by extensometers attached to ridges on the adaptors at either end of the specimen. It was assumed that no deformation took place outside the gauge length or in the adaptors. Temperature was monitored by two thermocouples attached to the specimen gauge length.

Results

Specimen 405 (215 °C / 100 MPa) is still under test. At the end of October 92 it had run approximately 17000 hours and reached a strain of 6.5%.
The results of all the creep tests carried out on Cu-OFP above 200 °C are given in the table below. The Larson-Miller parameter, P_{LM}, has been calculated as $P_{LM} = T(12 + \log t_f)$ where T is the temperature in Kelvins.

Test	Temp (°C)	Stress (MPa)	t_f (hour)	ss creep rate (h^{-1})	ss creep rate (s^{-1})	ε_f (%)	P_{LM} (10^3)
401	215	120	7848	4.5×10^{-5}	1.25×10^{-8}	35.5	7.76
402	215	140	1451	2.23×10^{-4}	6.25×10^{-8}	38.5	7.40
405	215	100	--->	2.12×10^{-6}	5.89×10^{-10}	---	---
406	215	160	52	3.0×10^{-4}	8.5×10^{-8}	32.1	6.69
407	215	150	192	1.19×10^{-3}	3.3×10^{-7}	40.7	6.97
410	300	100	220	1.08×10^{-3}	3.0×10^{-7}	44.0	8.22
411	450	30	195	8.9×10^{-4}	2.5×10^{-7}	32.1	10.33
412	250	100	4796	3.58×10^{-5}	9.94×10^{-9}	41.6	8.20
413	250	120	656	5.23×10^{-4}	1.45×10^{-7}	57.6	7.75

Creep curves for the three tests carried out at 100 MPa are given in Figs. A1-A3.

Discussion

See the discussion in part B.

Part B Creep tests below 200 °C

Experimental

Creep tests were performed under constant load in air in uniaxial tension on cylindrical specimens with a 5 mm diameter and a 50 mm gauge length. Deformation was measured by extensometers attached to ridges on the adaptors at either end of the specimen. It was assumed that no deformation took place outside the gauge length or in the adaptors. Temperature was monitored by two thermocouples attached to the specimen gauge length.

Four tests were carried out, as specified below

Test mark	Temp (°C)	Stress (MPa)	Start date
420	150	150	92-01-08
421	100	150	92-01-14
422	75	150	92-01-08
423	100	100	92-01-09

Results

At the time of writing all creep tests were continuing. Specimen 423 has not reached its steady-state creep regime. Graphical representations of strain versus time, log. strain versus log. time and log. strain rate versus strain are given for all four tests in Figs. B1 to B4. An overview of the first 2500 hours is shown in Fig. B5.

Discussion

From Figs. B1 to B4 it can be seen that the tests are still in or have recently finished primary creep. Primary creep of copper has been described by Kouta and Webster [B2] using the following equation:

$$\varepsilon = A \exp(-Q/RT)^k \sigma^n t^k \qquad (B1)$$

where ε is the strain, σ the stress, t the time, Q the activation energy, R the gas constant and T the temperature in Kelvins. A, n and k are constants. For a given creep test at constant stress (equivalent to constant load at low strains and low n values) and constant temperature a plot of log. strain versus log. time should result in a straight line with gradient k. This is shown to be the case in

Figs. A1 to A3 and B1 to B4. The values of k for tests 420 to 423 are 0.24, 0.17, 0.15 and 0.15 respectively and under an applied stress of 100 MPa the values k were 0.15,0.33 and 0.5 at 100, 250 and 300 °C respectively. k has previously been found to increase with increasing stress or temperature, [B2].

At high stresses materials creep by dislocation glide alone (the so-called power law breakdown regime) rather than by diffusional controlled climb or climb plus glide (power law creep) which will occur during service. Frost and Ashby [B3] state that for fcc materials power law creep breakdown occurs at an applied stress to elastic modulus ratio $\sigma/E \sim 10^{-3}$. For copper they give a more specific value of 1.26×10^{-3} and this value is shown on all their deformation mechanism maps. The shear elastic modulus at 300 K, μ_o, is given as 4.21×10^4 MPa [B3] and $d\mu/dT$ is -16.76. Assuming that $\sigma_t / \sigma_s = 2.66$ where σ_t is the tensile stress and σ_s is the shear stress, the σ_s / μ ratio has been calculated for a variety of creep conditions. Values greater than 1.26×10^{-3} indicate power law breakdown, *i.e.* deformation occurs by dislocation glide alone and not by dislocation climb or a combination of glide plus climb.

Test mark	Stress (MPa)	Temp (°C)	T/T_m	σ_s / μ
420	150	150	0.312	$1.44\ 10^{-3}$
421	150	100	0.275	$1.38\ 10^{-3}$
422	150	75	0.18	$1.36\ 10^{-3}$
410	100	300	0.422	$1.00\ 10^{-3}$
412	100	250	0.386	$9.8\ 10^{-4}$
405	100	215	0.36	$9.6\ 10^{-4}$
423	100	100	0.275	$9.2\ 10^{-4}$

The values above indicate that specimens 420 to 422 are not deforming in the power law regime but the other specimens are deforming by thermally activated processes. The canisters are initially subjected to conditions of about 100 °C and 100 MPa; the temperature and stress will gradually decrease during service, [B4]. These values are within the power-law creep regime.

Steady-state creep in the power law creep regime can be described by the following equation:

$$\dot{\varepsilon} = A\, \sigma^n \exp(-Q/RT) \qquad (B2)$$

where $\dot{\varepsilon}$ is the creep rate and the other symbols are the same as in Eqn. B1. At constant stress a plot of log. creep rate versus 1/T yields a straight line of

gradient - Q / 2.3 R. Such a plot is given in Fig. B6 for tests 420-422 , which have the same applied stress of 150 MPa. From Fig. B6 Q, the activation energy, has been calculated as 30 to 40 kJ / mole. Typical activation energy values of diffusional processes in copper are given by Frost and Ashby [B3];

Q for lattice (volume) diffusion, Q_v = 197 kJ / mole

Q for boundary diffusion, Q_b = 104 kJ / mole

Q for core diffusion, Q_c = 117 kJ / mole

A value of 40 kJ / mole indicates that power law creep is not occurring at these stresses and temperatures, which was inferred from the table above. All future creep tests should be carried out with a σ_s / μ ratio of less than 1.26×10^{-3} to ensure that the deformation mechanisms occurring in the laboratory are applicable to those occurring during service.

A graph of log. creep rate versus 1/T was also plotted for a constant stress of 100 MPa. Test 423 was used in the analysis together with specimens 405 (215 °C), 410 (300 °C) and 412 (250 °C). Details of the last three tests can be found in Part A. The resulting graph is shown in Fig. B7. Q for the three highest temperatures was found to be close to 197 kJ/mole, which corresponds to volume diffusion. (See Fig. B7). The datum point corresponding to specimen 423 does not fall near the other 3, which indicates that a steady-state creep rate has not yet been reached. The steady-state creep rate can be estimated from Fig. B7 by extrapolation; if deformation is controlled by boundary diffusion the creep rate will be about 5×10^{-10} per hour. Extrapolation of Fig. B4 indicates that this will occur at about 5% strain and 900 years. If the deformation is controlled by volume diffusion, the creep rate will be even lower.

References

B1 Henderson, P. J., Österberg, J.-O. and Ivarsson, B. G. "Low Temperature Creep of Copper Intended for Nuclear Waste Containers" Institute of Metals Report IM-2780 (Oct 1991) and SKB Technical Report 92-04 (March 1992)

B2 Kouta, F.H.H. and Webster, G.A. "Creep Behaviour of 99.85 pure copper" First Int. Conf. on Current Advances in Mechanical Design and Production Pergamon Press, Oxford (1981)

B3 Frost, H. J. and Ashby M. F. "Deformation Mechanism Maps - The Plasticity and Creep of Metals and Ceramics" Pergamon, Oxford (1982)

B4 Josefson, L. "Creep deformation and void growth in copper canisters for spent nuclear fuel". 1992-06-22.

Part C Stress Relaxation

Experimental

The stress relaxation tests were performed in servo-hydraulic machines on cylindrical specimens which were 60 mm long with a 25 mm gauge length and ridges for extensometry. A drawing of the specimens is given in Fig. C1. The strain was controlled by Super Linear Variable Capacitance (SLVC) transducers located outside the furnace at the lower end of the extensometer limbs. SLVC transducers have good long term stability and the error in the strain control was less than $\pm$ 0.3% (apart from the first test no. 12). This is 0.3% of the total strain on the specimen (*e.g.* 0.3%x0.2%) and not a strain of 0.3% . The temperature was controlled to within $\pm$ 1 °C and this represents the largest source of error. (With an initial constant strain of 0.2 % and taking the coefficient of thermal expansion to be 17×10^{-6} one degree change in temperature gives rise to an error of 0.8%). Fluctuations in the load readings are due to fluctuations in the load cell output and not a real variation in load. The source of this error has now been traced.

The first two tests (nos. 12 and 25) were carried out at 75 and 100 °C with an initial stress of 100 MPa. The specimens were loaded slowly until 100 MPa was reached, then the strain was held constant and the stress decay monitored. However, it is likely that stress relaxation was occurring during loading so the strain levels are much higher for these two tests than for the subsequent ones. The remaining tests (21, 18 and 13) were loaded rapidly to a strain level corresponding to an elastic stress of 150,150 and 250 MPa respectively. Three tests were performed on specimen no. 18. The first, 18-1 was performed on the as-received material and was terminated by a power failure, 18-2 was a continuation after the power failure and the third test performed on the same specimen was in compression, 18-3. The tests are detailed in the table below.

Test mark	Temp (°C)	Strain (%)	Initial Stress (MPa)	Notes
12	75	0.4	100	slow loading
25	100	0.3	100	slow loading
21	100	0.12	150 (elastic)	
18-1	75	0.12	150(elastic)	
18-2	75	0.12		restarted after power failure
18-3	75	?		in compression
13-1	150	0.2	250 (elastic)	
13-2	150	0.2		restarted after power failure

Results and Discussion

Plots of stress versus time for all the tests are shown in Figs. C2-C10. At 75 °C the stress drops by about 30 % of its original value within the first 200 hours. At higher temperatures the stress relaxation is slightly greater. During relaxation elastic strain is converted into plastic strain. The total strain remains constant. Therefore:

$$d\sigma/Edt + d\varepsilon/dt = 0 \qquad (C1)$$

where $d\sigma/Edt$ is the elastic strain rate (negative) and $d\varepsilon/dt$ the plastic strain rate (positive). Plots of strain rate versus time for Tests 18-1 and 21 are displayed in Figs. C11 and C12. Fig. C13 gives the variation of strain rate with time for all the stress relaxation tests. The strain rates are remarkably similar for all the tests and do not appear to depend on temperature or initial stress.

Part D
Tensile testing up to 600 °C

Experimental

The tensile tests were performed in a servo-hydraulic machine on cylindrical specimens which were 60 mm long with a 25 mm gauge length and ridges for extensometry. A drawing of the specimens is given in Fig. D1. The strain was recorded by Super Linear Variable Capacitance (SLVC) transducers located outside the furnace at the lower end of the extensometer limbs. Tests were carried out from room temperature to 200 °C at strain rates of 10^{-2} to 10^{-5} per second and from room temperature to 600 °C at a strain rate of 10^{-4} per second. The deformation rate was kept constant throughout each test and was not increased after yielding had occurred.

Results and Discussion

A summary of all the results is given in Table D1. Some important results are displayed graphically in Figs. D2 to D12 . Figs. D2 to D5 show the stress -strain curves up to 5 % for tests performed at 26, 100, 150 and 200 °C respectively at a number of different strain rates. There is obviously something unusual about the test performed at 26°C/ 10^{-4} per sec (see Fig. D2), probably due to prior plastic deformation, so the values of the 0.2% and 1% proof stresses (Rp0.2 and Rp1.0) from this test have been omitted in the other figures. The ultimate tensile strength (Rm) was not affected. The proof stresses and the tensile strength up to 200 °C at 10^{-3} and 10^{-5} per second are shown in Figs. D6 and D7 respectively. The proof stresses are unaffected by temperature up to 200 °C, but there is a monotonic decrease in Rm, due to a decrease in work hardening. The same behaviour is shown in Fig. D8 where the strain rate is 10^{-4} per second.

Figures D9 to D11 show the effect of strain rate. There appears to be a slight increase in the proof stresses at high strain rates. Ductility was unaffected by strain rate and showed a slight increase with increasing temperature. Fig. D12 shows the elongation at fracture with respect to temperature; there is no drop in ductility at higher temperatures as seen in oxygen-free high purity copper (see Fig. D13). This is an important result as it indicates that Cu-OFP is unlikely to suffer from the low creep ductility displayed by Cu-OF in a previous investigation, [D1].

The values of the 0.2% proof stress at room temperature are slightly greater than the value of the yield strength (*i.e.* 46 MPa) quoted by the manufacturer, [D1]. However, copper has no well-defined yield point and the 0.1% proof stress may have been taken to represent yield. The values of the ultimate tensile strength

are in agreement with the manufacturer's value of 239 MPa.

Reference

D1 Henderson, P. J., Österberg, J.-O. and Ivarsson, B. G. "Low Temperature Creep of Copper Intended for Nuclear Waste Containers" Institute of Metals . Report IM-2780 (Oct 1991) and SKB Technical Report 92-04 (March 1992)

CONCLUSIONS

Creep, stress relaxation and tensile tests have been carried out on oxygen-free phosphorus copper,(Cu-OFP). At 100 °C and 100 MPa,(the maximum anticipated service temperature and stress) creep deformation is controlled by diffusional processes. The steady-state creep rate has been estimated to be about $5x10^{-10}$ per hour. For all future creep testing the stress to elastic modulus ratio should be kept below 1.26×10^{-3} to ensure that deformation is diffusion-controlled.

Stress relaxation tests showed that the initial stress in constrained Cu-OFP fell by about 30 % within the first 200 hours at 75°C. This reduces the risk of deformation due to residual stresses.

Tensile testing revealed that Cu-OFP displayed excellent ductility (~40%) which did not vary with strain rate or temperature. This is in contrast to oxygen-free high purity copper in which ductility falls to a low level with decreasing strain rate or increasing temperature. Cu-OFP is therefore more suitable as a canister material as it less likely that cracking will occur at low strains because of deformation during service.

ACKNOWLEDGEMENTS

This project was entirely funded by SKB AB, Sweden's Nuclear Fuel and Waste Management company and the copper was supplied by Outokumpu Poricopper Oy, Finland. Lars Werme (SKB) and Rolf Sandström (IM) are thanked for their helpful comments.

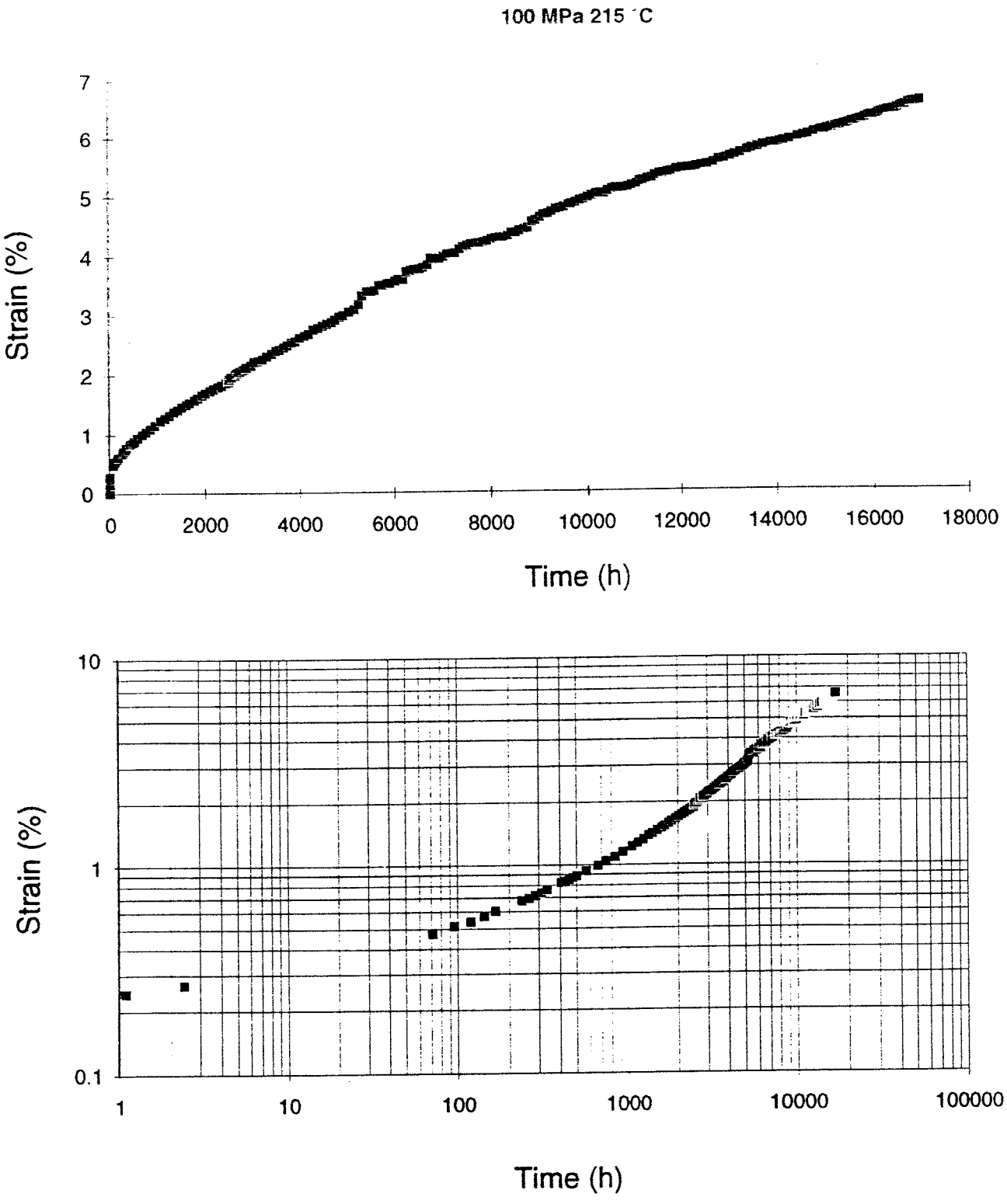

Fig. A1 Creep curves for specimen 405

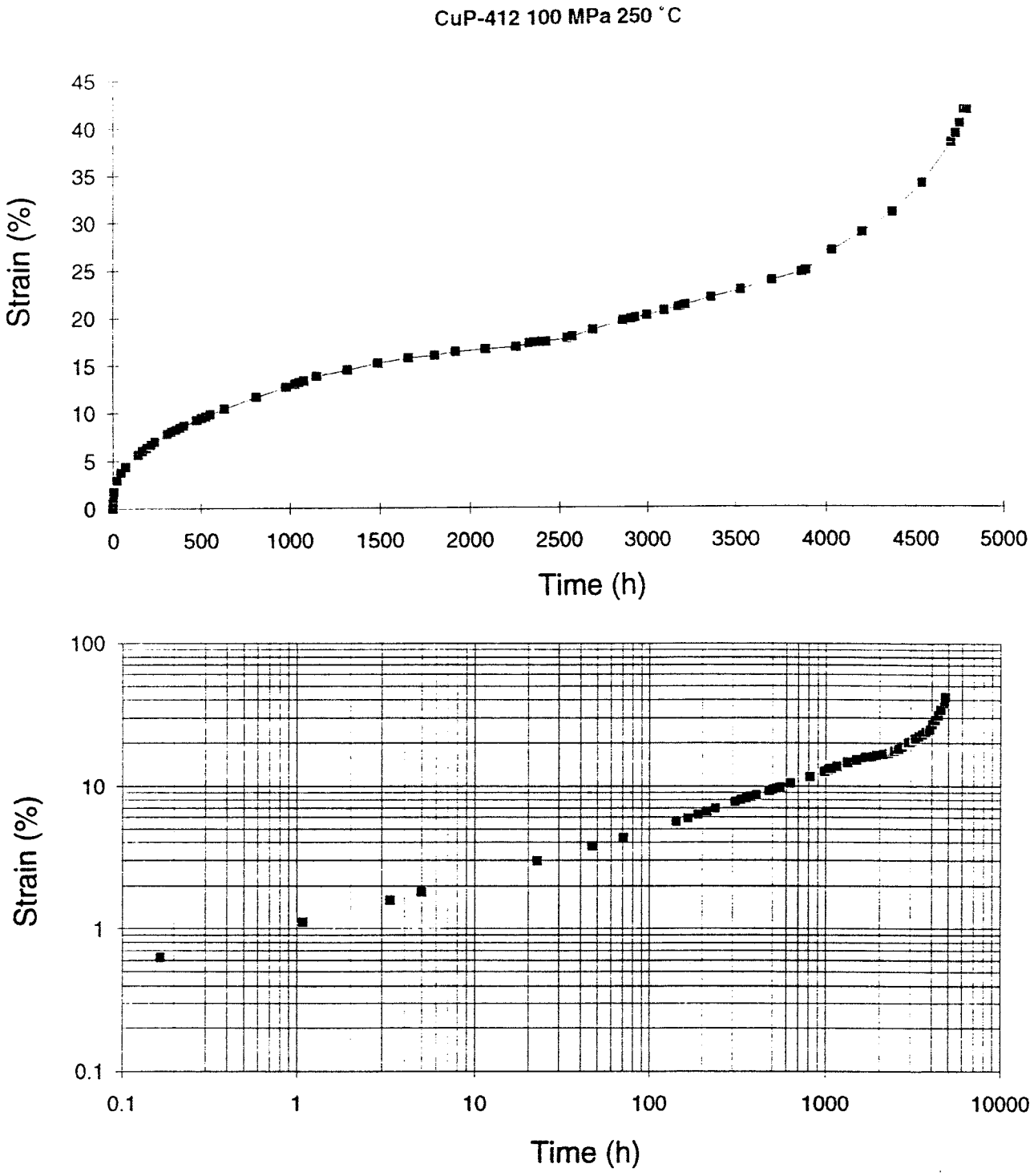

Fig. A2 Creep curves for specimen 412

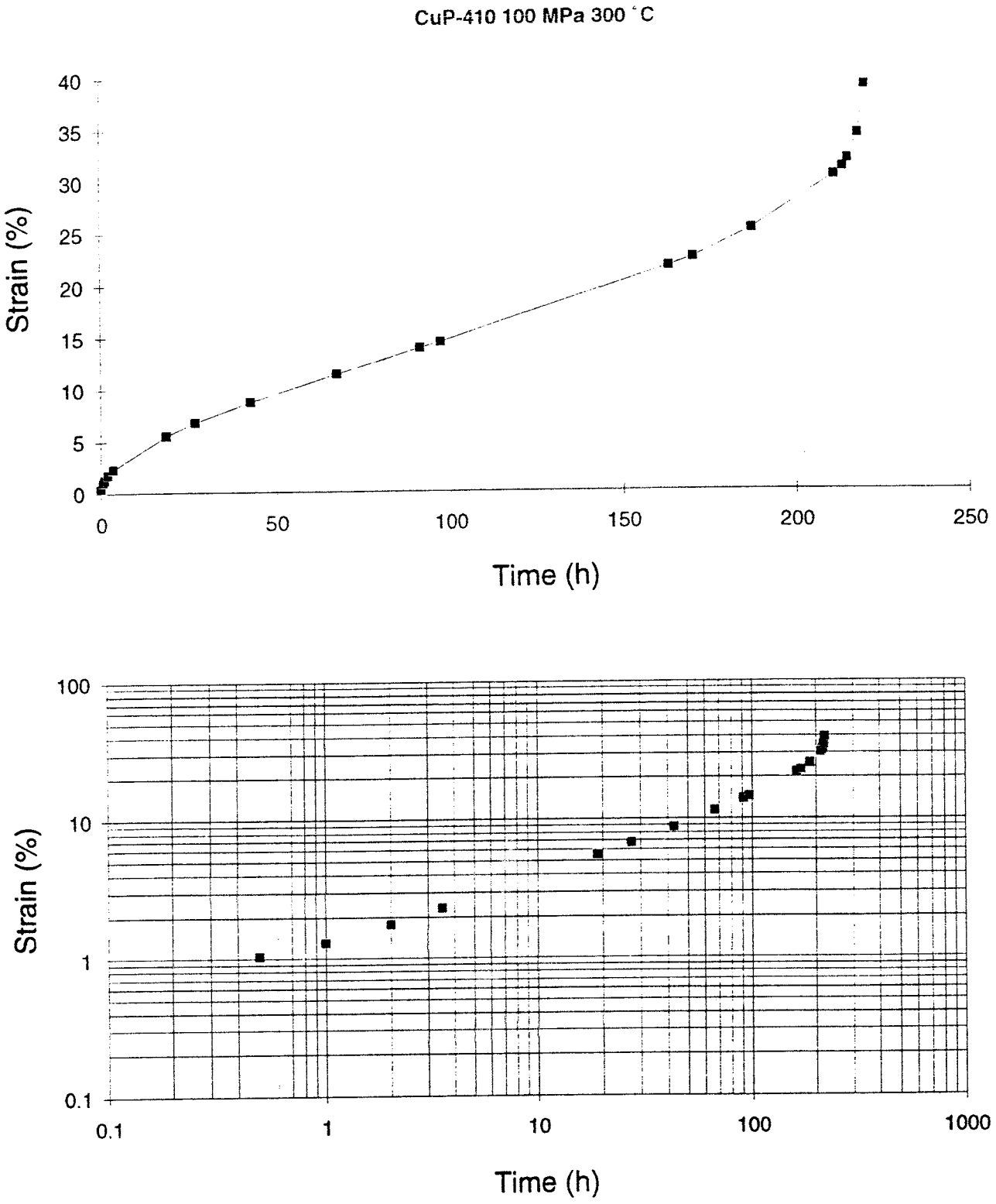

Fig. A3 Creep curves for specimen 410

Fig. B1 Creep results for specimen 420

150 °C/ 150 MPa

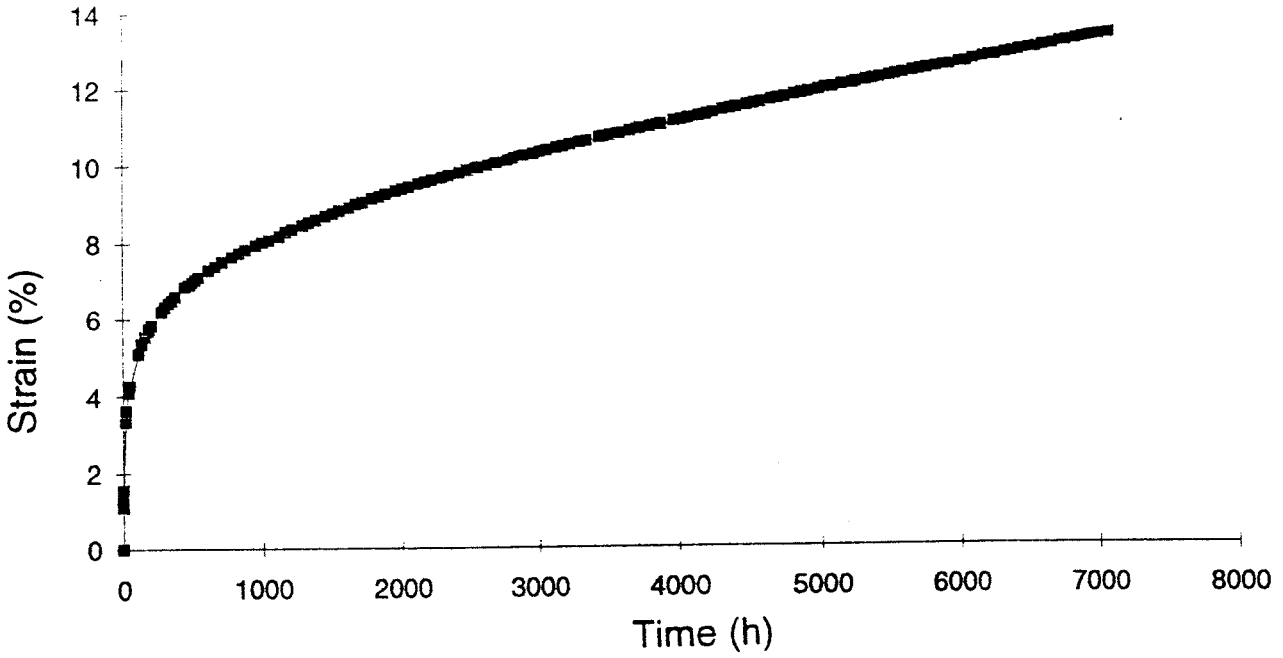

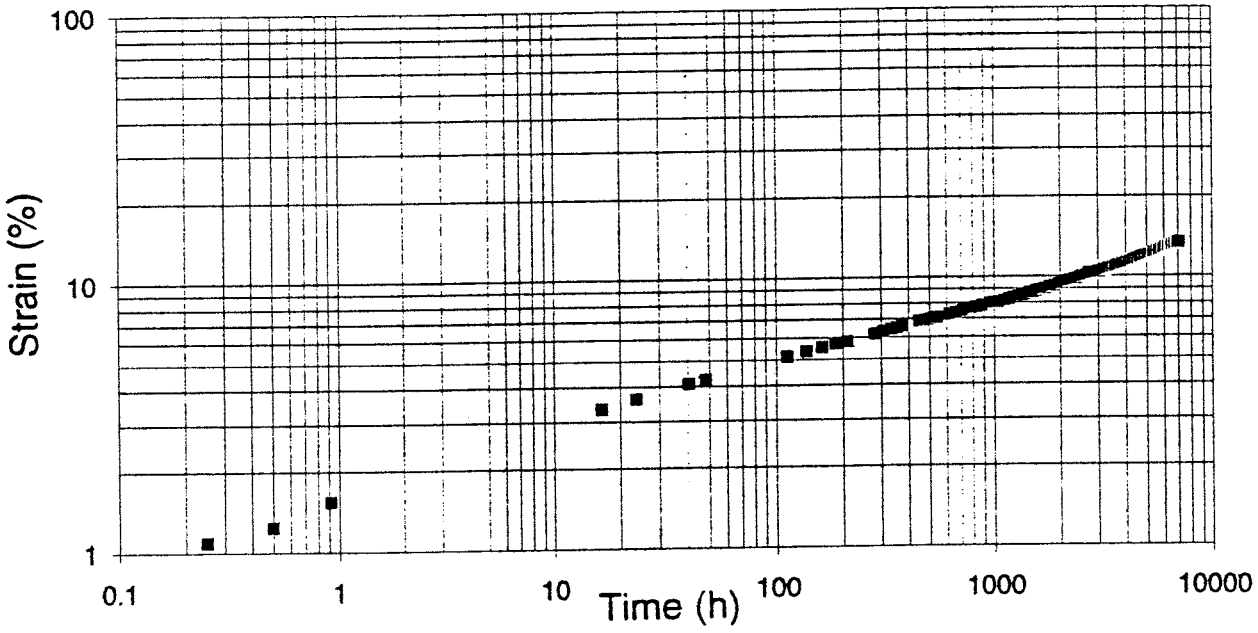

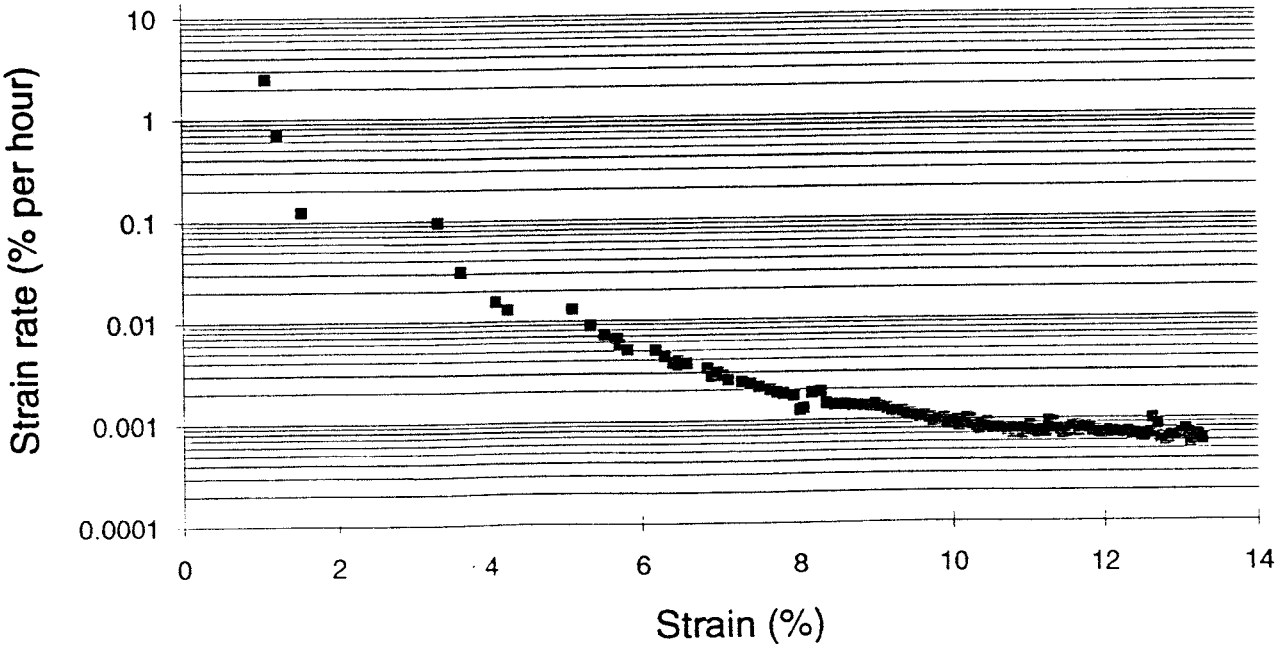

Fig. B2 Creep results for specimen 421

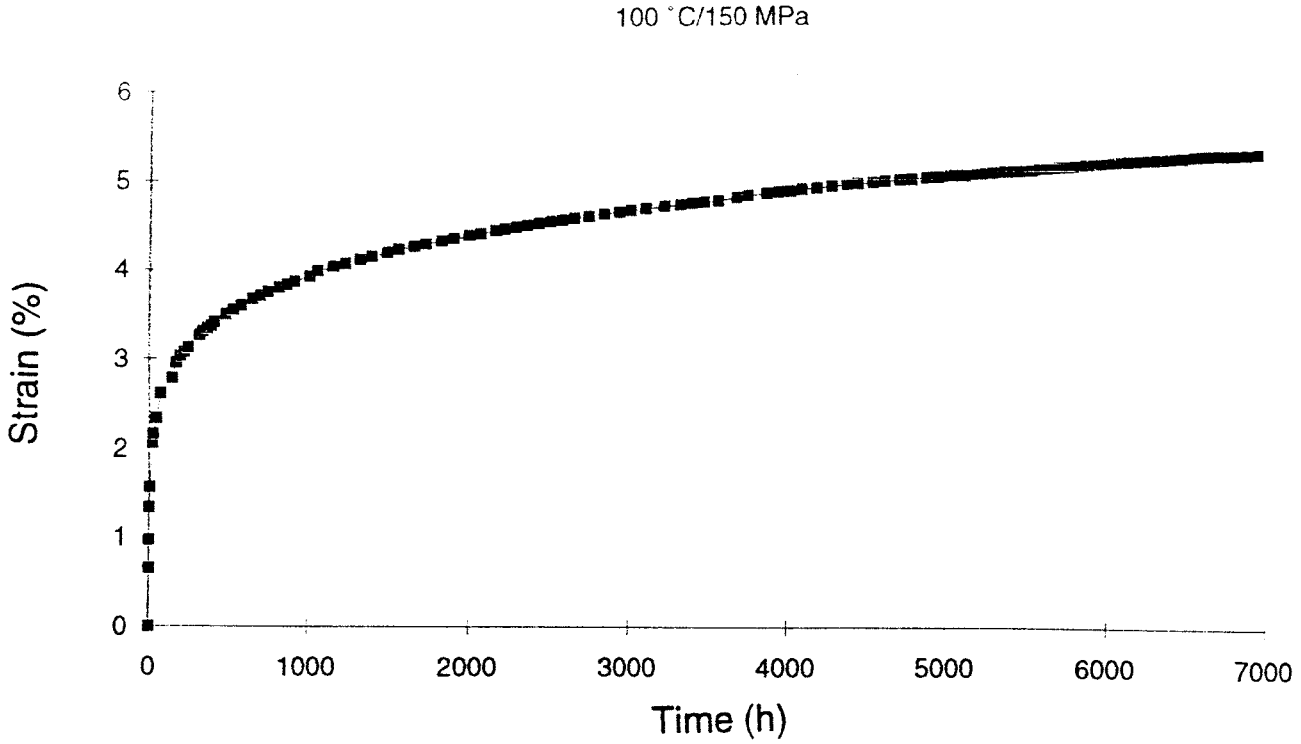

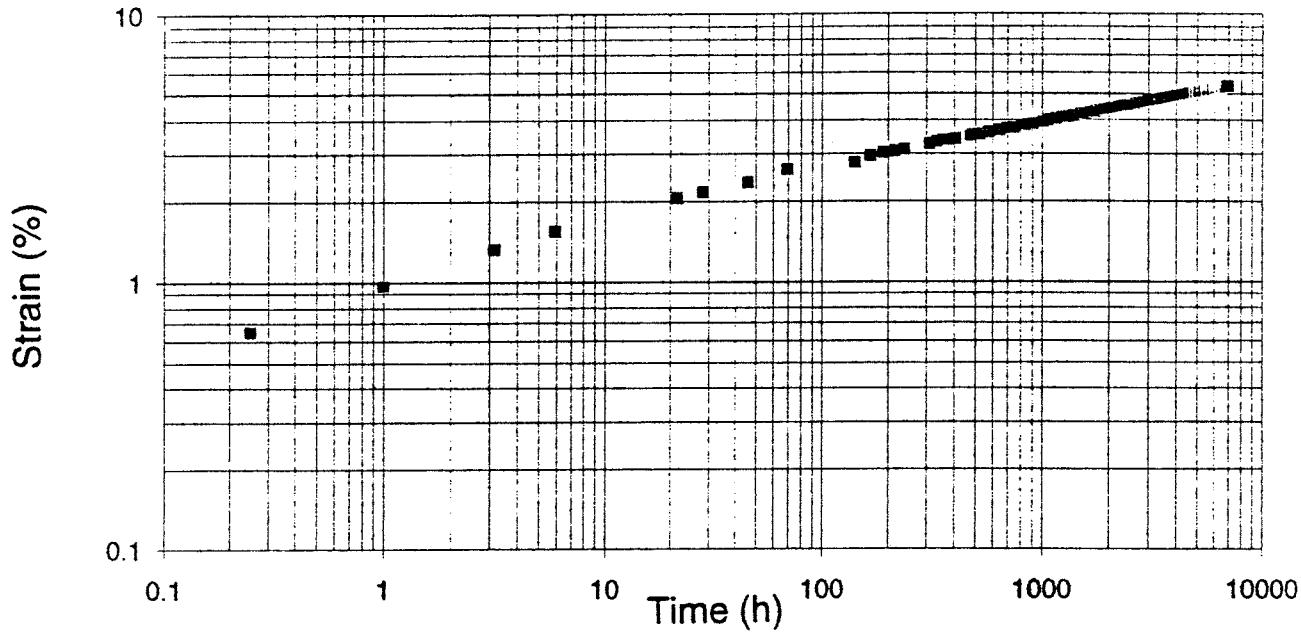

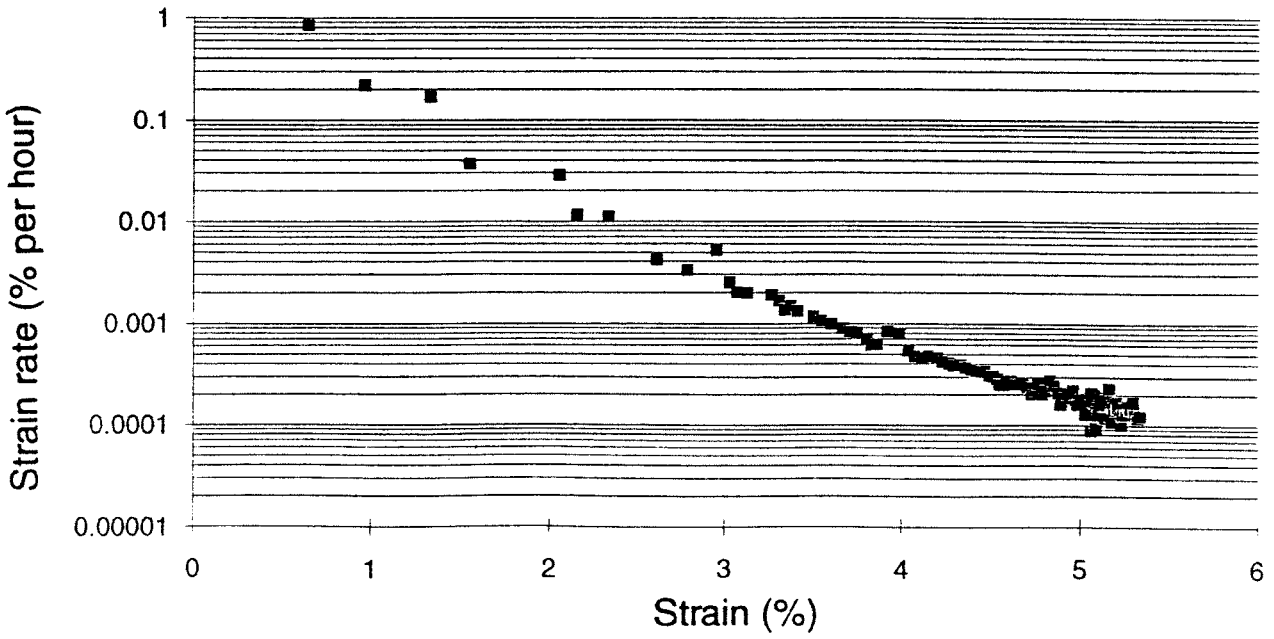

Fig. B3 Creep results for specimen 422

75 °C / 150 MPa

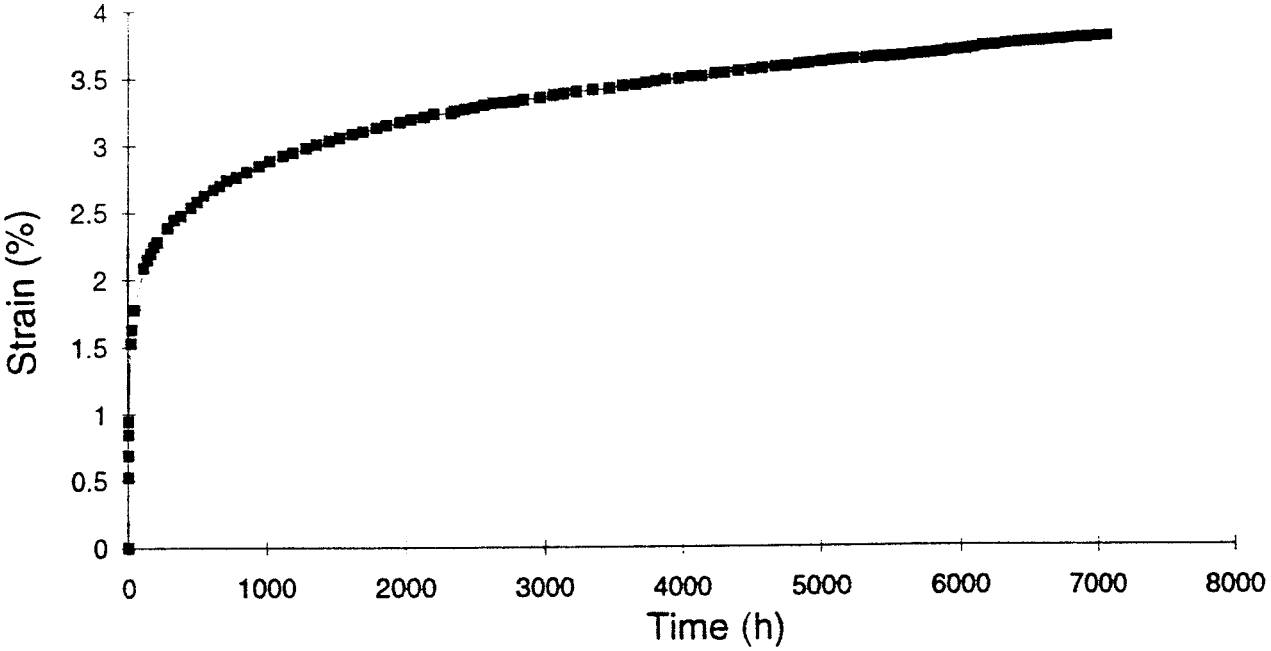

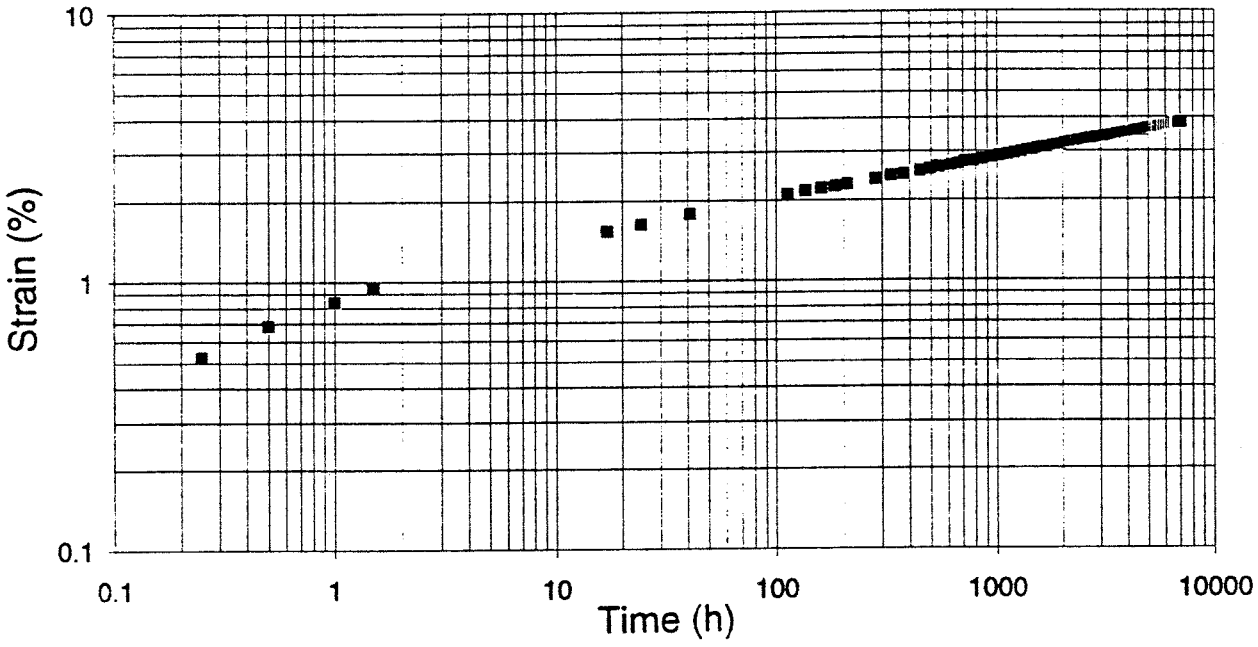

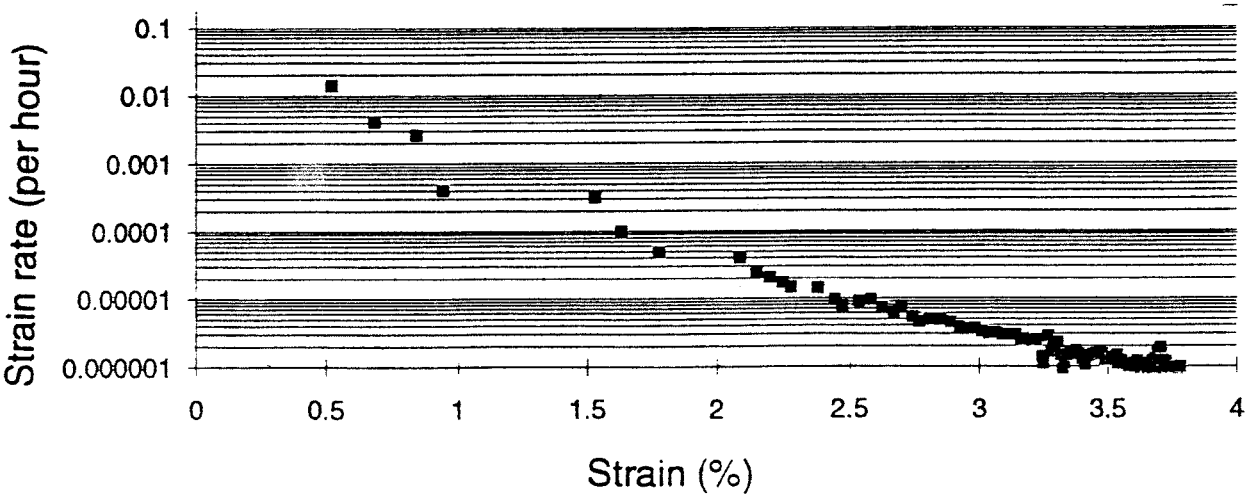

Fig. B4 Creep results for specimen 423

100 °C / 100 MPa

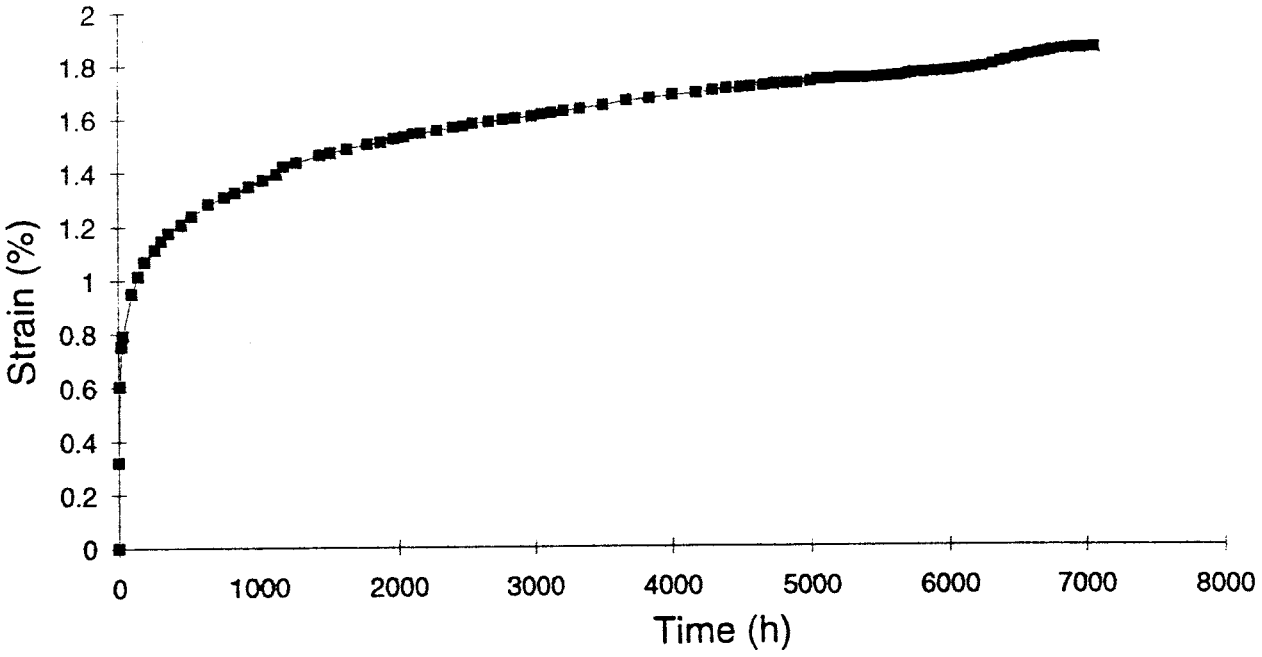

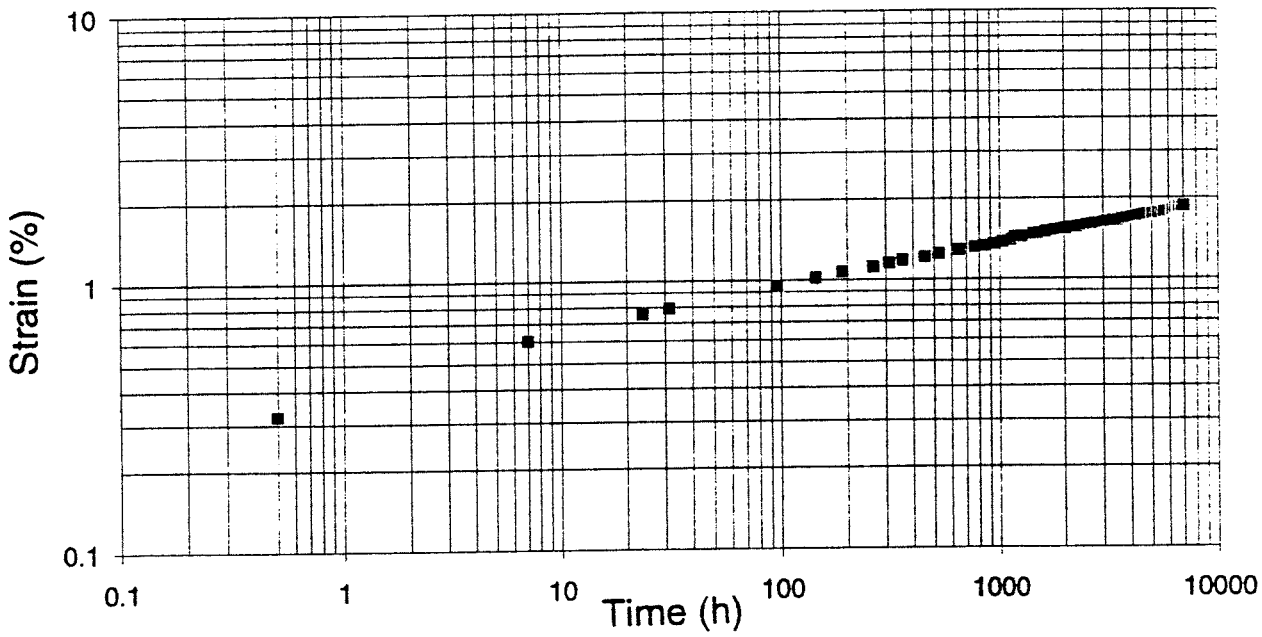

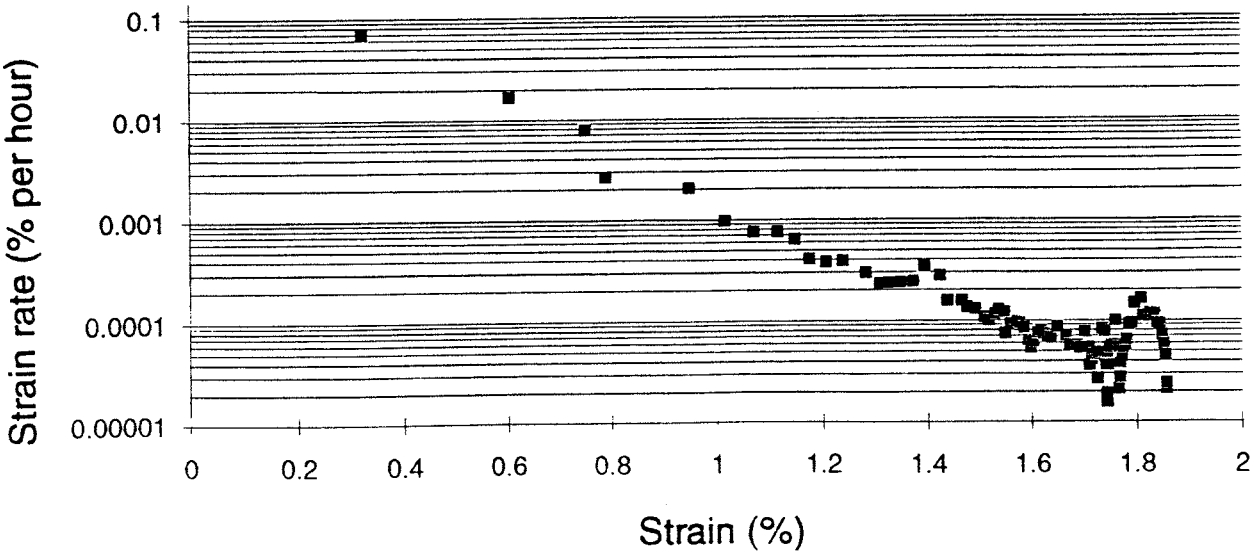

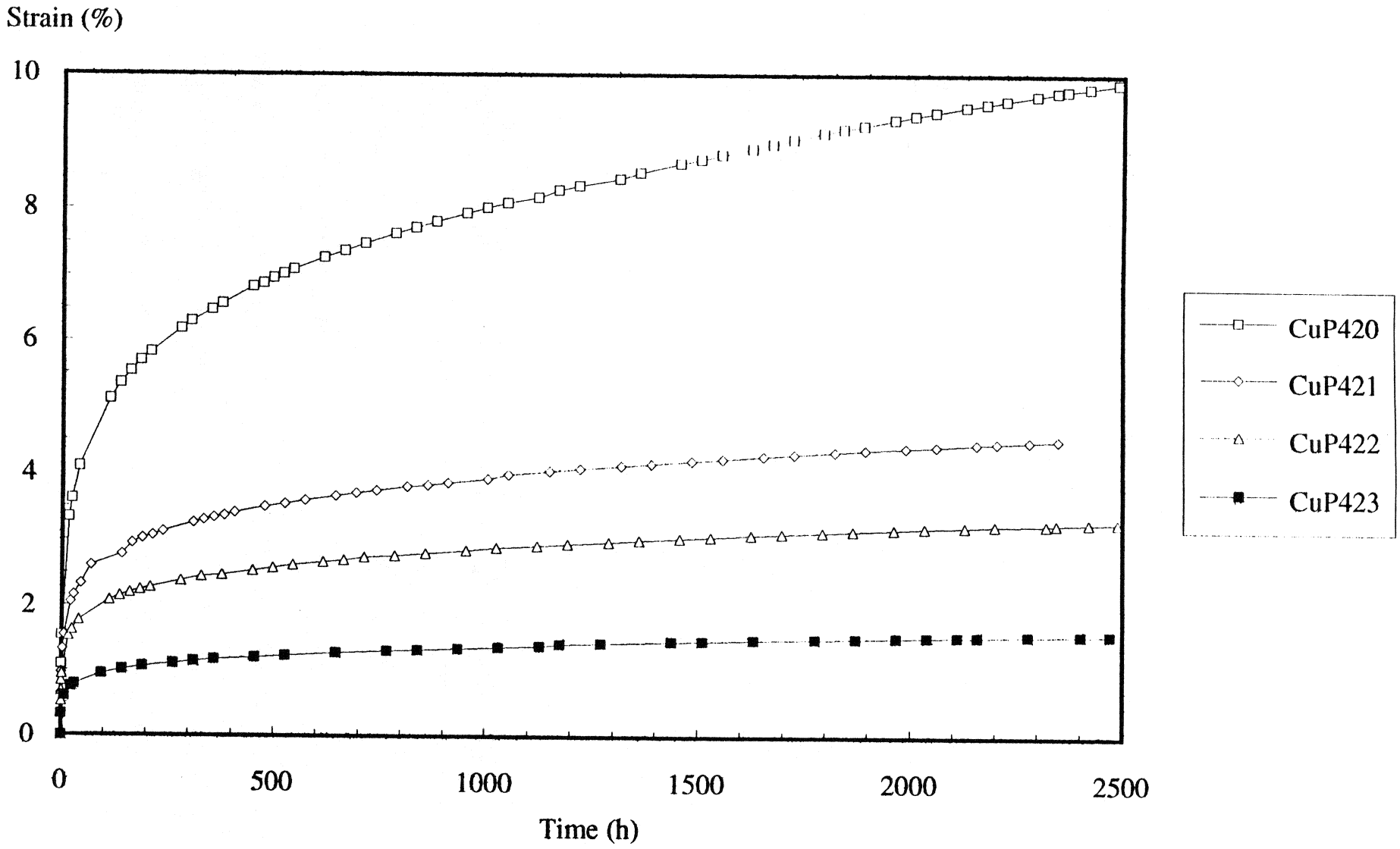

Fig. B5 Creep strain versus time for the first 2500 hours

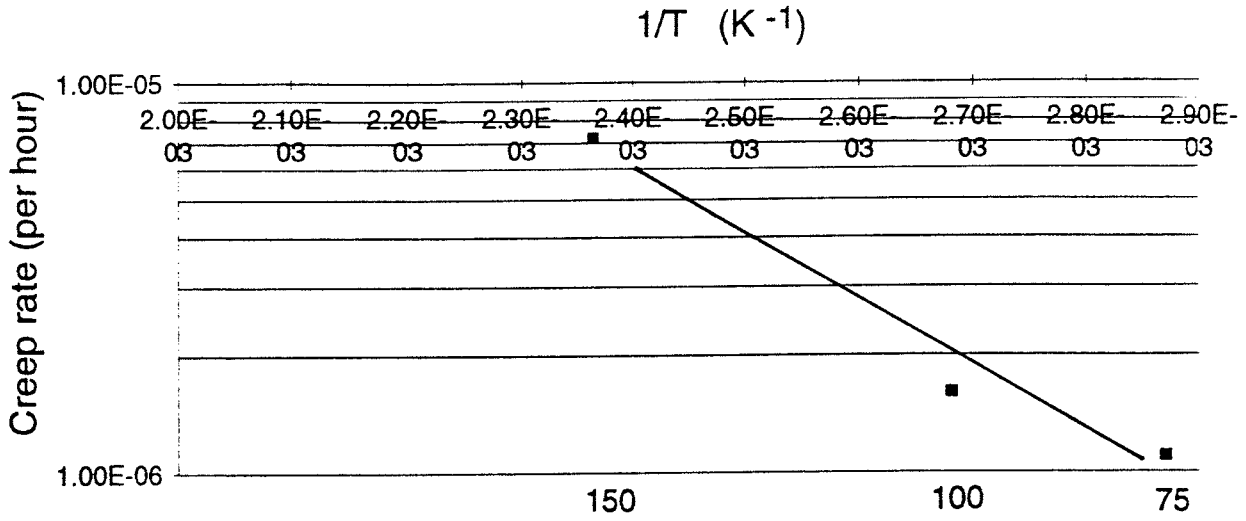

Fig. B6 Relationship between creep rate and temperature at a constant stress of 150 MPa.

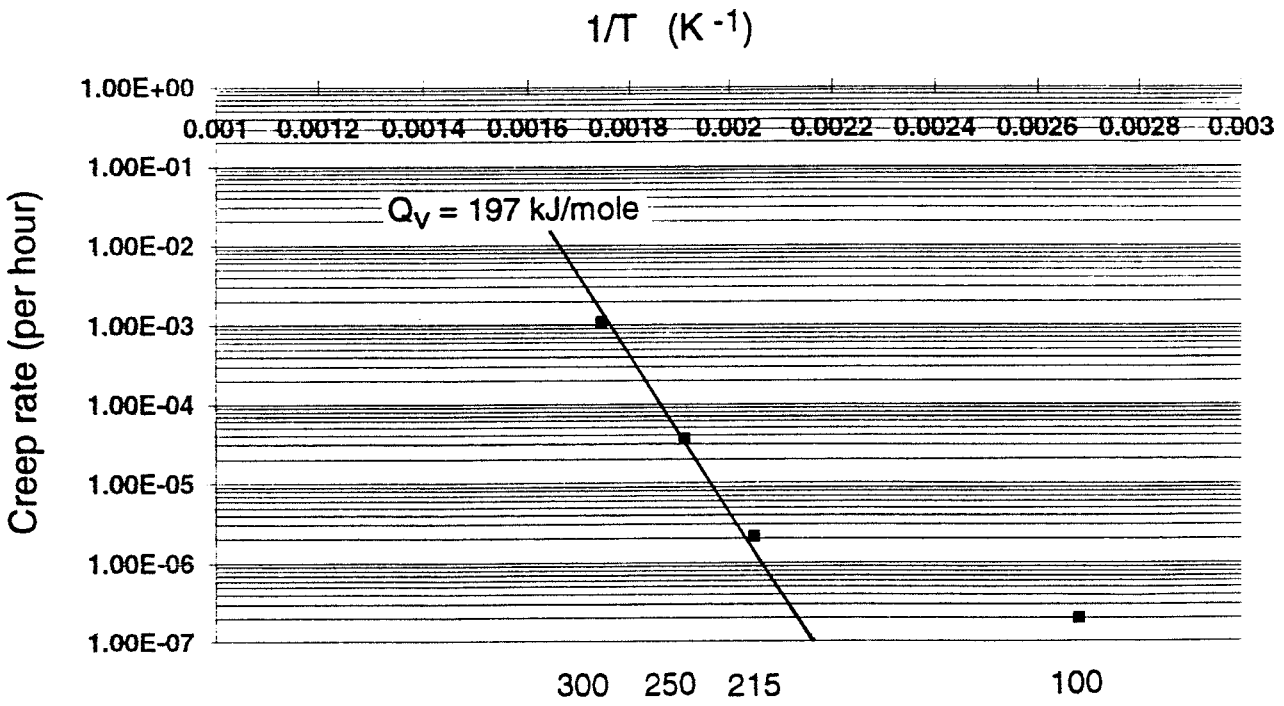

Fig. B7 Relationship between creep rate and temperature at a constant stress of 100 MPa.

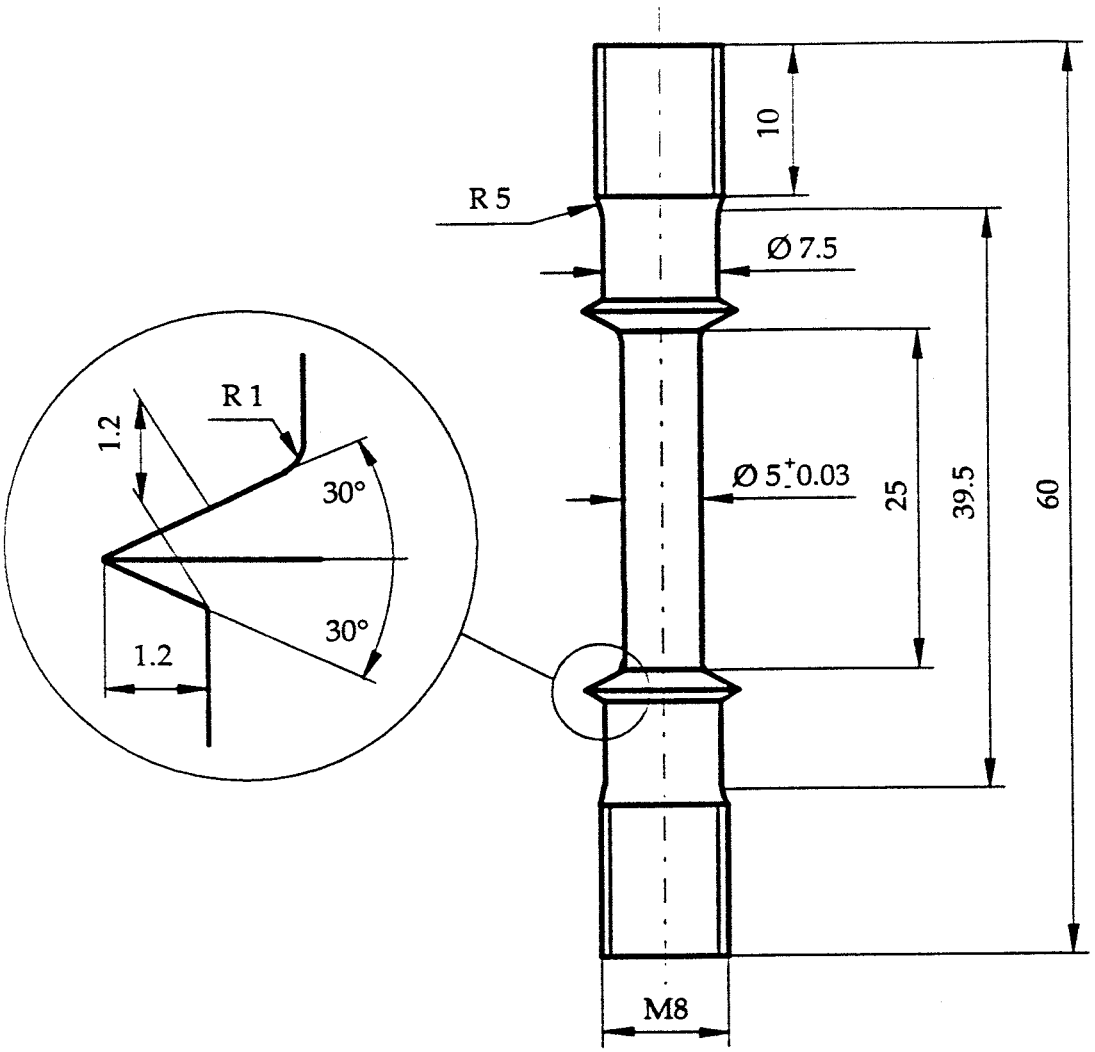

Fig. C1 Drawing of the specimens used for stress relaxation. Dimensions in mm.

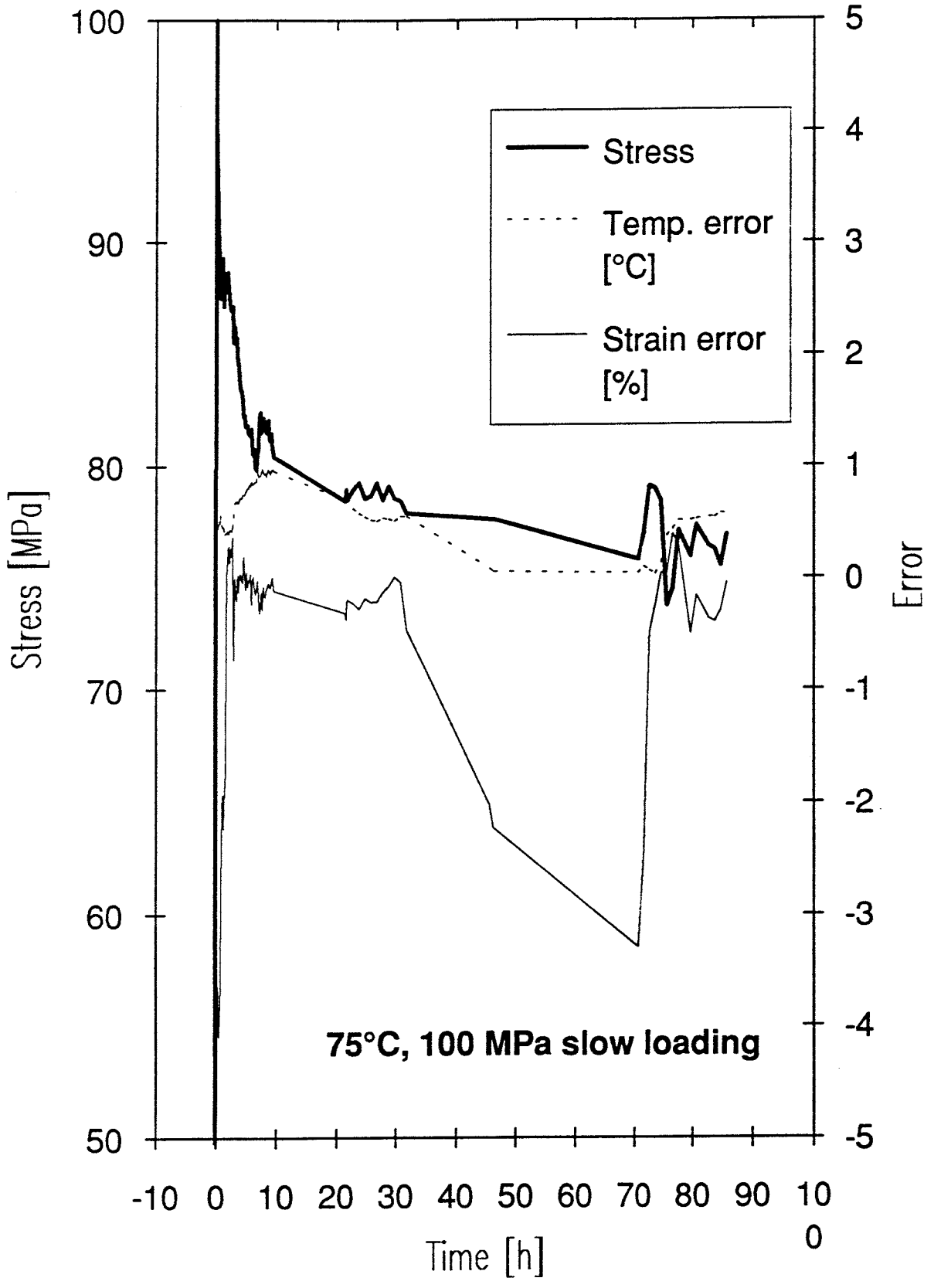

Fig. C2 Plot of stress against time for Test 12, (75°C,initial stress 100 MPa)

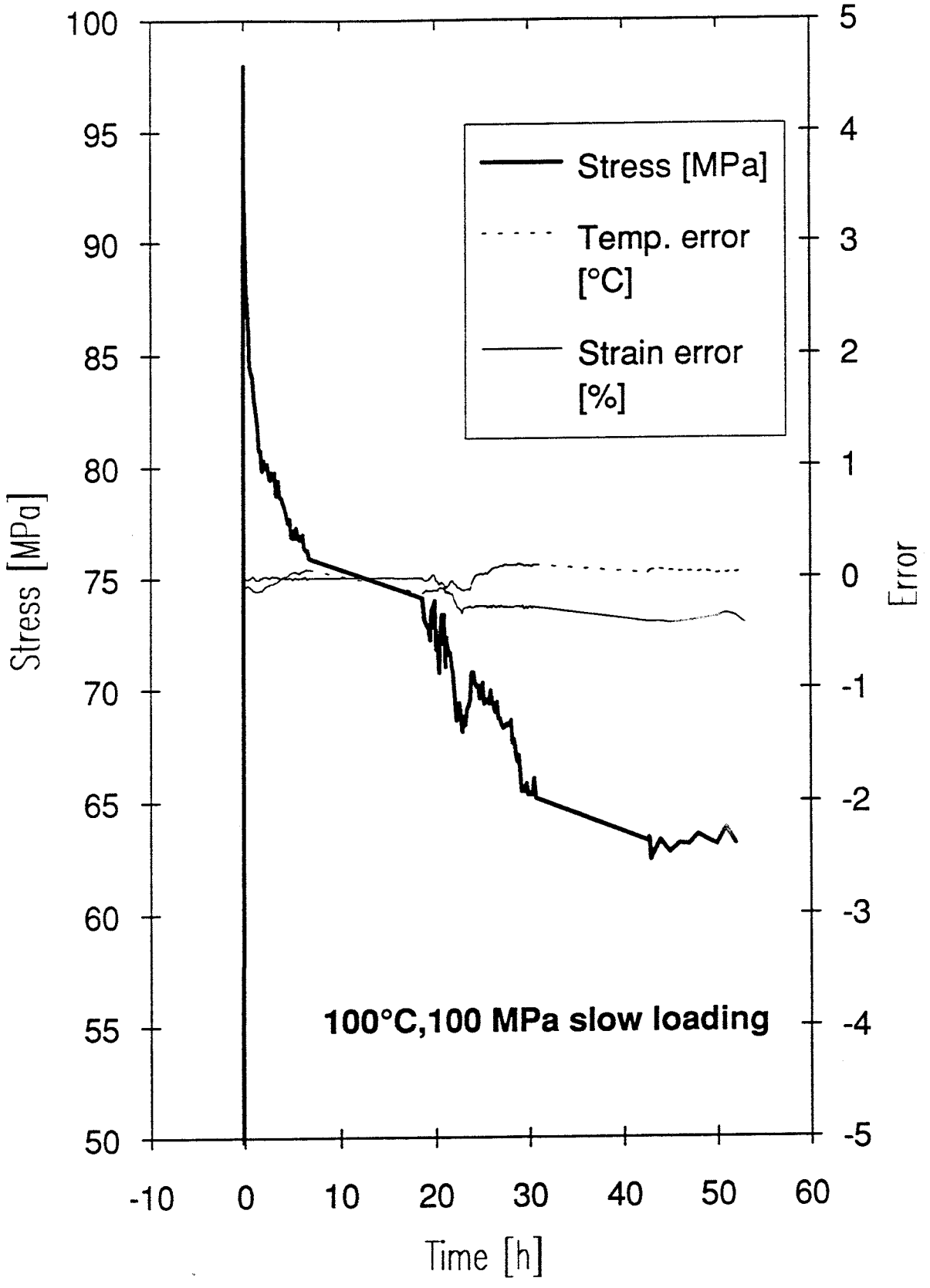

Fig. C3 Plot of stress against time for Test 25, (100°C, initial stress 100 MPa)

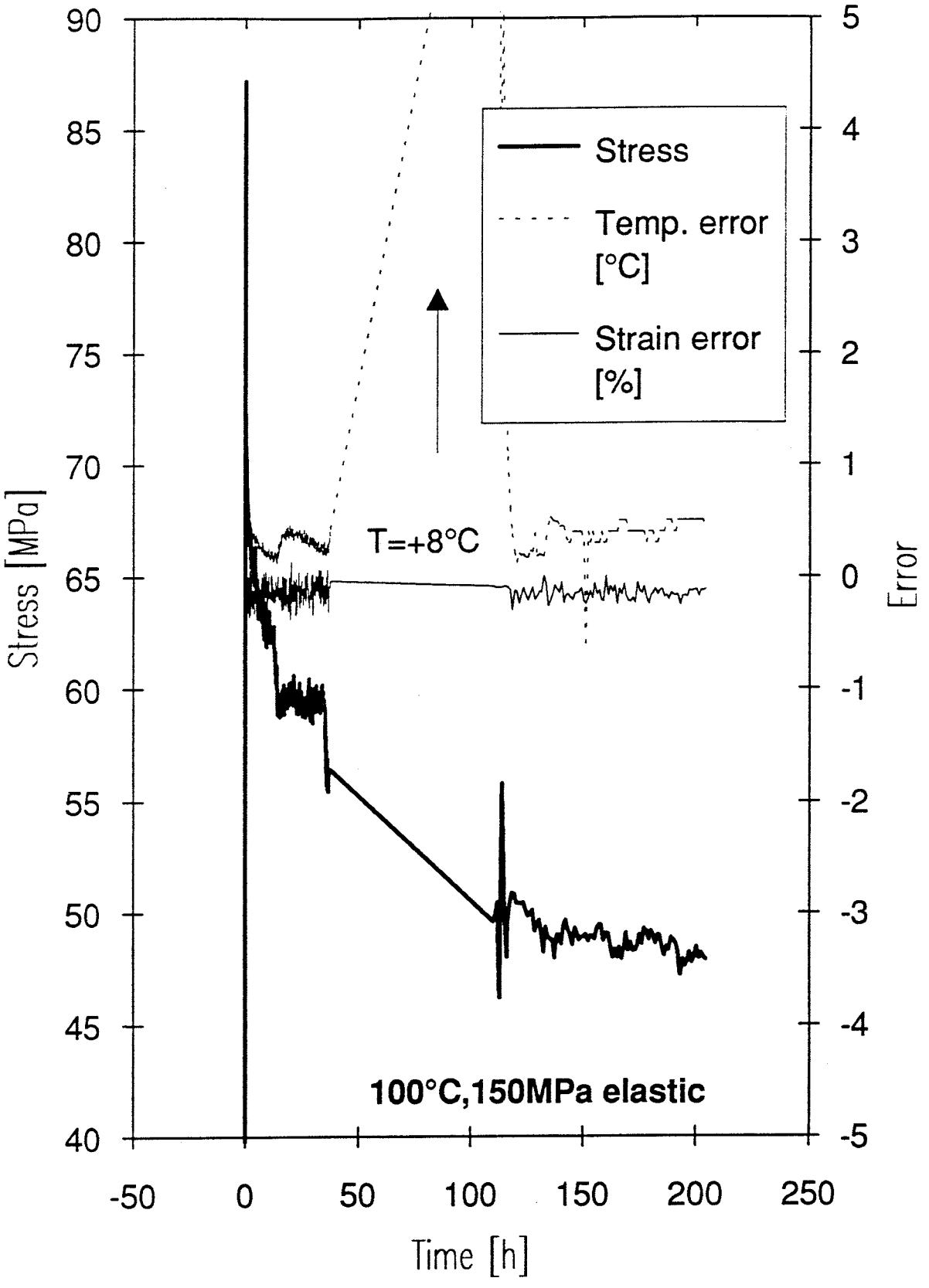

Fig. C4 Plot of stress against time for Test 21, (100°C, initial stress 150 MPa elastic)

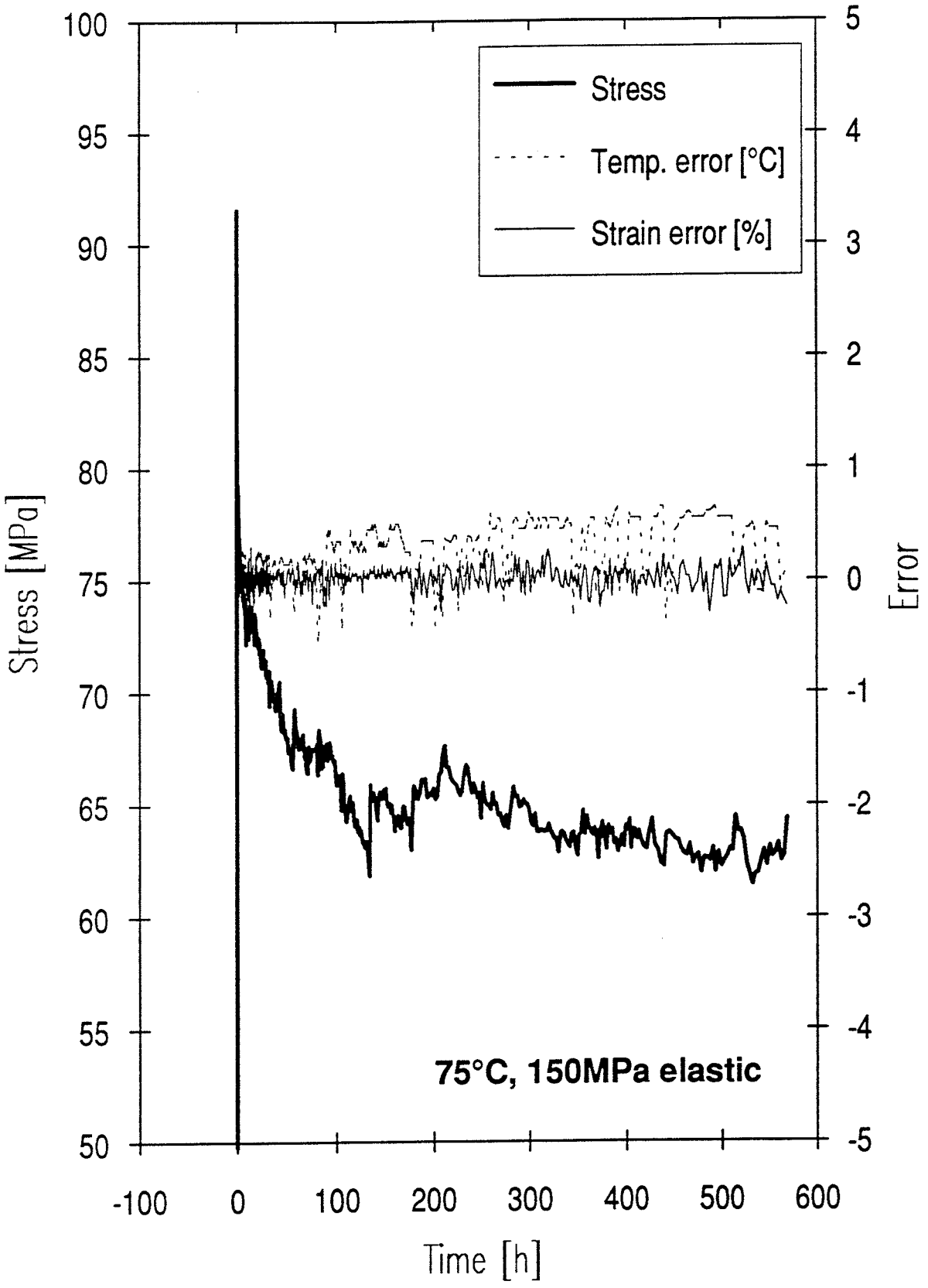

Fig. C5 Plot of stress against time for Test 18-1,(75°C,initial stress 150 MPa elastic)

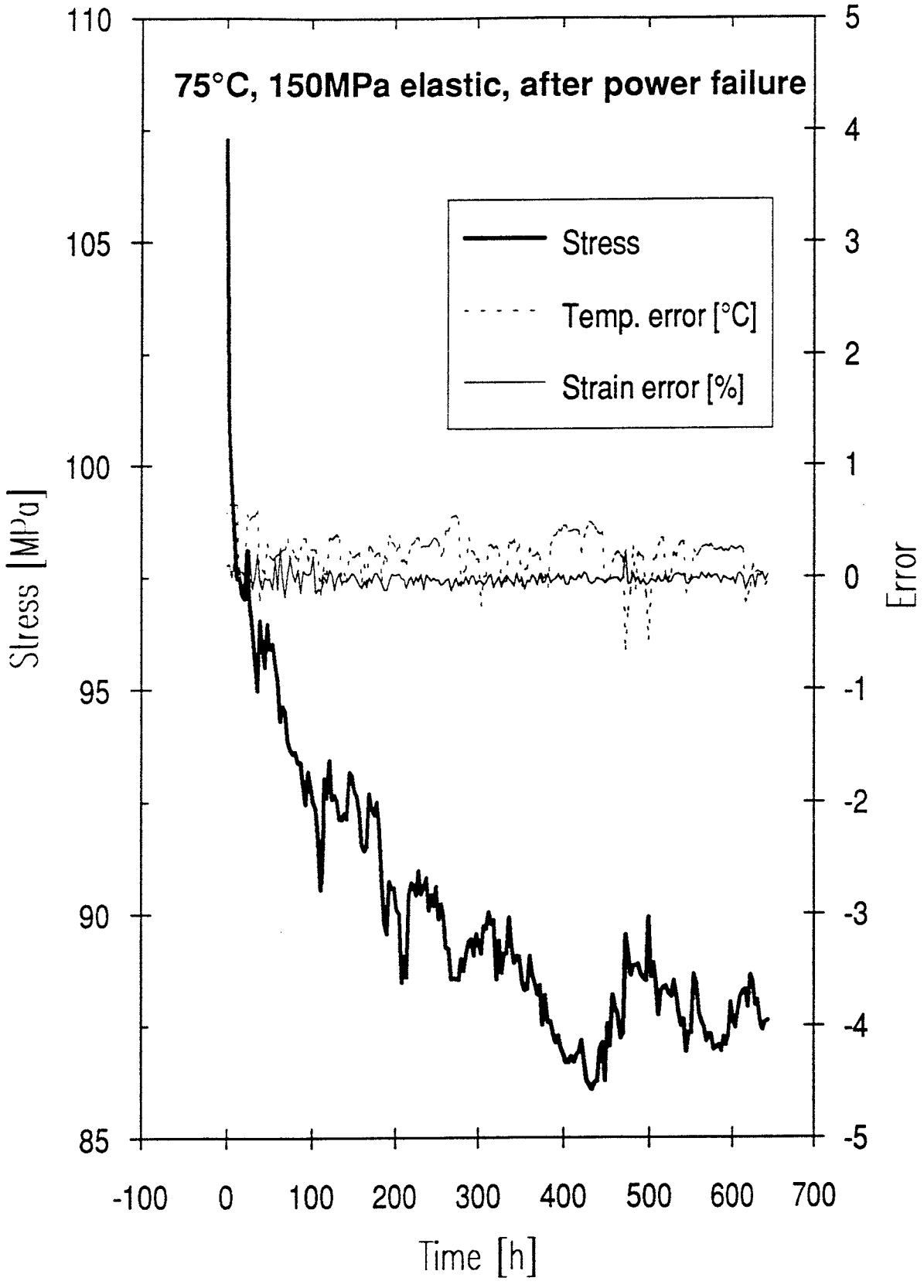

Fig. C6 Plot of stress against time for Test 18-2,(75°C,initial stress 150 MPa)
Continuation of 18-1,re-started after power failure

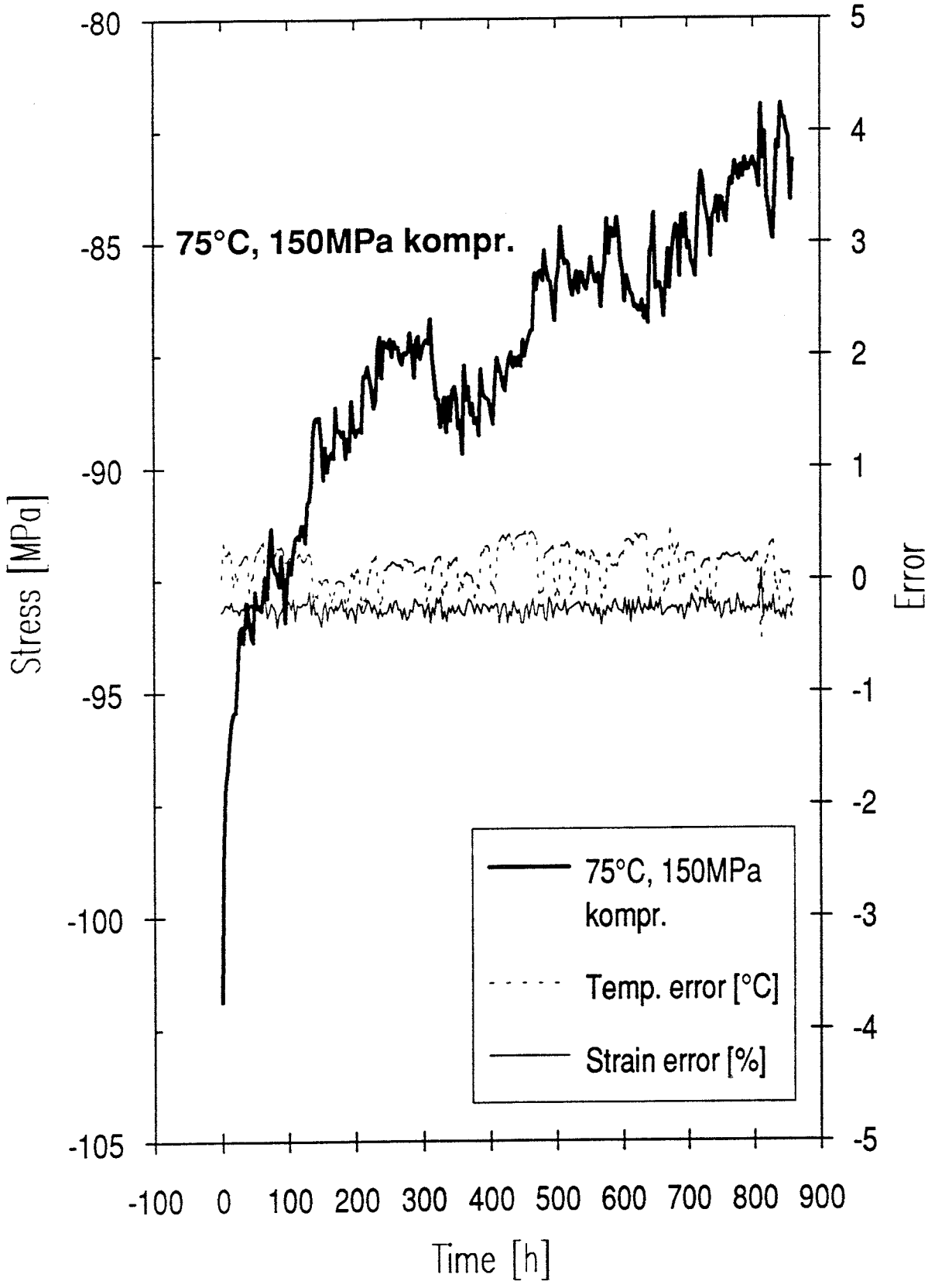

Fig. C7 Plot of stress against time for Test 18-3,(75°C,initial stress 150 MPa) Stress applied in compression

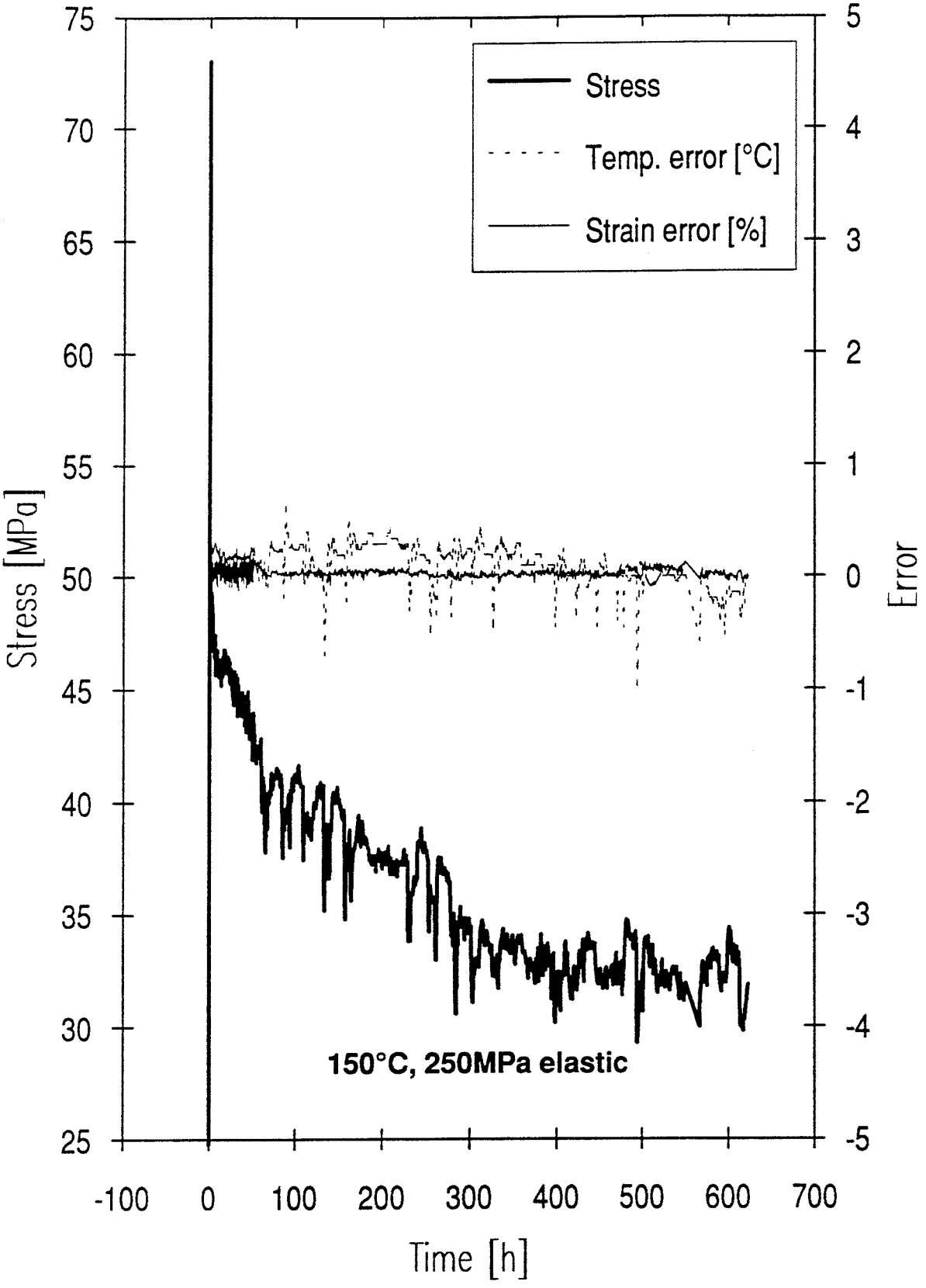

Fig. C8 Plot of stress against time for Test 13-1,(150°C,initial stress 150 MPa)

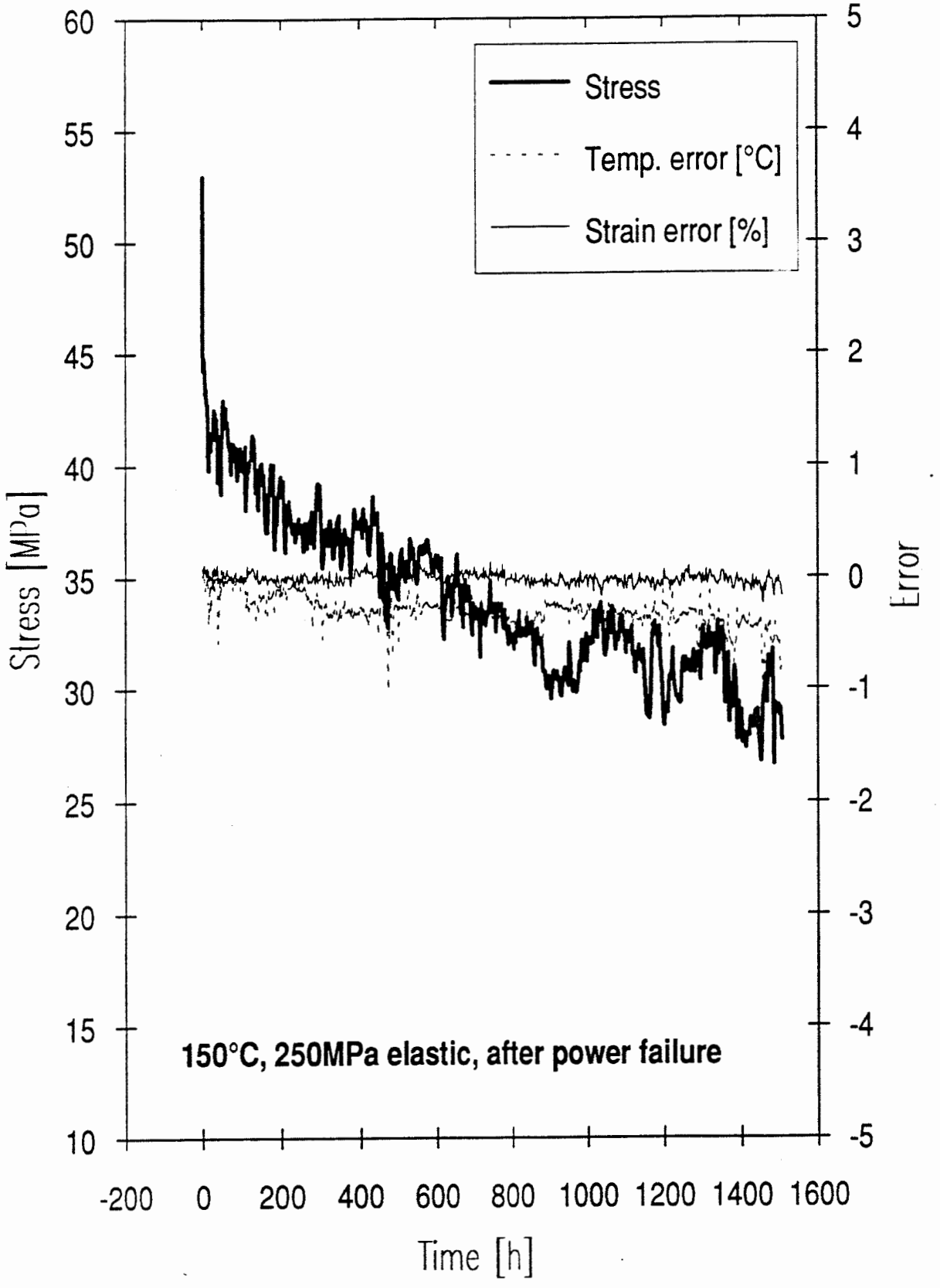

Fig. C9 Plot of stress against time for Test 13-2,(150°C,initial stress 150 MPa) Continuation of 13-1, re-started after power failure.

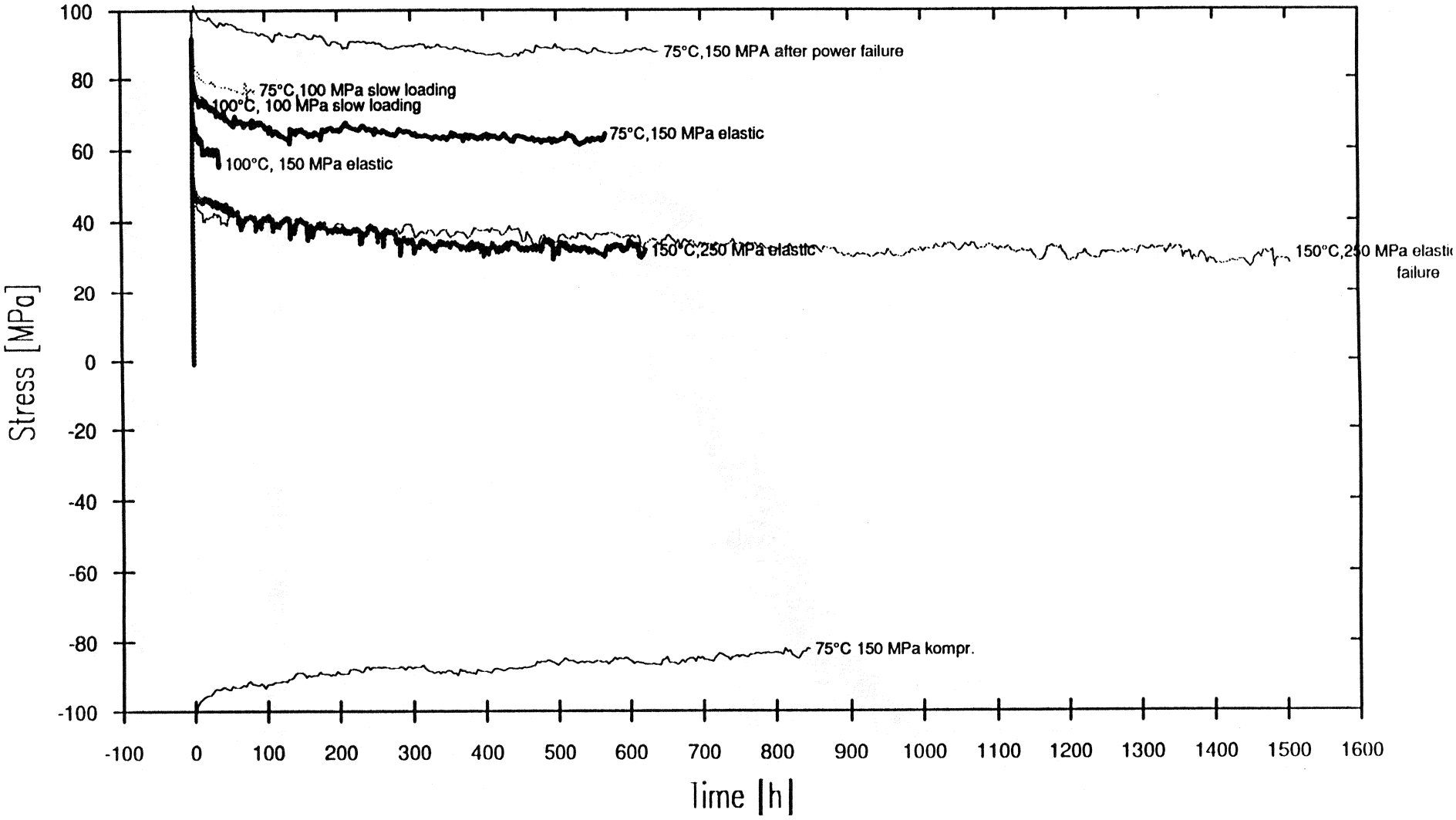

Fig. C10 Plot of stress versus time for all the stress relaxation tests.

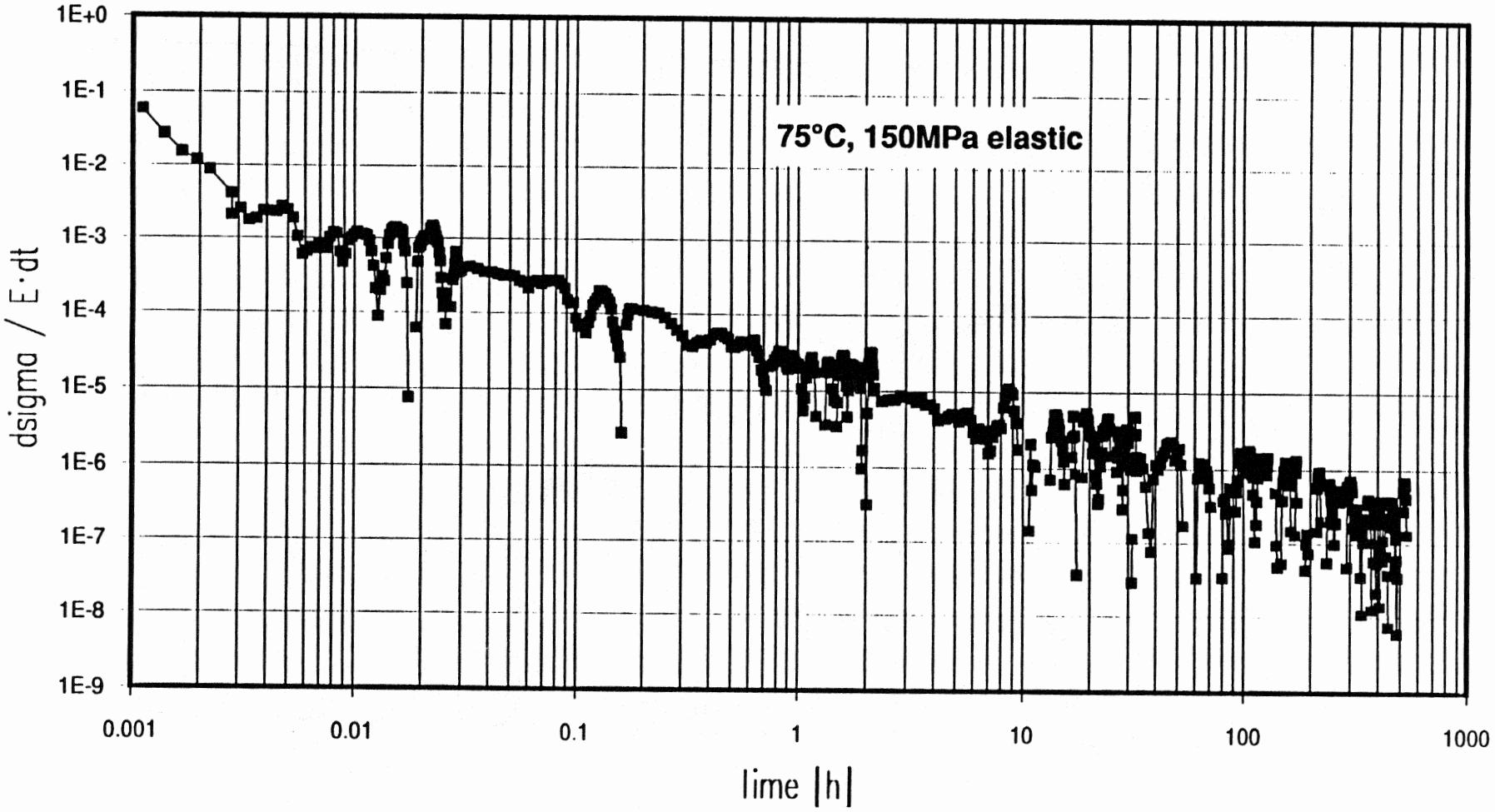

Fig. C11 Plot of plastic strain rate versus time for specimen 18-1,(75°C/150MPa).

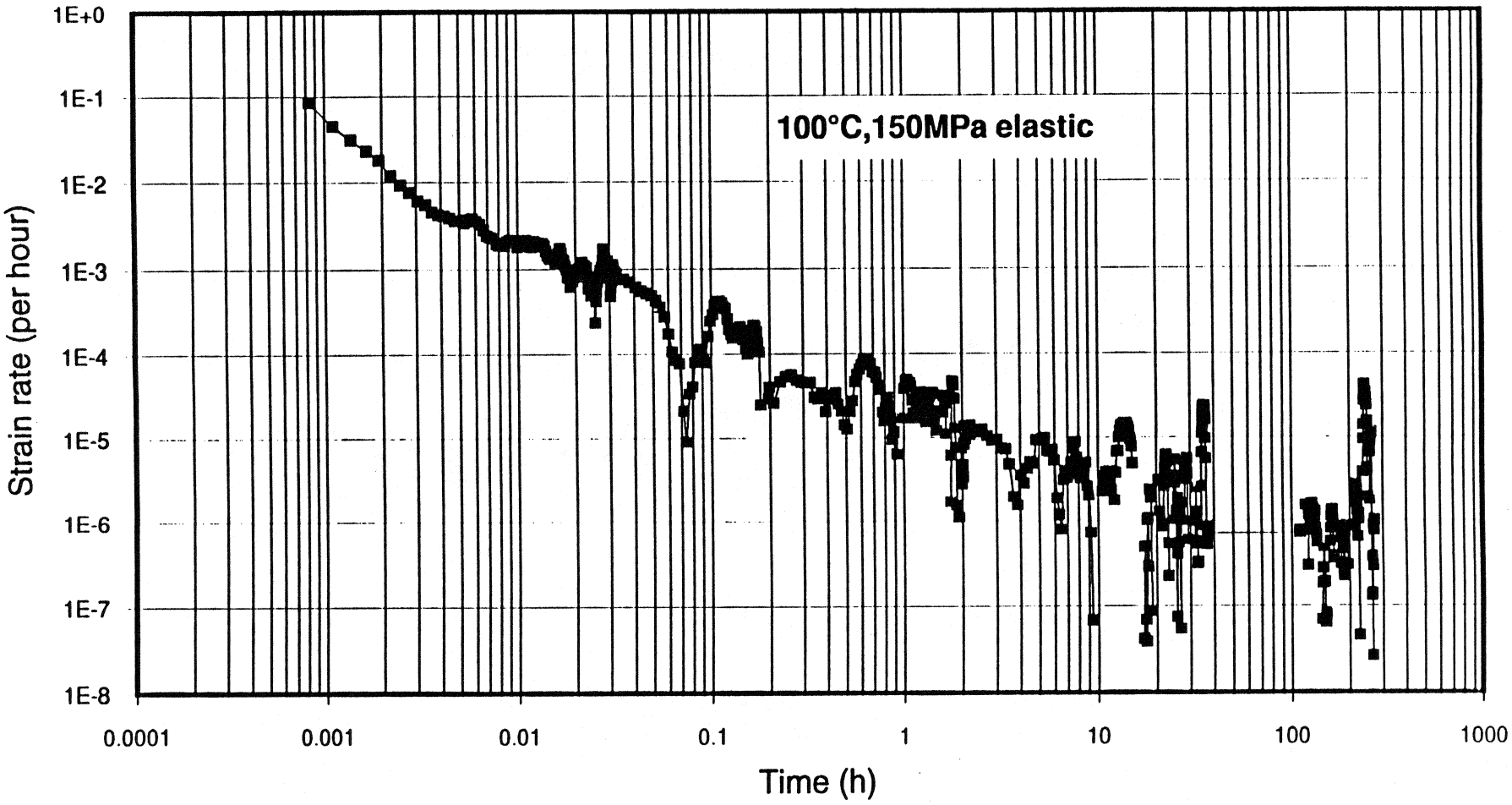

Fig. C12 Plot of plastic strain rate versus time for no. 21, (100°C/150MPa)

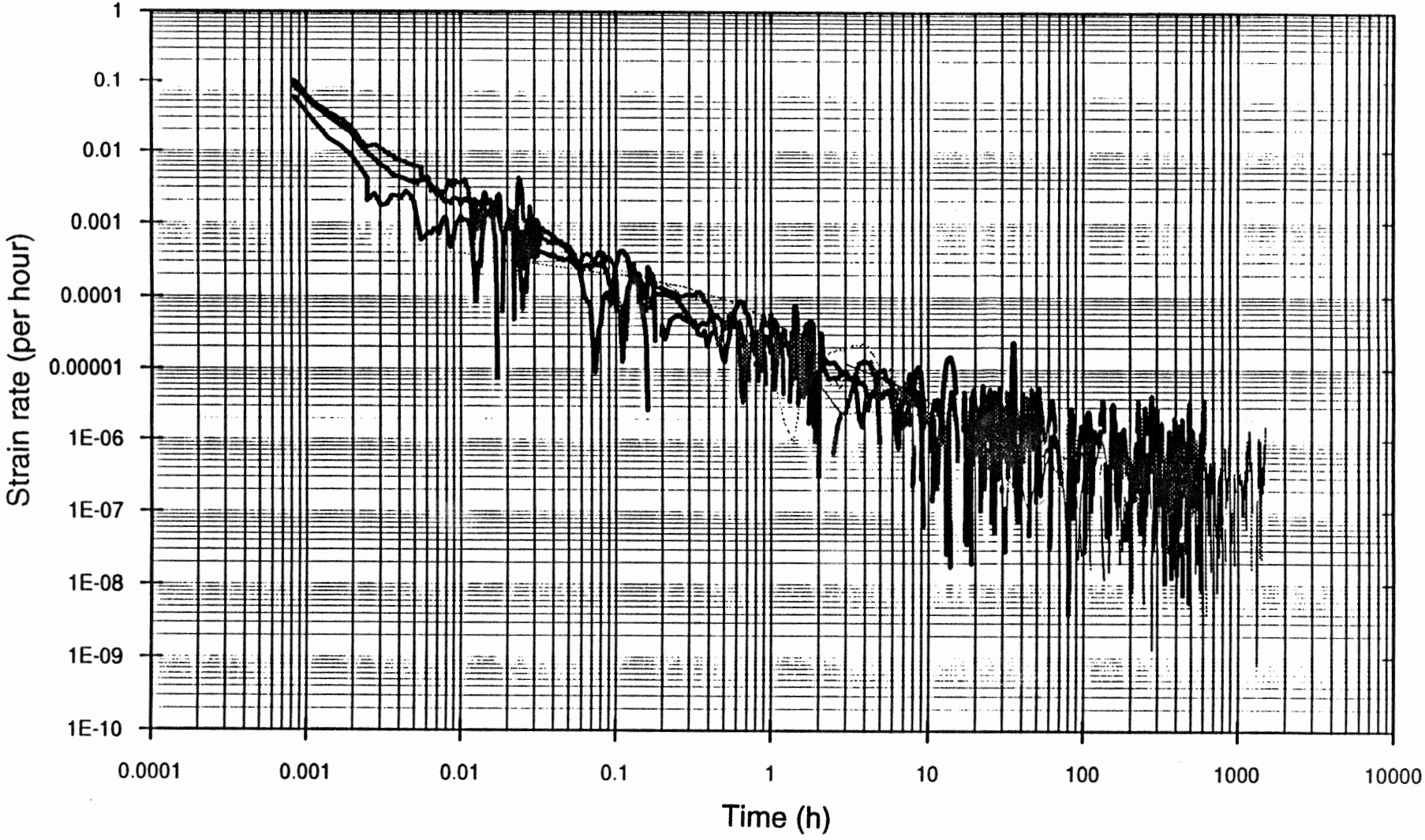

Fig. C13 Plot of plastic strain rate versus time for all the stress relaxation tests.

Prov	Start Längd [mm]	Min diam. [mm]	Min area. [mm²]	Provmask. nr.	Tempertur [°C]	Datum	Anm.	Prov	Mät resultat Drag hast. [mm/s]	E-modul [N/mm²]	Fm (tidb.) [N]	Fm (x/y) [N]	Längd [mm]	Min diam. [mm]	Rp0.2 [MPa]	Rp1.0 [MPa]	Rm [MPa]	A5 [%]	Z [%]	Resultat Drag hast. [/s]
1	24.277	4.972	19.42	2.3	26			1	6.31E-02		4820	4730	36.079	1.33	82	103	248	48.6	93	2.5E-03
2	24.609	4.924	19.04	2.3	26		Kasserad	2					36.392	1.3				47.9	93	
3	26.848	5.014	19.75	2.4	250	92:05:06	för.v.urtag	3	2.85E-03		3260				67	96	165			1.1E-04
4	27.002	4.924	19.04	2.5	200	92:05:07		4	2.96E-03		3480		38.793	1.74	85	94	183	43.7	88	1.2E-04
5	27.057	4.982	19.49	2.4	100	92:04:24		5	1.55E-02	1.36E+05	4260	4200	39.137	1.53	85	100	219	44.6	91	6.2E-04
6	27.333	5.01	19.71	2.3	26			6	0.059		4837	4850	40.436	1.31	90	109	245	47.9	93	2.4E-03
7	27.446	4.991	19.56	2.3	100	92:05:06		7	3.00E-04		4180		40.424	1.41	91	105	214	47.3	92	1.2E-05
8	27.519	5.007	19.69	2.3	400	92:07:04		8	3.00E-03		1980		44.686	0.414	46	57	101	62.4	99	1.2E-04
9	27.382	4.996	19.60	2.3	500	92:07:06		9	2.90E-03		1232		42.688	0.0145	34	43	63	55.9	100	1.2E-04
10	27.256	4.995	19.60	2.5	150	92:05:06		10	3.50E-02		3940	3940	39.162	1.35	79	105	201	43.7	93	1.4E-03
11	27.292	5.002	19.65	2.3	300	92:07:02		11	3.25E-03		3040		41.047	1.27	82	101	155	50.4	94	1.3E-04
12	27.321	5.012	19.73	2.5	150	92:04:14	Rel./Högh.	12	6.60E-01		4520		39.31	1.3			229	43.9	93	2.6E-02
13	27.458	5.001	19.64	2.3	150	92:07:17	Relaxation	13												
14	27.528	5.002	19.65	2.3	150	92:04:26		14												
15	27.337	5.015	19.75	2.5	150			15	1.49E-03	1.20E+05	3880	3900	39.346	1.44	67	109	196	43.9	92	6.0E-05
16	27.67	5.001	19.64	2.3	100	92:07:08		16	3.00E-03		4160		39.704	1.42	93	115	212	43.5	92	1.2E-04
17	27.436	4.995	19.60	2.4	200			17	2.90E-02		3740	3510	39.335	1.42	91	125	191	43.4	92	1.2E-03
18	27.39	5.021	19.80	2.5	75		Relaxation	18												
19	27.389	5.001	19.64			92:07:19		19												
20	27.511	5.003	19.66	2.3	600	92:07:14		20	2.90E-03		640		44.819	0.135	21	25	33	62.9	100	1.2E-04
21	27.143	5.012	19.73	2.5	100		Relaxation	21					30.904	4.662				13.9	13	
22	27.452	4.994	19.59	2.3	26			22	2.52E-02		4820	4820	40.105	1.36	86	122	246	46.1	93	1.0E-03
23	27.722	4.996	19.60	2.5	150	92:04:29		23	3.00E-04		3700		40.622	1.616	61	120	189	46.5	90	1.2E-05
24	27.485	5.008	19.70	2.3	26			24	2.51E-03		4789		40.236	1.22	97	202	243	46.4	94	1.0E-04
25	27.499	4.996	19.60	2.5	100	92:04:02	Rel./Plast.	25	3.12E-02		4450	4400	44.48	1.25	176	189	227	61.8	94	1.2E-03
26	27.603	4.995	19.60		200			26												
27	27.607	4.995	19.60					27												
28	27.523	4.974	19.43	2.3	26	92:04:21		28	1.60E-04		4540	4530	39.773	1.3	68	110	234	44.5	93	6.4E-06
29	27.57	4.996	19.60	2.4		92:07:13	Kasserad	29							22	27				
30	27.711	4.986	19.53	2.3	150	92:04:23	Höghast.	30	3.50E-01		4200		39.778	1.24	101	[135]	215	43.5	94	1.4E-02
31	27.744	4.992	19.57	2.3	200	92:07:15		31	3.00E-04		3460		41.712	1.39	75	91	177	50.3	92	1.2E-05

[mm]

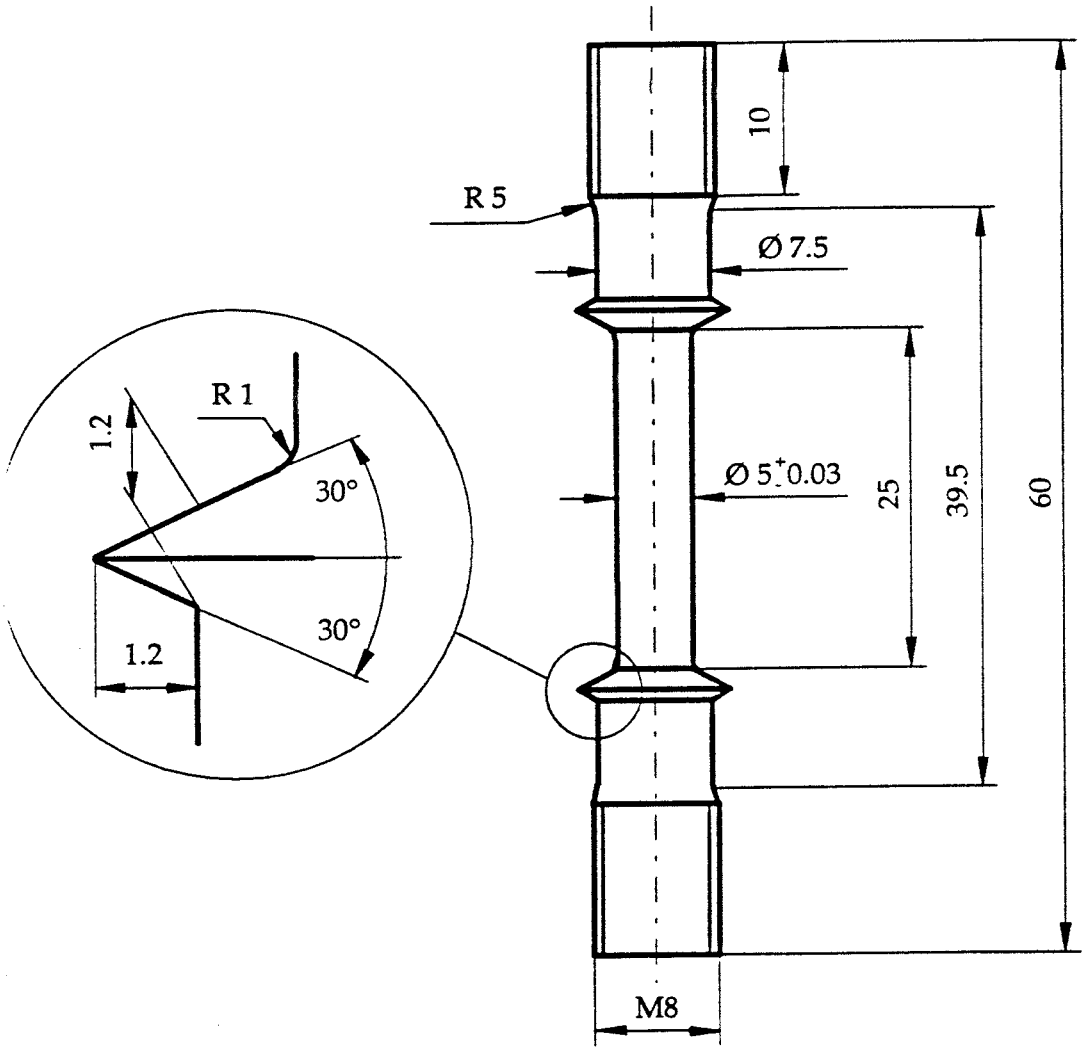

Diametern kan göras mindre på mitten inom den angivna toleransvidden.
Metriska gängor enligt SMS 2.
Maskinbearbetade ytor inom försökslängden inklusive de kälade partierna skall vara jämna, släta och fria från brottanvisningar.

Fig. D1 Drawing of the specimens used for tensile testing. Dimensions in mm.

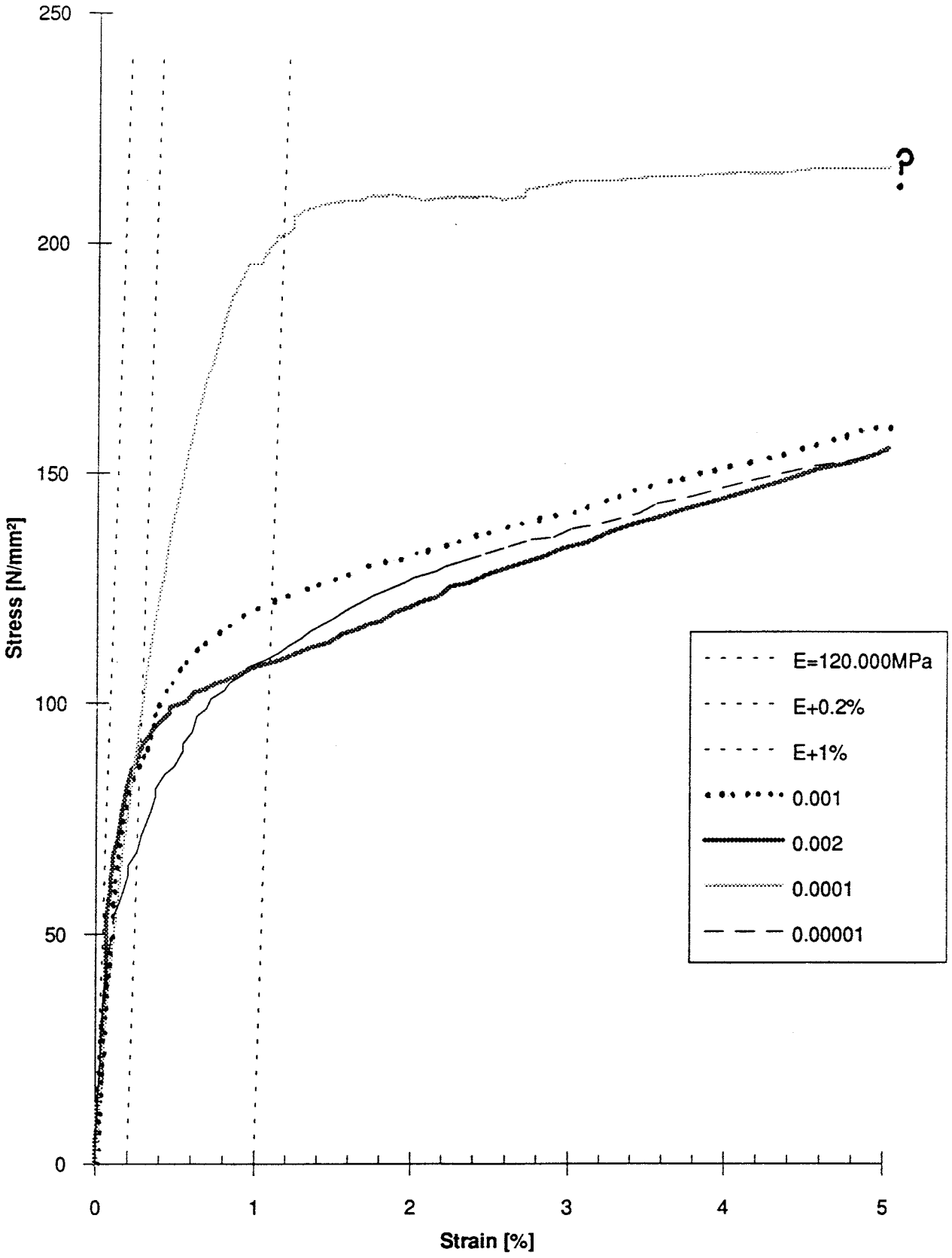

Fig. D2 Stress-strain curves for Cu-OFP at 26 °C.

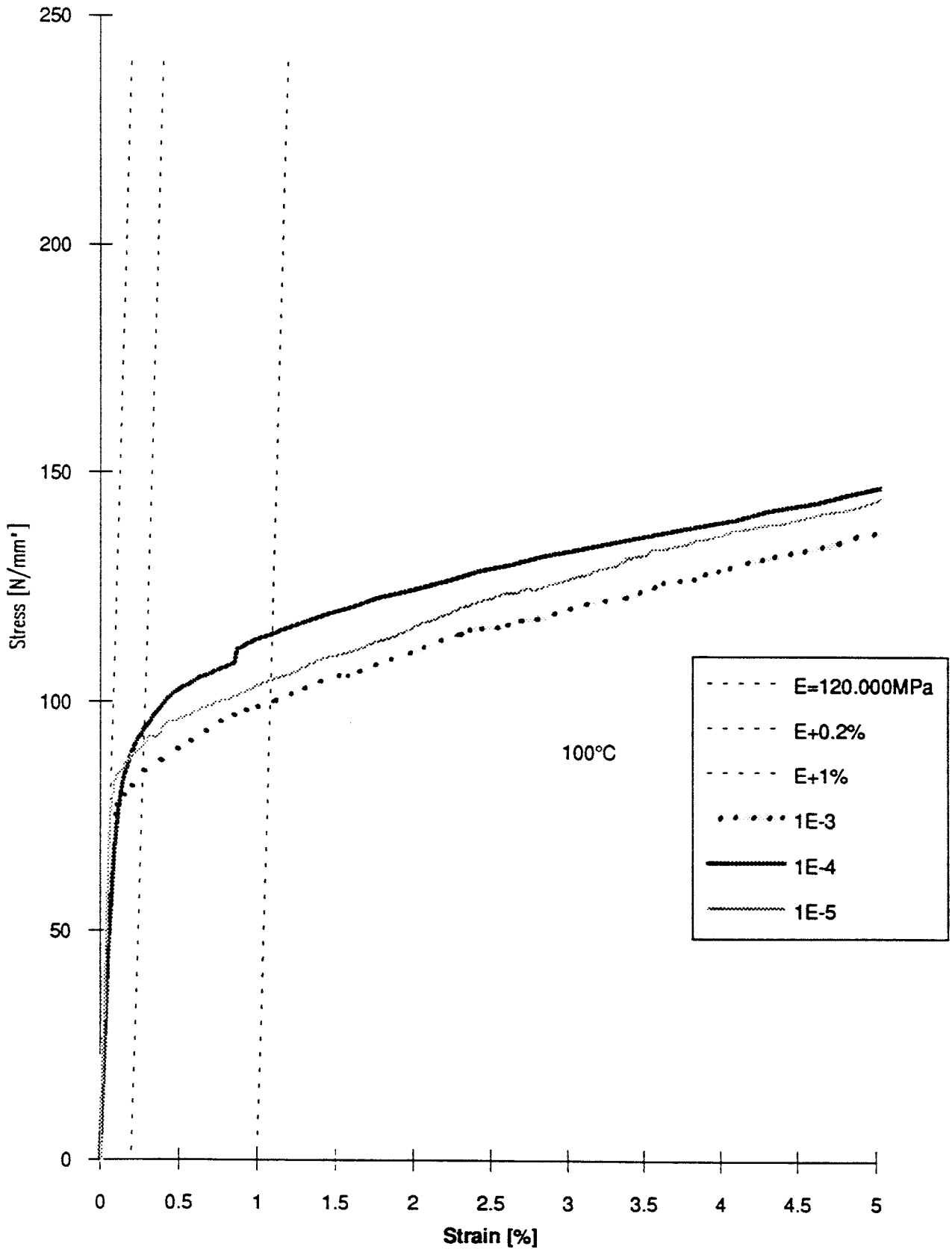

Fig. D3 Stress-strain curves for Cu-OFP at 100 °C.

Fig. D4

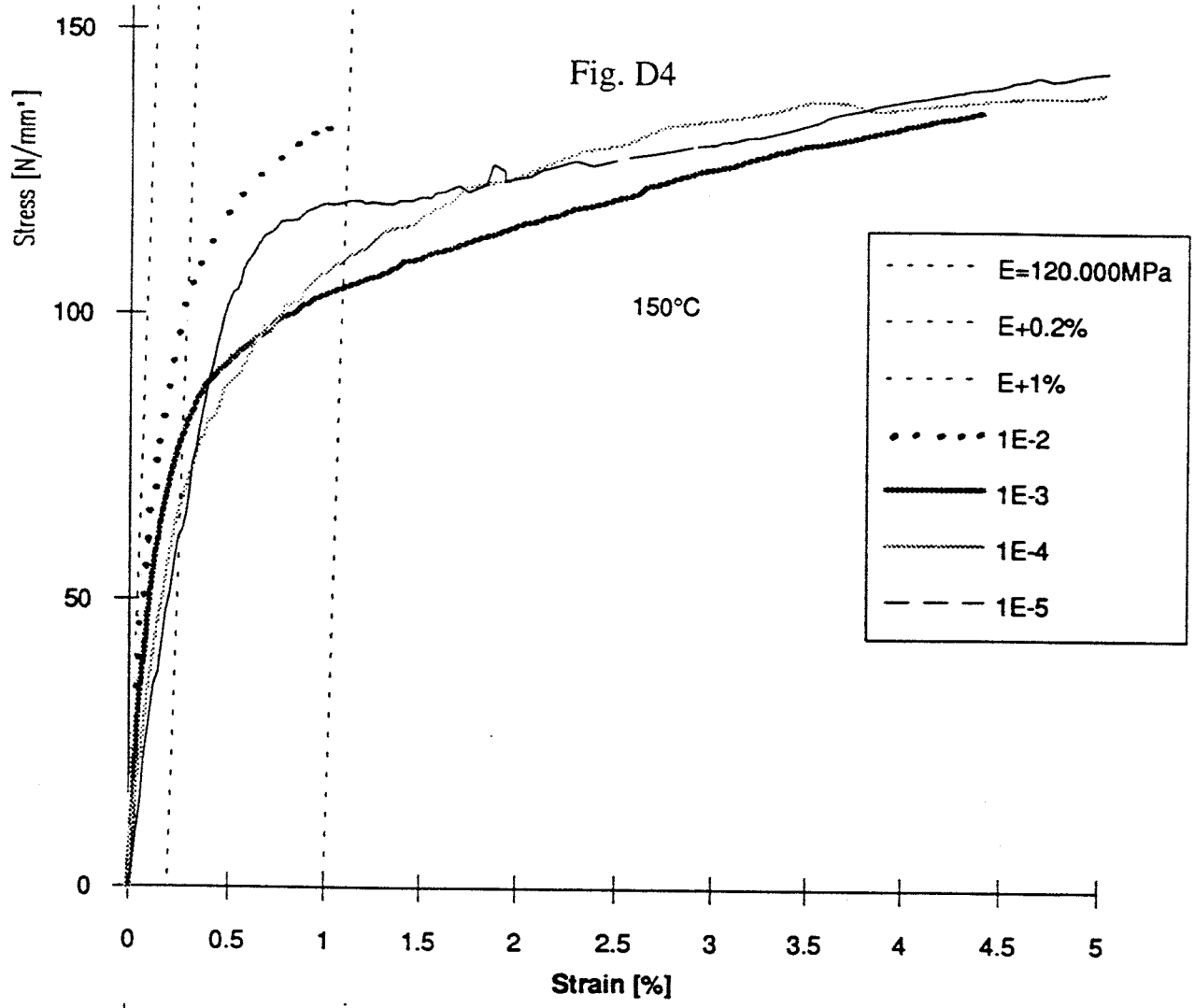
Stress [N/mm²]
150
100
50
0
0
0.5
1
1.5
2
2.5
3
3.5
4
4.5
5
Strain [%]
150°C
E=120.000MPa
E+0.2%
E+1%
1E-2
1E-3
1E-4
1E-5

Fig. D5

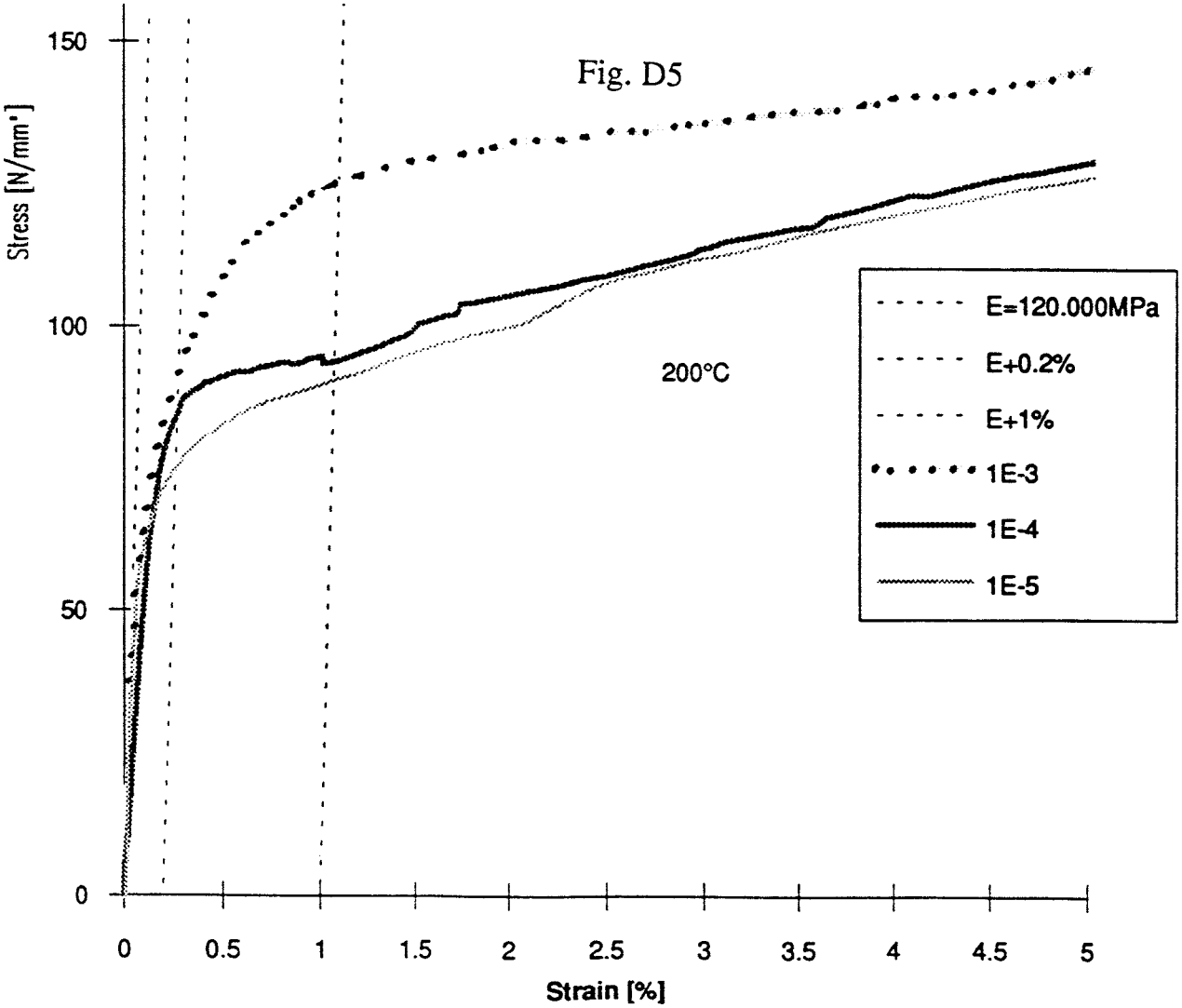
Stress [N/mm²]
150
100
50
0
0
0.5
1
1.5
2
2.5
3
3.5
4
4.5
5
Strain [%]
200°C
E=120.000MPa
E+0.2%
E+1%
1E-3
1E-4
1E-5

Fig. D6 **1E-3**

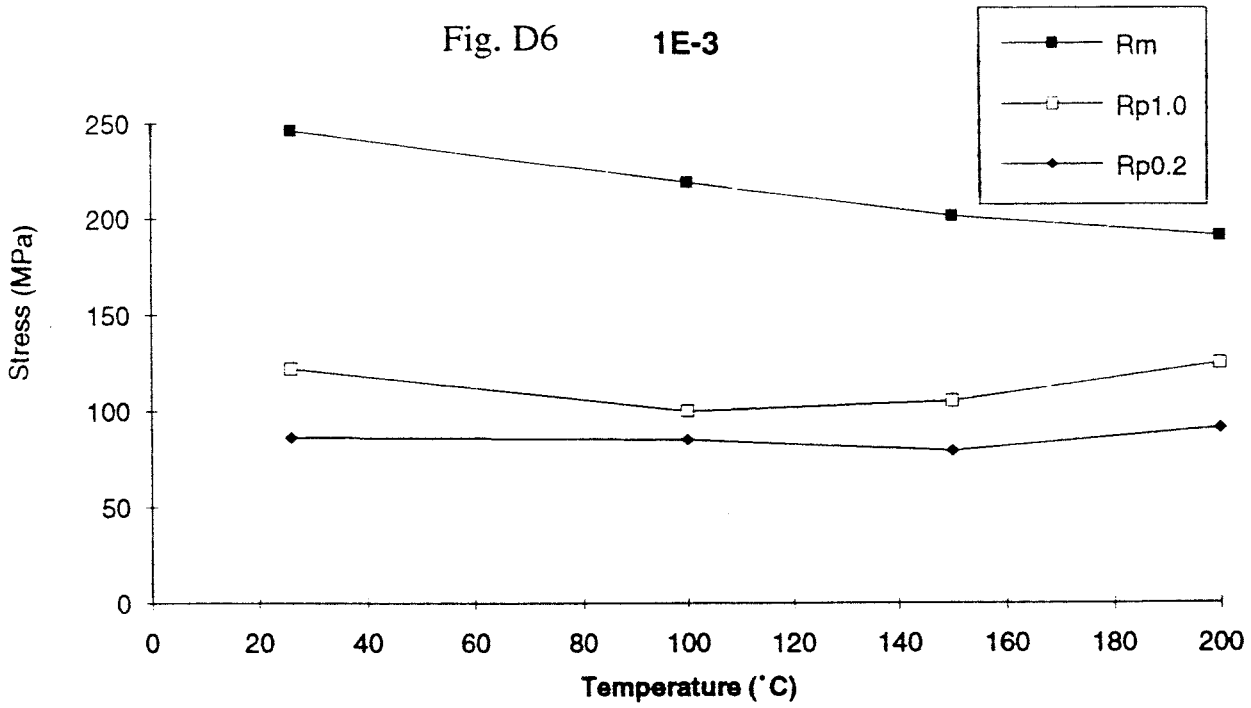

Fig. D7 **1E-5**

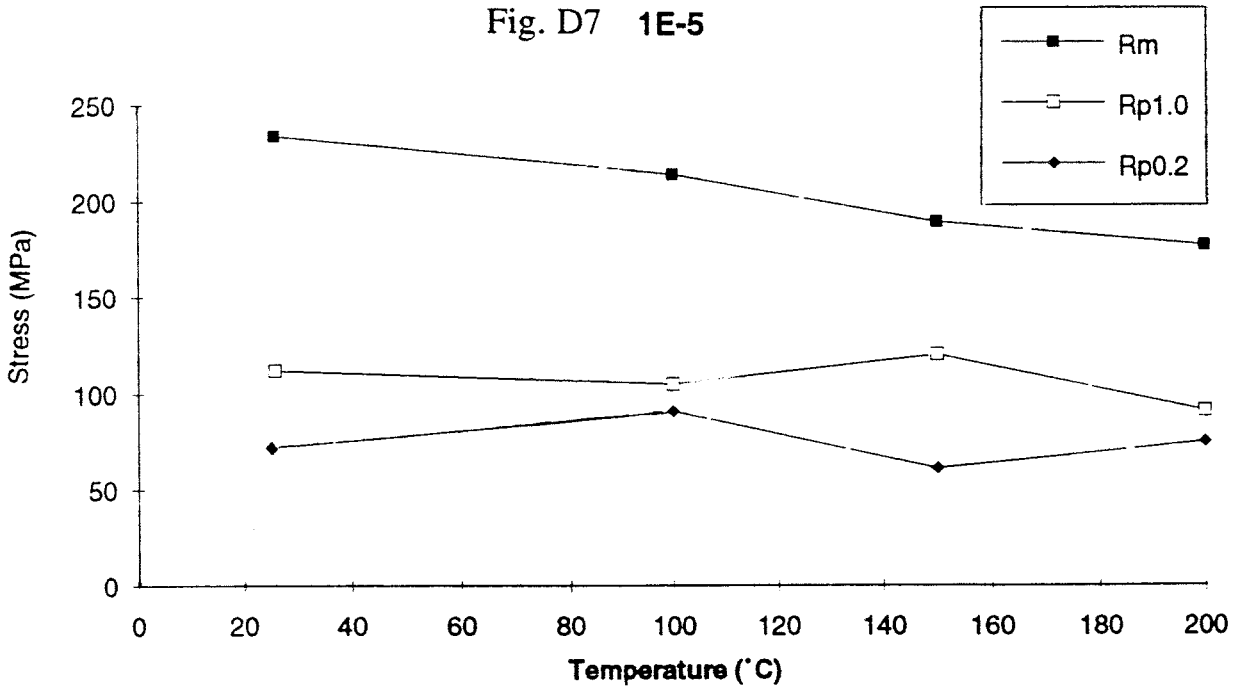

Fig. D8 **1E-4**

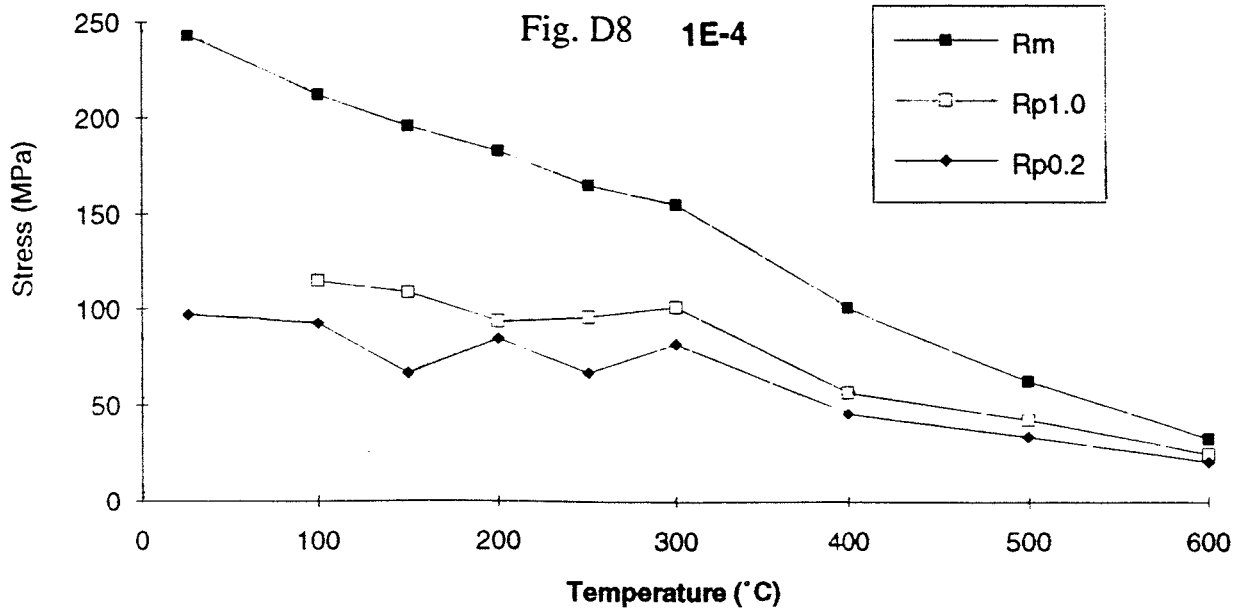

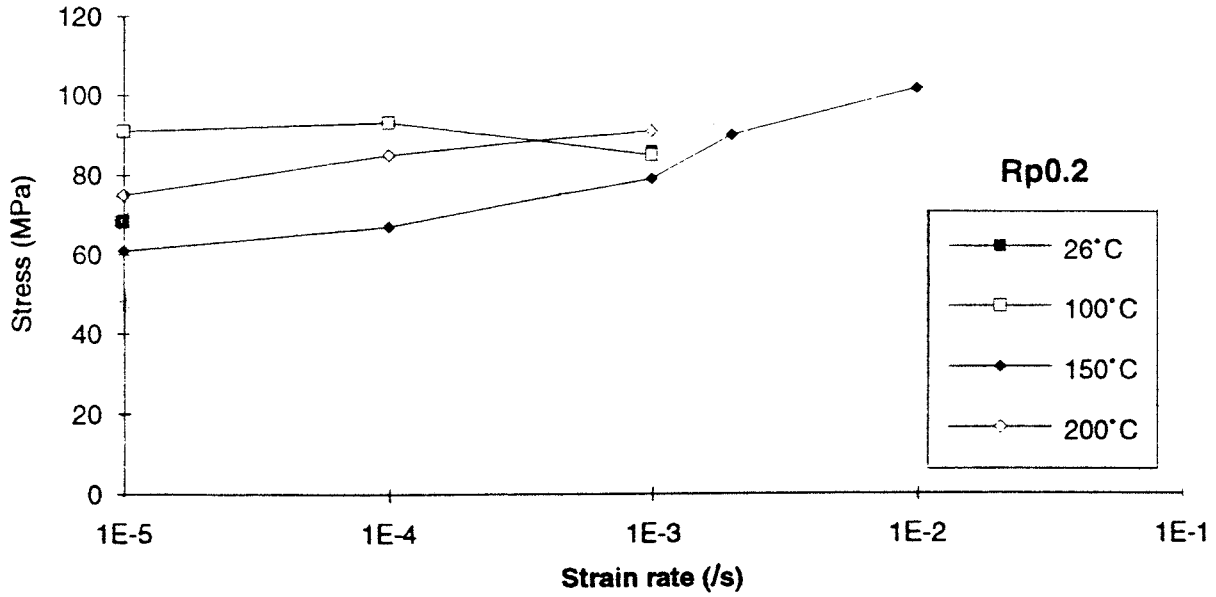

Fig. D9 Variation of 0.2% proof stress with strain rate.

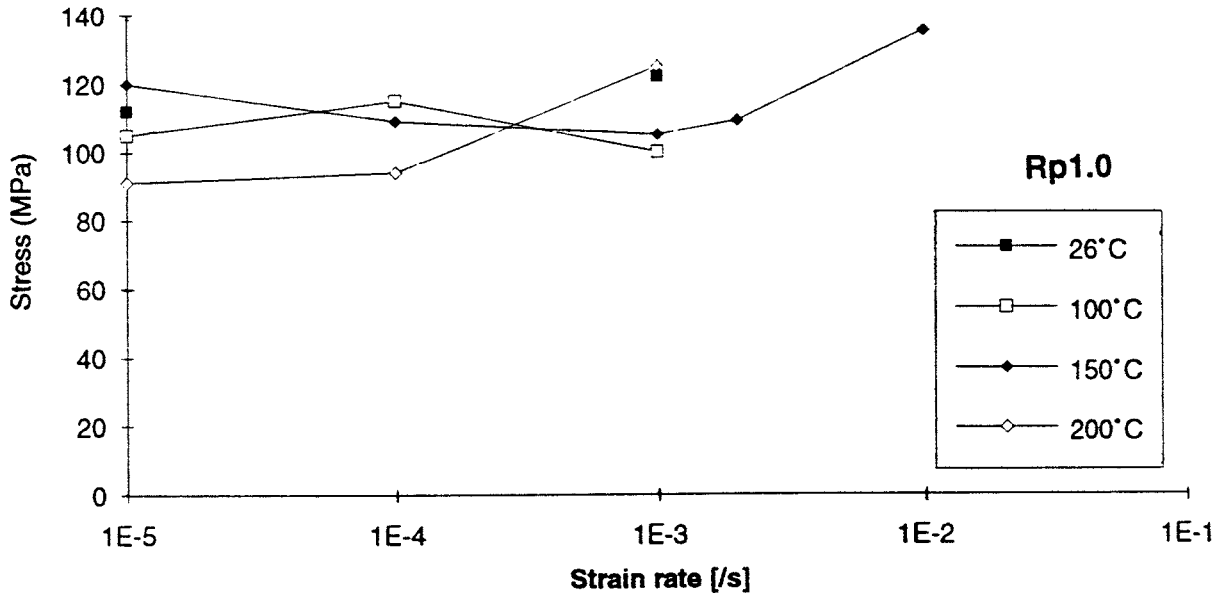

Fig. D10 Variation of 1.0% proof stress with strain rate.

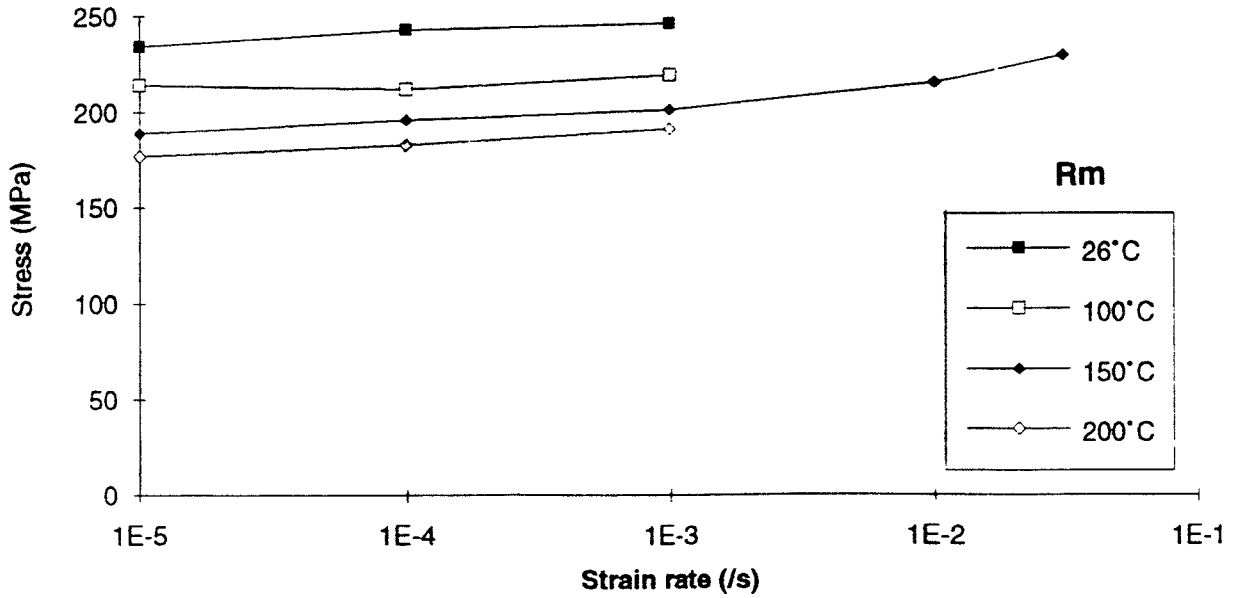

Fig. D11 Variation of ultimate tensile strength with strain rate.

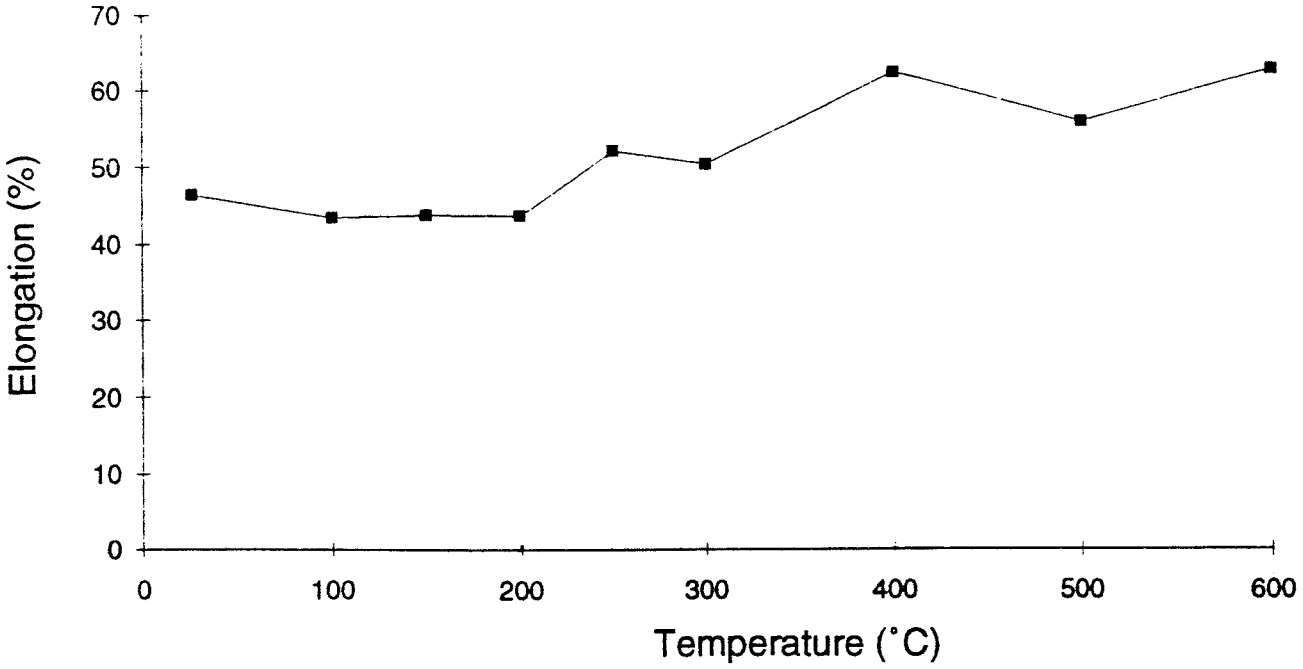

Fig. D12 Variation of elongation at rupture with temperature for a strain rate of $1 \times 10^{-4}\ s^{-1}$.

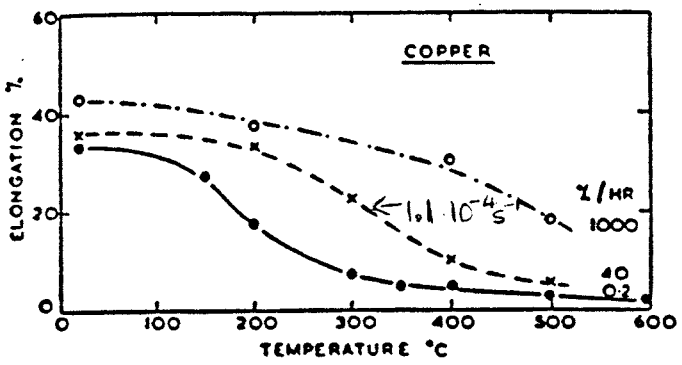

Influence of strain rate and temperature on the ductility of copper.

Fig. D13 Variation of elongation at rupture with temperature and strain rate for oxygen-free high purity copper.
(From J. N. Greenwood et al. Acta Metall. 2, pp 250-258, (1954)).

Appendix IV

Creep Deformation and Void Growth in Copper Canisters for Spent Nuclear Fuel

Lennart Josefson
Chalmers University of Technology

Chalmers University of Technology
Division of Solid Mechanics

Dr Lennart Josefson

1992-06-22

SKB:s referensgrupp för mekanisk integritet hos kapslar för använt kärnbränsle

Creep deformation and void growth in copper canisters for spent nuclear fuel

In the current proposal for the design of canisters for spent nuclear fuel the copper material will be initially subject to temperatures of, roughly, 100 °C, and stress levels of 100 MPa. Both temperatures and stress levels will gradually decrease during the design life of the canister. The deformation mechanism maps presented in Cocks and Asby (1982) indicate that the dominant deformation mechanism would be power law creep with a possible shift to diffusional flow for very long times. The void growth mechanism maps in Cocks and Ashby (1982), on the other hand, would indicate that surface difffusion would dominate void growth with a possible influence also of power law creep.

The estimations of material parameters in constitutive relations for creep deformation and void growth are based on results from creep tests on copper reported in Hendersson et al. (1991). Two materials have been studied in particular:

- **Cu-P Ser 400**: which is a phosphorus de-oxidised copper. This material was tested at, primarily, 215 °C, and it was found to exhibit transcrystalline fracture with large values for the fracture strain, ε_f = 30 - 40%. The grain size was 45 μm.
- **OFHC Ser 000-100-200**: which is a oxygen free high conductivity copper. This material was also tested at 215 °C, but with reported intercrystalline fracture and low fracture strains ε_f = 1 % except for three tests in Series 200 where ε_f = 10%. The grain size was 60 μm for Ser 000, 370 μm for Ser 100 and 45 μm for Ser 200.

Creep deformation

Although there exist several more or less empirical relations that describe creep deformation we propose that it would be sufficient to use the simple Norton-Bailey relation Eqn (1), which describes the secondary part of the creep curve only by use of two material parameters B and n.

$$\dot{\varepsilon}^c = B\sigma^n \tag{1}$$

In the present loading case, where the long time behaviour is of particular interest, it is believed that an accurate modelling of primary creep is not motivated. More complex relations may be proposed, but their potential is restricted by difficulties in obtaining values for the entering material parameters. Some other examples of phenomenologically based

constitutive relations for the present Copper material (and loading situation) can be found in Ivarsson and Österberg (1991). The Norton-Bailey relation can be extended to multi-axial stress states by assuming isotropic creep deformation, hence

$$\dot{\varepsilon}_{ij}^{c} = B\,\sigma_{eff}^{n-1}\,s_{ij} \tag{2}$$

where σ_{eff} is the von Mises effective stress and s_{ij} is the stress deviator. The parameters B and n in Eqn (1) can be determined in different ways, see for example Bråthe and Josefson (1979). Here, they have been determined by using linear regression in a log $\dot{\varepsilon}_{min}$ - log σ plot. The following values were obtained, see also Figures 2 and 4 in Henderson et al. (1991).

- o **Cu-P Ser 400:** $B = 5.10 \cdot 10^{-27}$ and $n = 10.5$ ($[t]$ = h and $[\sigma]$ = MPa).
- o **OFHC Ser 000-100-200:** $B = 2.38 \cdot 10^{-15}$ and $n = 5.32$

One may note that when employing linear regression the stresses were normalized with a reference stress being equal to the arithmetic mean of the stress levels at 215 °C. Figures 1 and 2 show the resulting straight line fit for Cu-P and OFHC copper. The (average) strain rate can also be estimated as the strain to rupture ε_R divided by the time to rupture t_R.

$$\dot{\varepsilon}_{average}^{c} = \frac{\varepsilon_R}{t_R} \tag{3}$$

For OFHC copper, with a low elongation at fracture, one will then obtain values for B and n which are relatively close the one reported above, $B = 2.56 \cdot 10^{-14}$ and $n = 4.91$, see Figure 3. For the ductile Cu-P copper there will be a larger difference between these values and the one above.

It is believed that the copper canister will be subject to prescribed deformation rather than prescribed loads during its design life. Thus, it would be better to determine material parameters from relaxation tests instead of creep tests. Such relaxations are included in the work of this Reference group. However, at the moment these relaxation tests have not been completed.

It is difficult to quantify the temperature dependence for the parameters B and n since sufficient data is available for 215 °C only. Here we propose the straightforward approach to include an Arrhenius term, indicating diffusional flow, hence

$$\dot{\varepsilon}_{ij}^{c} = B_0 e^{(-Q_c/RT)}\,\sigma_{eff}^{n-1}\,s_{ij} \tag{4}$$

Here Q_c = is the activation energy for creep deformation, R = Gas constant = 8.31 J/mol K and T is the absolute temperature. Using the value Q_s = 205 kJ/mol valid for surface diffusion one obtains $B_0 = 4.59 \cdot 10^{-5}$.

Void growth

In Cocks and Ashby (1982) three void growth mechanisms based on physical processes leading to creep fracture are compared with proposals based on continuum damage theories. These three mechanisms are power law creep, boundary diffusion and surface diffusion.

As indicated above, the physical process controlling void growth in OFHC copper would be surface diffusion with a resulting intergranular fracture. Thus, the void growth can be expressed as

$$\dot{\omega} = C\sqrt{\omega}\left(\frac{\sigma}{1-\omega}\right)^3 \tag{5}$$

where the fraction of voids in the grain boundaries is denoted ω. The appearance of this relation have been discussed by Pettersson (1992). After modifying values for the diffusion constant, which is included in the constant C, it was found that use of Eqn (5) would give very large rupture times (influence of power law creep was neglected), for the case when the stress σ is constant. Rupture was assumed to occur when the fraction of voids is ω = 0.25.

For the corresponding case of transgranular creep fracture in Cu-P Cocks and Ashby (1982) propose power law creep relations, thus

$$\dot{\varepsilon}^c = B\left(1-\beta+\frac{\beta}{(1-\omega)^n}\right)\sigma_{eff}^n \tag{6}$$

$$\dot{\omega} = B\,\beta\left(\frac{1}{(1-\omega)^n}-(1-\omega)\right)\sigma_{eff}^n \tag{7}$$

where the factor β can account for combined axial and hydrostatic loadings. In the uni-axial case β = 0.6.

Transgranular void growth may also be modelled with the so-called Gurson model for porous media, see Gurson (1977). This model and some other similar models are discussed in the overview Tvergaard (1991).

The empirical way to describe successive deterioration of copper at elevated temperatures in continuum damage mechanics is to use the (single-coupled) Kachanov theory. Hence a scalar damage parameter ω is introduced. This parameter grows, from zero for undamaged material to unity for completely damaged material, with the damage rate

$$\dot{\omega} = C\left(\frac{\sigma_I}{1-\omega}\right)^{\nu} \tag{8}$$

where σ_I is the maximum principal stress and C and ν are material parameters. Note, that Eqn (8) predicts a non-zero void growth, $\dot{\omega}$ even when ω = 0. This is not the case for the physically based Eqn:s (5) and (7). According to Bråthe (1978) they are preferrably determined from creep rupture tests and use of linear regression in a log σ_R - log t_R plot. Here σ_R is the rupture stress, that is the force divided by the actual cross sectional area of the specimen at rupture. By using this empirical approach one obtains:

- **Cu-P Ser 400**: $C = 1.39 \cdot 10^{-41}$ and $\nu = 16.0$ ($[t]$ = h and $[\sigma]$ = MPa).
- **OFHC Ser 000-100-200:** $C = 2.21 \cdot 10^{-8}$ and $\nu = 2.41$

Figure 4 shows the obtained straight line fit for the case of Cu-P copper. One finds for OFHC copper a low value for the exponent ν which may justify the assumption of surface diffusion which would give the value 3 for this exponent. One may also note that the assumption of power law creep for Cu-P requires large deformation of the copper material, as seen in Henderson et al. (1991) $\varepsilon_f = 30$ %. The accumulated plastic deformation during the welding process is estimated to be much smaller, 5 %, except possibly at strong geometric discontinuities where the plastic strain may become 10 %. This limits the validity of the assumption of transgranular fracture as rupture mode for Cu-P copper.

However, if one for a moment assumes that Cu-P copper exhibits an intergranular fracture mode, the calculated value for $\nu = 16.0$ indicate that surface diffusion is not the dominant void growth mechanism. As shown in the void growth diagrams in Cocks and Ashby (1982), void growth may also be controlled by power law creep. The total void growth rate may then be approximately taken as the sum of the growth rates for surface diffusion and power law creep. Cocks and Ashby (1982) propose that formulas for power law void growth in grain boundaries will be roughly the same as Eqn:s (6) and (7).

Correlation of strain and rupture data

As indicated above, the two alternatives Cu-P and OFHC copper seem to behave differently at elevated temperatures, for example the fracture mode is different. This difference in creep behaviour can be demonstrated by plotting the so called Dobes-Millicka relation (see Bråthe and Josefson, 1979):

$$\log\frac{t_R}{\varepsilon_R} + m \log \dot{\varepsilon}_{min} = C^* \qquad (9)$$

The two parameters C^* and m, has been found to reduce the scatter in creep data better than the classical Monkman-Grant relation. The idea is that the stages of secondary and tertiary creep are not independent, they are parts of the same creep process. Hence, there should exist some relationship between stationary properties, like $\dot{\varepsilon}_{min}$, and rupture properties, like ε_R and t_R. Figure 5 shows a plot of t_R/ε_R vs $\dot{\varepsilon}_{min}$. Included in Fig. 5 are also values for parent metal of OFHC copper creep tested at 75 °C and at 110 °C (see Ivarsson and Österberg, 1988). This material is equivalent to OFHC Ser 000 copper. One finds that the experimental results does not form a straight line. The strong difference in fracture strain ε_f between Cu-P and OFHC copper is clearly displayed in Fig. 5 as the results for these two alloys form two groups near the horizontal and vertical axis. Normally the resulting line should have the slope -1 corresponding to $m = 1$. Equation (9) can not be used for extrapolation of creep data, but one may note that if the result of linear regression of data for Eqn (9) is that $m = 1$ then the approximation for $\dot{\varepsilon}_{min}$ in Eqn (3) is reasonable.

Extrapolation of creep rupture data.

Another way to show that Cu-P data differ from OFHC data is to use formulas proposed in Cocks and Ashby (1982) for extrapolation of creep rupture data. Contrary to most other phenomenological methods, see Manson and Ensign (1979), their method is based on formulas for microstructural changes, that is void growth caused by grain-boundary diffusion, surface diffusion and power law creep. Essentially, they propose that a single master curve should result if creep rupture data at different temperatures are replotted as P_1 versus P_2 where

$$P_1 = \log\sigma - H\left(\frac{1}{T}-\frac{1}{T_0}\right)$$

$$P_2 = \log t_R - J\left(\frac{1}{T}-\frac{1}{T_0}\right) \qquad (9)$$

and where T_0 is a reference temperature and the constants H and J are chosen to minimise the scatter. Figure 6 shows such a master curve for OFHC copper although based on creep data at higher temperatures than the ones of interest now. The corresponding curve for Cu-P and OFHC copper at lower temperatures are shown in Fig. 7. Included in Fig. 7 are also some creep test results for Cu-P copper at temperatures higher than 215 °C. Also here it is found that the Cu-P data deviates from the OFHC data. Note that the values for H and J used in Fig. 8 were determined from the elevated temperature data for OFHC copper referred to in Cocks and Asby (1982).

The purpose of extrapolation is to use uni-axial creep data at constant load and short times and high temperatures in the assessment of creep behaviour at longer times (lower stress levels), to histories of non-steady loads and temperatures or to more complex stress states. Cocks and Ashby (1982) also discusses the extrapolation to non-steady histories of stress and temperatures. They show that linear cumulative damage rules may give uncertain results if different damage mechanisms control the void growth at different stages of the loading history.

Rupture under relaxation

The copper canister will be subject to prescribed deformation rather than prescribed loadings during operation. Thus formulas for uni-axial creep relaxation may be used for an estimation of the rupture time. Hence,

$$\dot{\varepsilon}^e + \dot{\varepsilon}^c = 0 \qquad \text{or} \qquad \dot{\sigma}/E + \dot{\varepsilon}^c = 0 \qquad (10)$$

where E is the Young's modulus. Bråthe (1976) solved Eqn (10) with $\dot{\varepsilon}^c$ taken from Eqn (1) together with the damage relation, Eqn (8), both for the single-coupled case (that is as expressed here) or for the double-coupled case (where the damage ω enters the creep deformation equation as in Eqn:s (6) and (7)). The closed form solution for Eqn:s (1) and (8) in the single-coupled case was used for OFHC copper with material parameters for Eqn:s (1) and (8) above and with the initial stress σ = 100 MPa. The rupture time t_R was found to be roughly 8 years. One may note that these formulas assume isothermal conditions. If one attempts to use these formulas for Cu-P copper with material parameters B, n, C and ν as determined above one finds that the material will have an infinite life (in order to obtain a finite rupture time the initial stress must be much larger than 100 MPa).

It is also possible to numerically integrate Eqn:s (1) and (8) to obtain the same result. Figures 8 and 9 show calculated relaxation of stresses and increase of fraction of voids for Cu-P and OFHC copper for the single-coupled case after use of Eqn (8) for the void growth. The initial stress was 100 MPa and the initial fraction of voids, $\omega_i = 0.000001$. It is seen that the development of voids is much larger in OFHC copper. The differential equations (1) and (8) were solved numerically by use of a fourth order Runge-Kutta method. Figure 10 shows calculated, simultaneous, stress reduction and damage development in Cu-P copper after integrating Eqn:s (6) and (7), that is for the double-coupled case when formulas for transgranular void growth are employed. Also here the development of fraction of voids (damage) in Cu-P is seen to be very low and the rupture time is very large. As noted above the same formulas can be used also for an assumed case of power law creep based void growth in the grain boundaries.

Summary

The Cu-P copper material seems to have a sufficiently high ductility resulting in a low development of voids both within the grains and possibly in the grain boundaries.

Creep deformation for this copper alloy is proposed to be modelled with Norton-Bailey relation for secondary creep. Two different formulas for development of voids are proposed, either a phenomenological approach based on Eqn (1) and Eqn (8) for the damage evolution, or a physically based approach based on simultaneous solution of Eqn:s (6) and (7).

References

Bråthe, L., 1976, Rupture under relaxation, *Proceedings of The VII International Congress on Rheology*, held in Göteborg, Sweden, pp. 616-617.

Bråthe, L., 1978, Estimation of Kachanov parameters and extrapolation from isothermal creep rupture data, *International Journal of Mechanical Sciences*, Vol. 20, pp. 617-624.

Bråthe, L., and Josefson, L., 1979, Estimation of Norton-Bailey parameters from creep rupture data, *Metal Science*, Vol. 13, pp. 660-664.

Cocks, A.C.F., and Ashby, M.F., 1982, On creep fracture by void growth, *Progress in Materials Science*, Vol. 27, pp. 189-244.

Gurson, A.L., 1977, Continuum theory of ductile rupture by void nucleation and growth - I. Yield criteria and flow rules for porous ductile media, *ASME Journal of Engineering Materials and Technology*, Vol 99, pp. 2-15.

Henderson, P.J., Österberg, J.-O., and Ivarsson, B.G., 1991, Low temperature creep of copper intended for nuclear waste containers, *Research Report IM-2780*, Swedish Institute for Metals Research, Stockholm, Sweden.

Ivarsson, B., and Österberg, J.-O., 1988, Creep properties of welded joints in OFHC copper for nuclear waste disposal, *SKB Technical Report 88-20*, Swedish Nuclear Fuel and Waste Management Co, Stockholm, Sweden.

Manson, S.S., and Ensign, C.R., 1979, A quarter-century of progress in the development of correlation and extrapolation methods for creep rupture data, *ASME Journal of Engineering Materials and Technology*, Vol. 101, pp. 317-325.

Pettersson, K., 1992, Creep and creep fracture of copper canisters for nuclear waste, Division of Mechanical Metallurgy, Royal Institute of Technology, Stockholm, Sweden, Appendix II, This Report.

Tvergaard, V., 1991, Mechanical modelling of ductile fracture, *Meccanica*, Vol 26, pp. 11-16.

Figure 1 Linear regression of σ vs $\dot{\varepsilon}_{min}$ for Cu-P copper Series 400.

Figure 2 Linear regression of σ vs $\dot{\varepsilon}_{min}$ for OFHC copper Series 000-100-200.

Figure 3 Linear regression of σ vs $\dot{\varepsilon}_{average} = \frac{\varepsilon_R}{t_R}$ for OFHC copper Series 000-100-200.

Figure 4 Linear regression of σ vs t_R for OFHC copper Series 000-100-200.

Figure 5 Dobes-Millicka relation for Cu-P copper Series 400, OFHC copper Series 000-100-200 and OFHC copper (parent metal) at 75 °C and at 110 °C (OFHC Ser 000).

Figure 6 Extrapolation procedure based on formulas for void growth applied to data for OFHC copper, from Cocks and Ashby (1982).

Figure 7 Extrapolation procedure for Cu-P copper Series 400, OFHC copper Series 000-100-200 and OFHC copper (parent metal) at 75 °C and at 110 °C (OFHC Ser 000).

Figure 8 Calculated stress relaxation and void fraction development in Cu-P copper using single coupled damage theory.

Figure 9 Calculated stress relaxation and void fraction development in OFHC copper Series 000-100-200 using single coupled damage theory.

Figure 10 Calculated stress relaxation and void fraction development in Cu-P copper using formulas for transgranular creep fracture and a double-coupled theory.

Figure 1

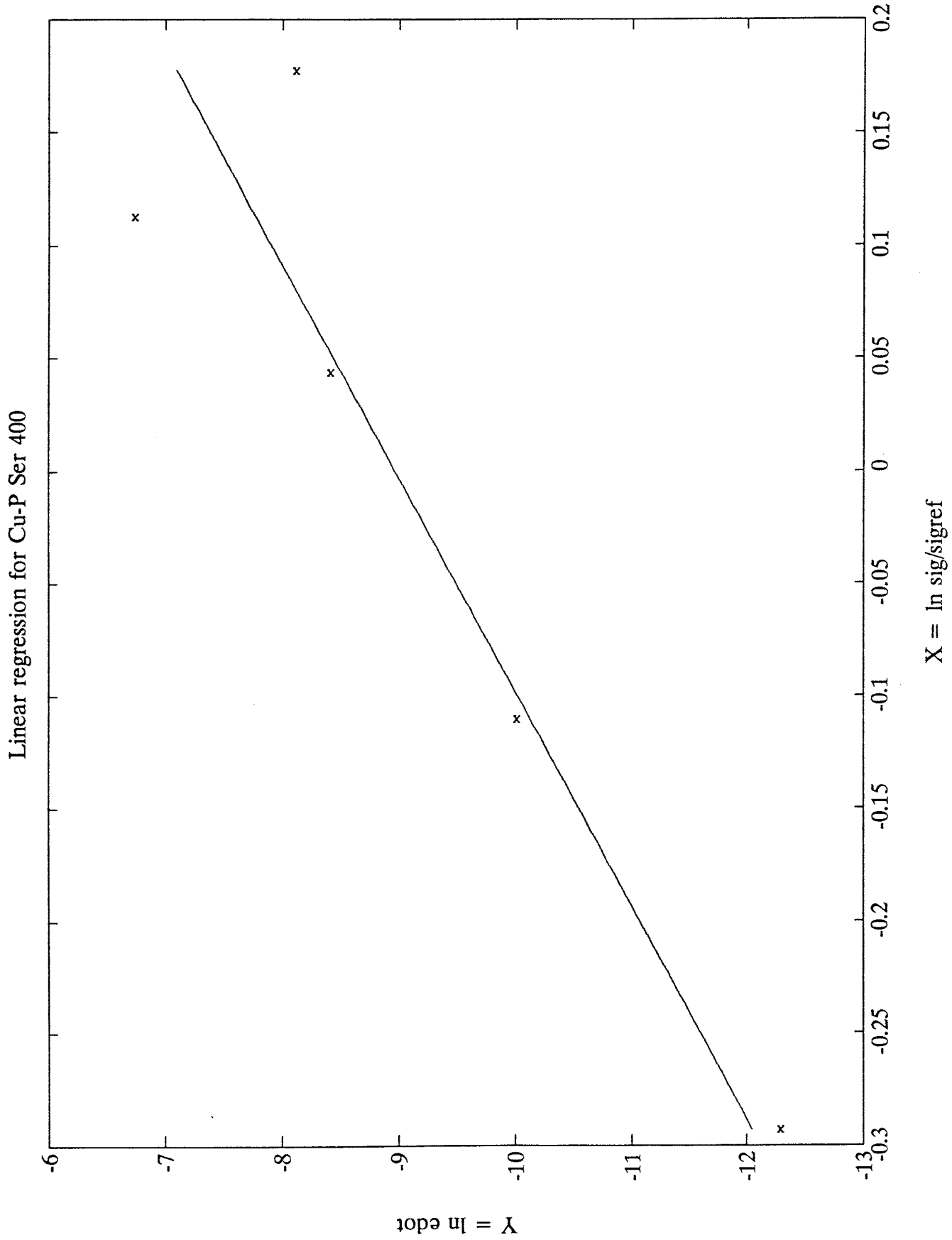
Linear regression for Cu-P Ser 400
Y = ln edot
X = ln sig/sigref
-6
-7
-8
-9
-10
-11
-12
-13
0.2
0.15
0.1
0.05
0
-0.05
-0.1
-0.15
-0.2
-0.25
-0.3

Figure 2

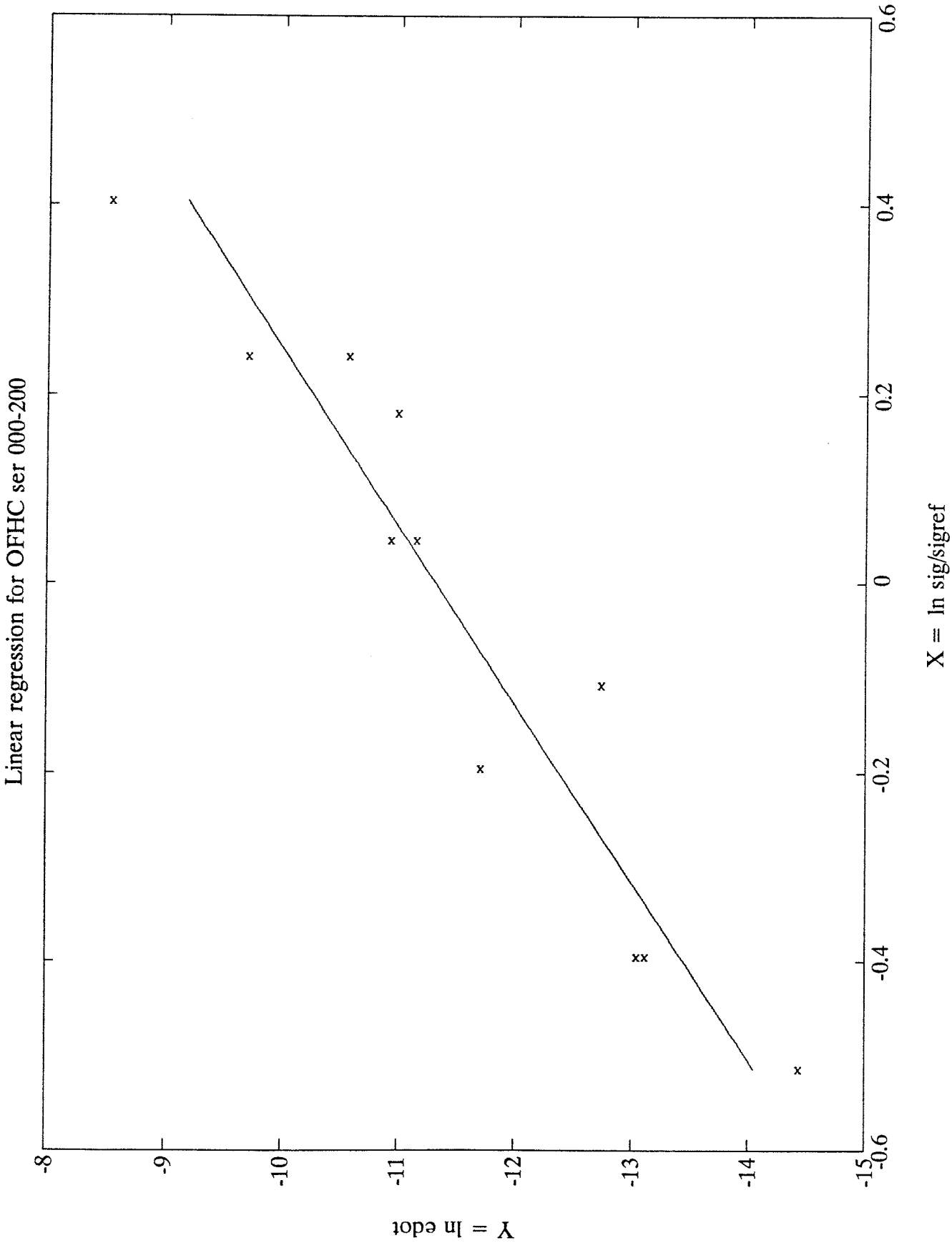
Linear regression for OFHC ser 000-200
Y = ln edot
X = ln sig/sigref
-8
-9
-10
-11
-12
-13
-14
-15
0.6
0.4
0.2
0
-0.2
-0.4
-0.6

Figure 3

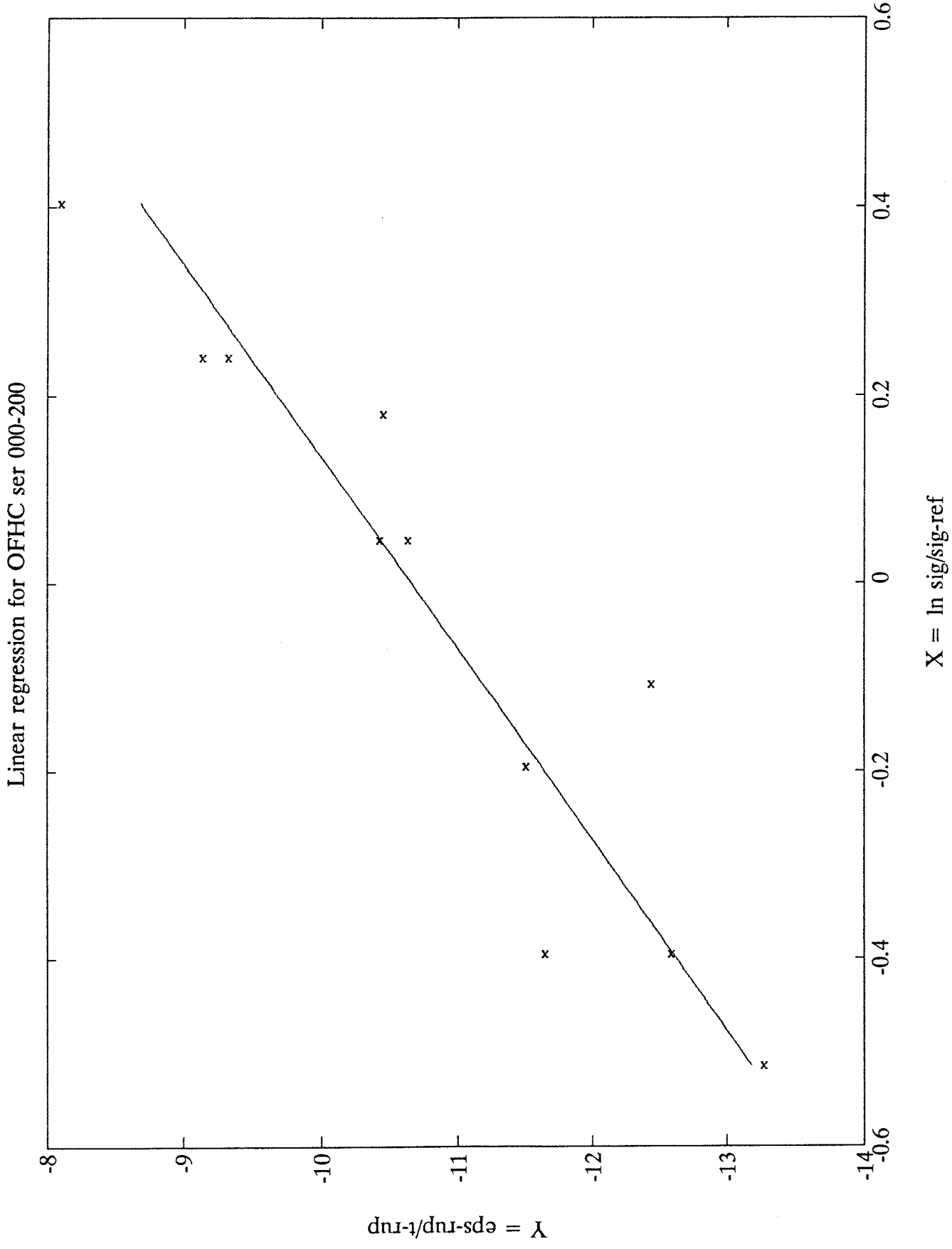
Linear regression for OFHC ser 000-200
Y = eps-rup/t-rup
X = ln sig/sig-ref
-8
-9
-10
-11
-12
-13
-14
0.6
0.4
0.2
0
-0.2
-0.4
-0.6

Figure 4

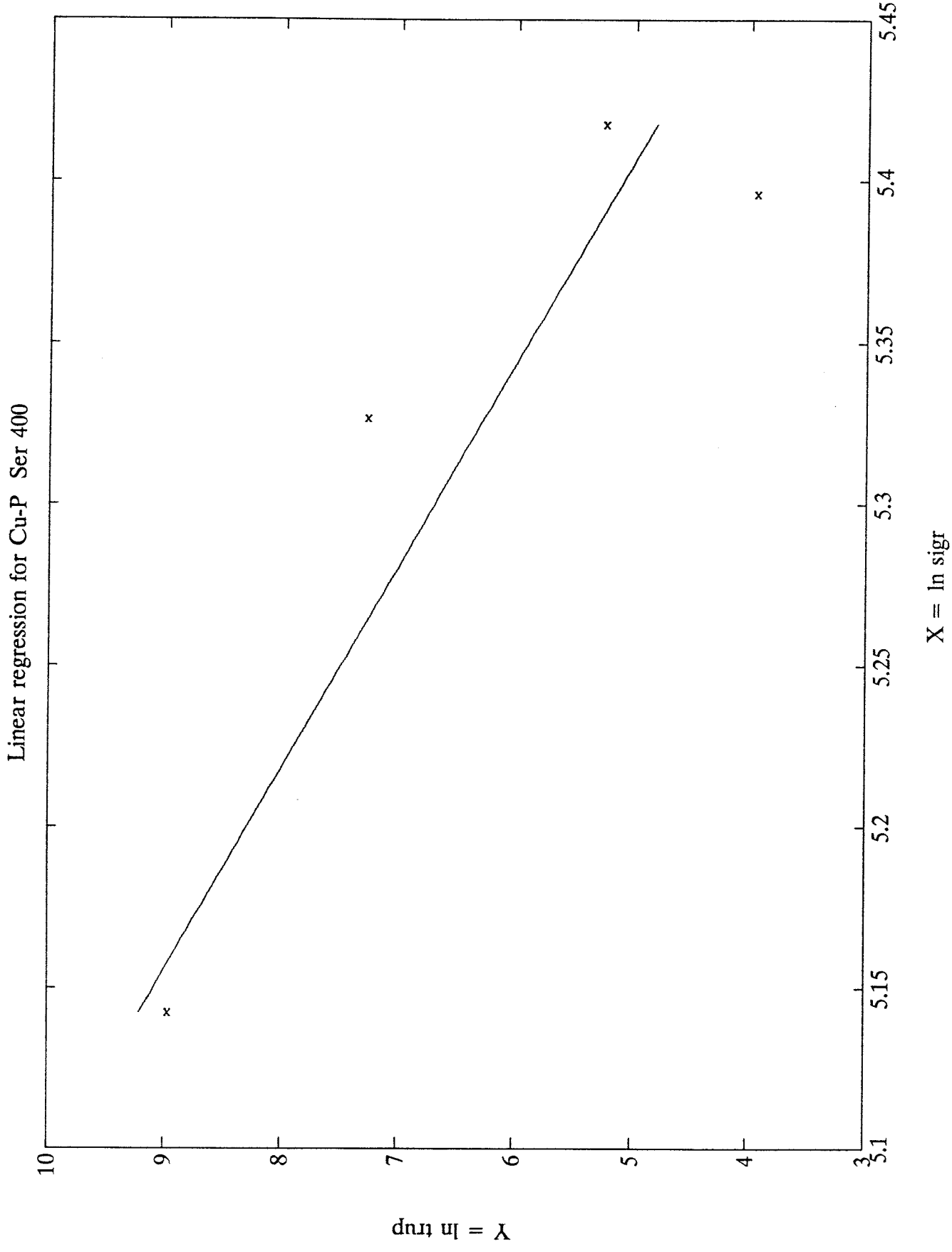
Linear regression for Cu-P Ser 400
Y = ln trup
X = ln sigr
10
9
8
7
6
5
4
3
5.1
5.15
5.2
5.25
5.3
5.35
5.4
5.45

Figure 5

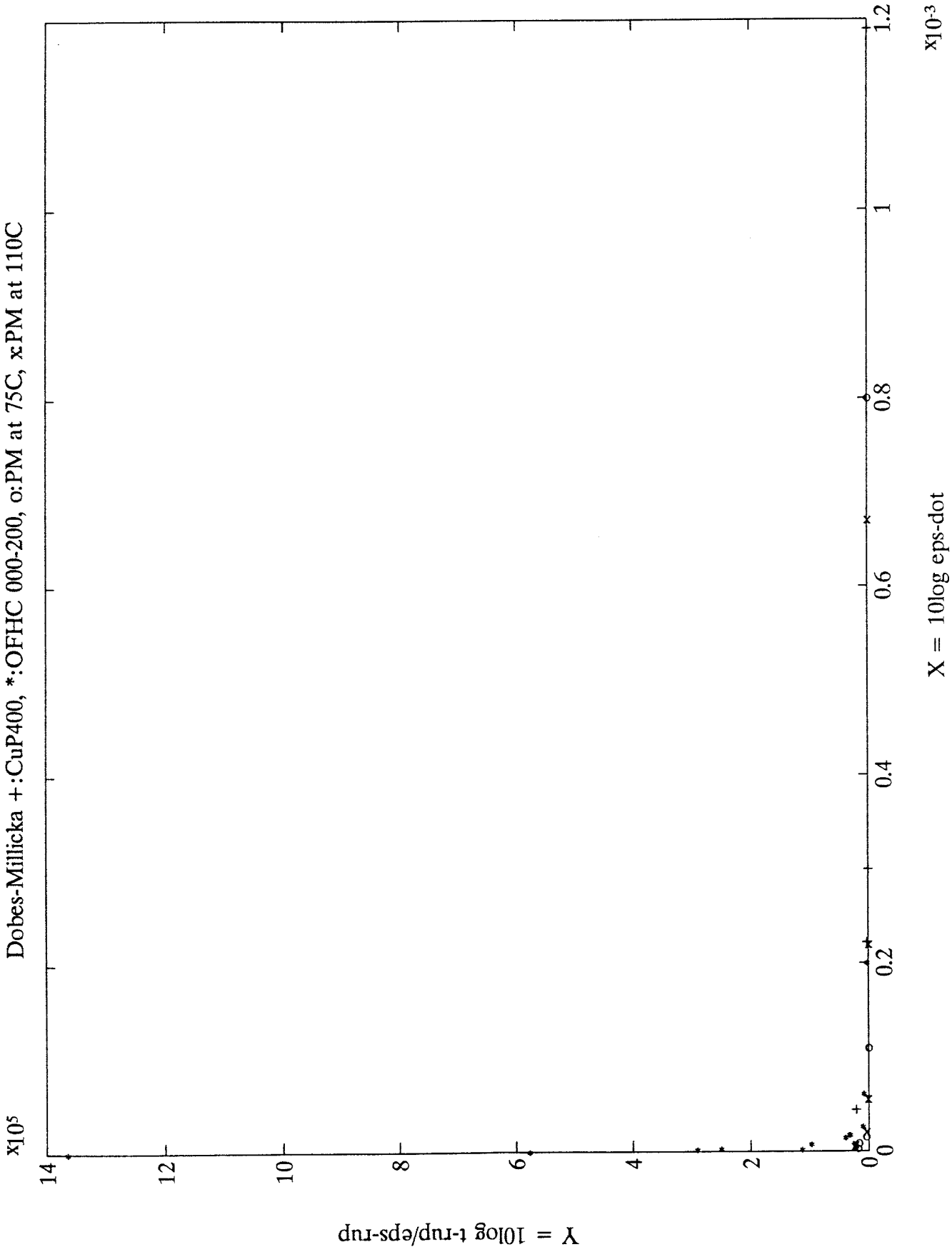
Dobes-Millicka +:CuP400, *:OFHC 000-200, o:PM at 75C, x:PM at 110C
x10^5
14
12
10
8
6
4
2
0
0
0.2
0.4
0.6
0.8
1
1.2
x10^-3
Y = 10log t-rup/eps-rup
X = 10log eps-dot

Figure 6

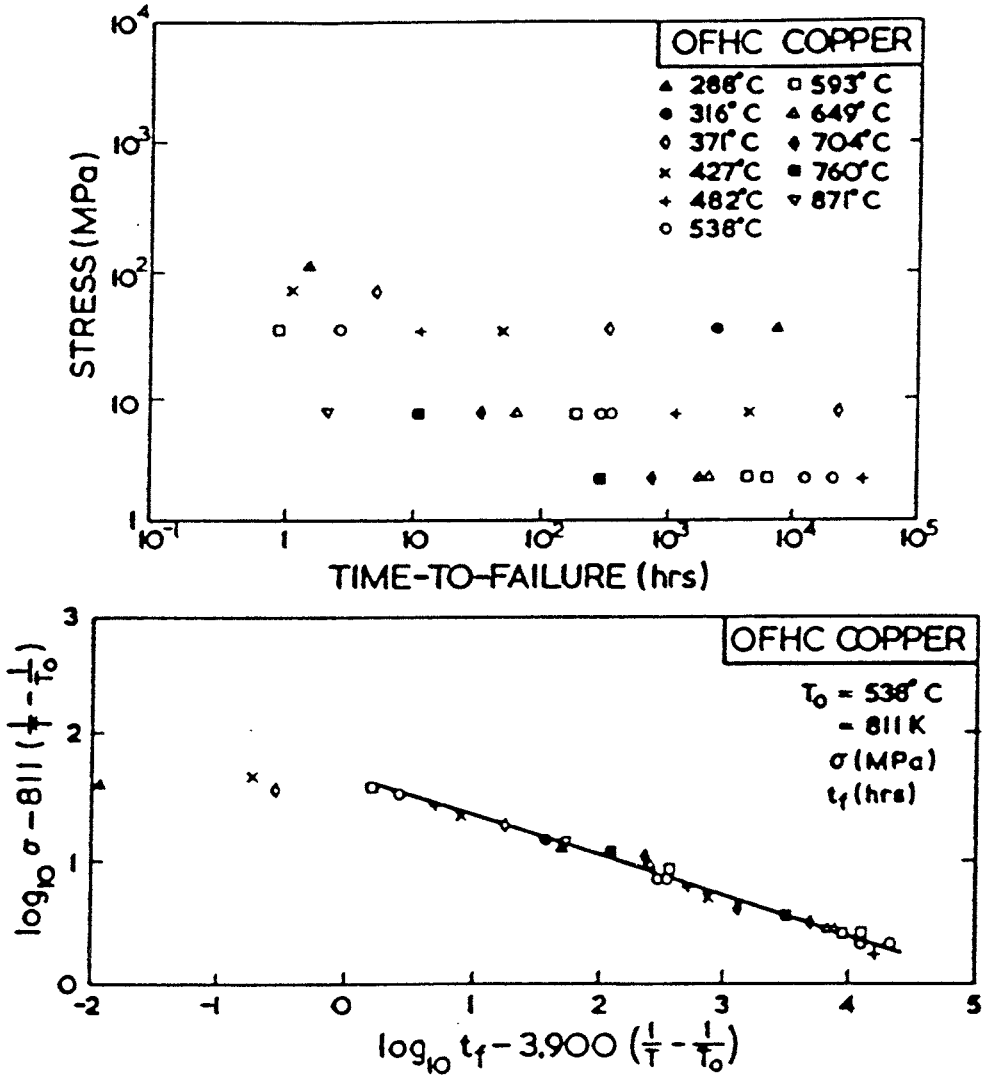
OFHC COPPER
288°C
316°C
371°C
427°C
482°C
538°C
593°C
649°C
704°C
760°C
871°C
STRESS (MPa)
TIME-TO-FAILURE (hrs)
OFHC COPPER
T_0 = 538°C
= 811 K
σ (MPa)
t_f (hrs)
$\log_{10}\sigma - 811\left(\frac{1}{T}-\frac{1}{T_0}\right)$
$\log_{10} t_f - 3.900\left(\frac{1}{T}-\frac{1}{T_0}\right)$

Figure 7

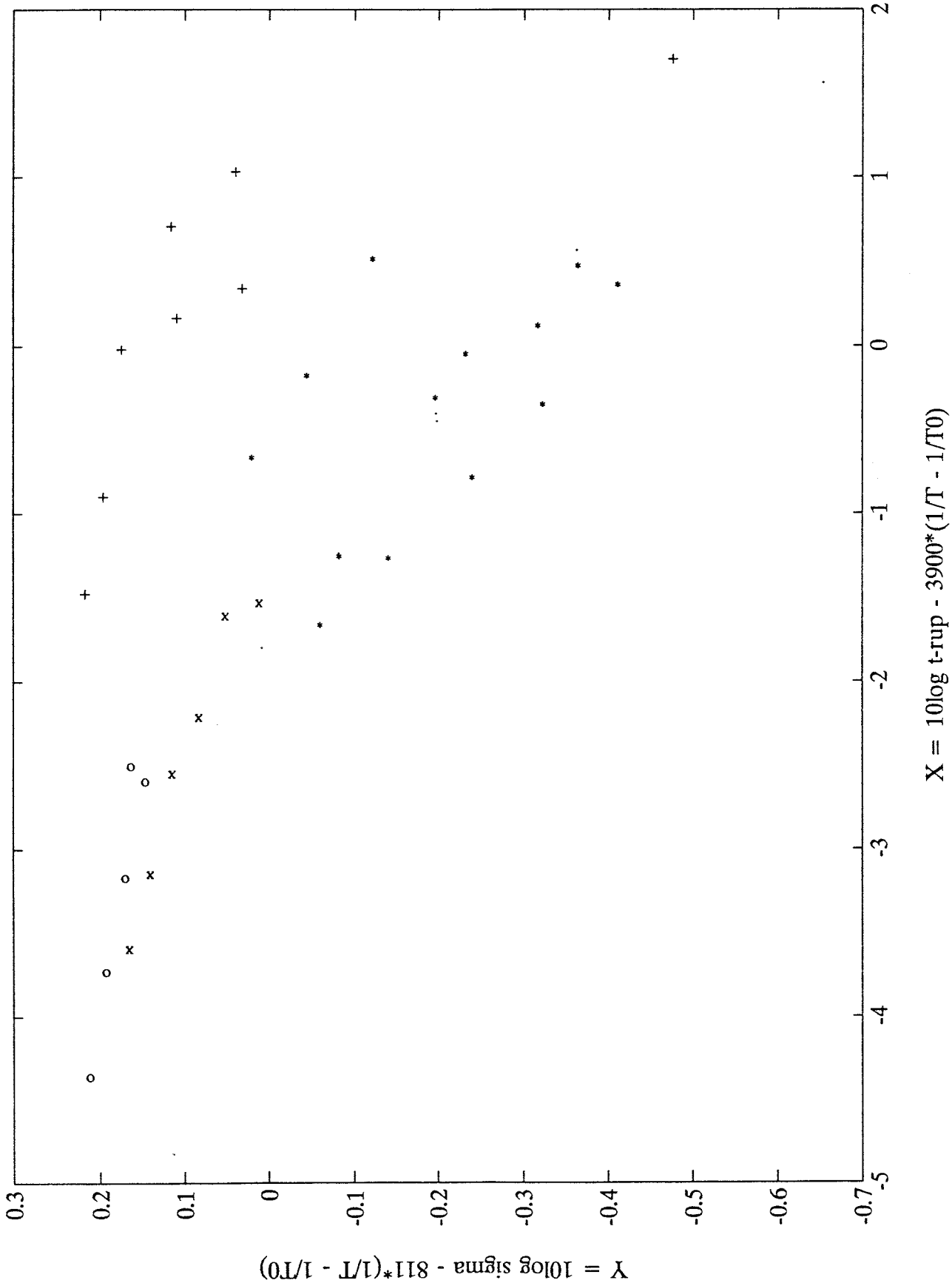
+: CuP, *: OFHC, o: PM 75C, x: PM 110C, .: OFHC 000 180, 250C
Y = 10log sigma - 811*(1/T - 1/T0)
X = 10log t-rup - 3900*(1/T - 1/T0)
0.3
0.2
0.1
0
-0.1
-0.2
-0.3
-0.4
-0.5
-0.6
-0.7
2
1
0
-1
-2
-3
-4
-5

Figure 8

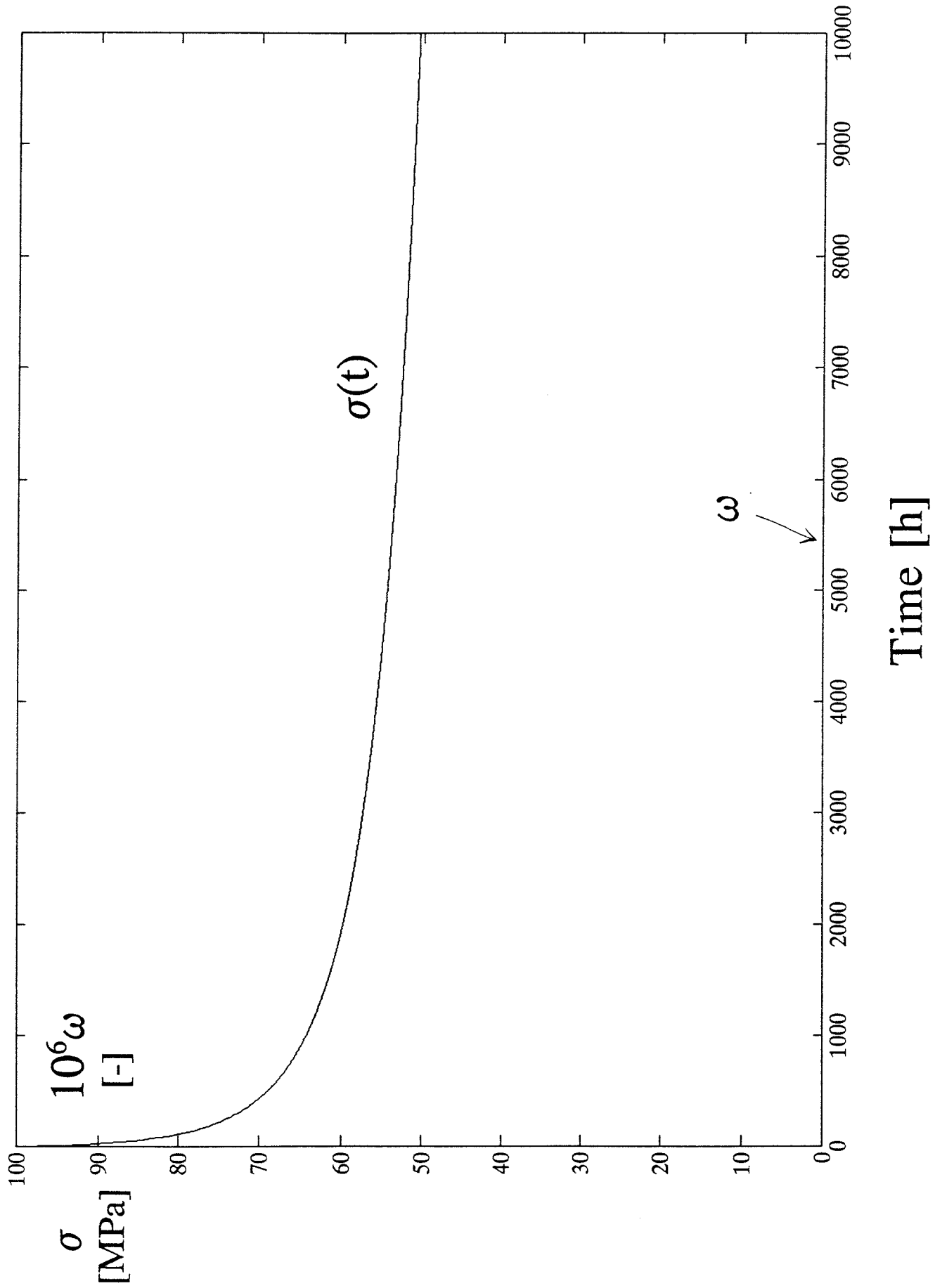
σ [MPa]
$10^6\omega$ [-]
σ(t)
ω
Time [h]
0
10
20
30
40
50
60
70
80
90
100
1000
2000
3000
4000
5000
6000
7000
8000
9000
10000

Figure 9

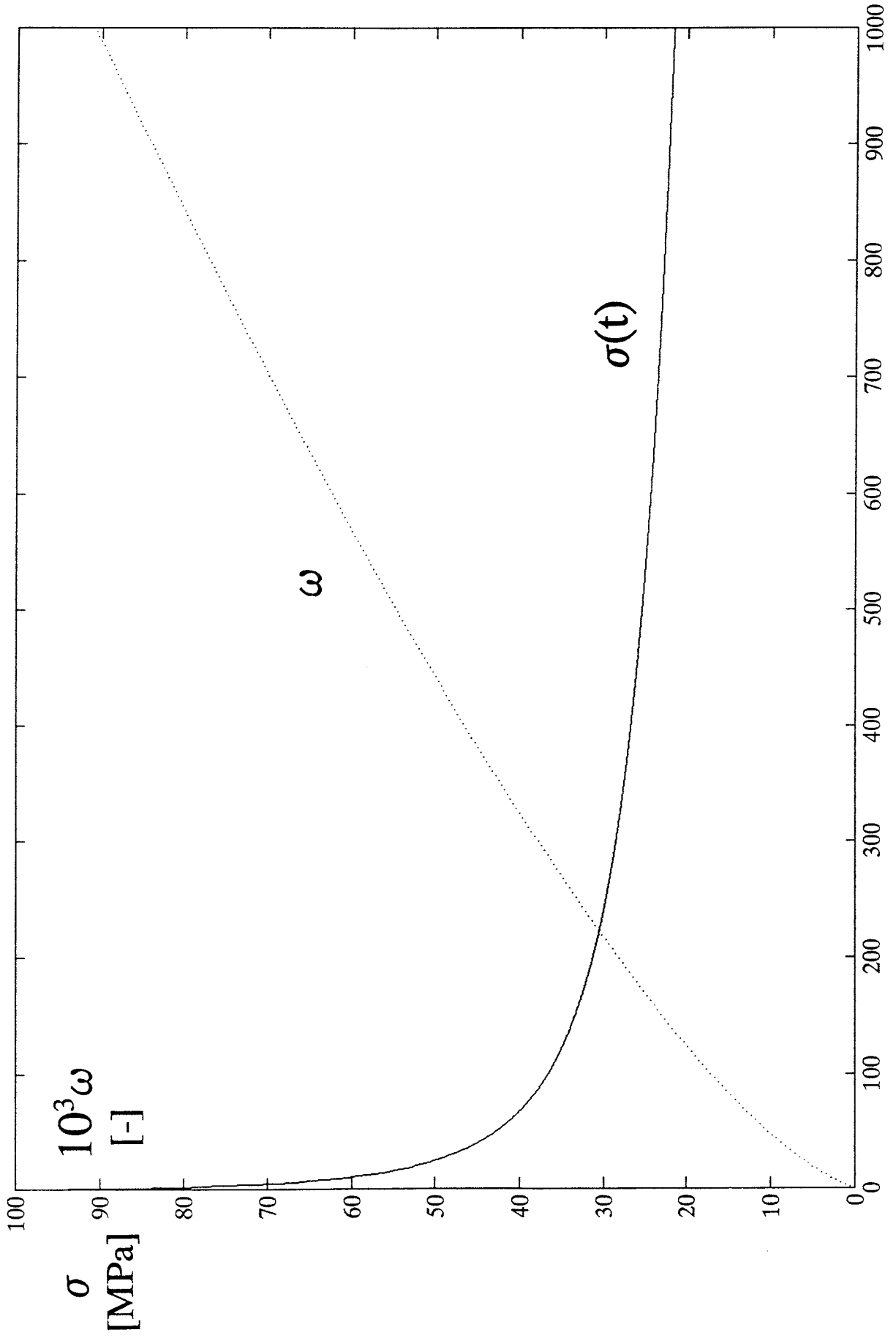
σ [MPa]
$10^3\omega$ [-]
ω
σ(t)
Time [h]
0
10
20
30
40
50
60
70
80
90
100
0
100
200
300
400
500
600
700
800
900
1000

Figure 10

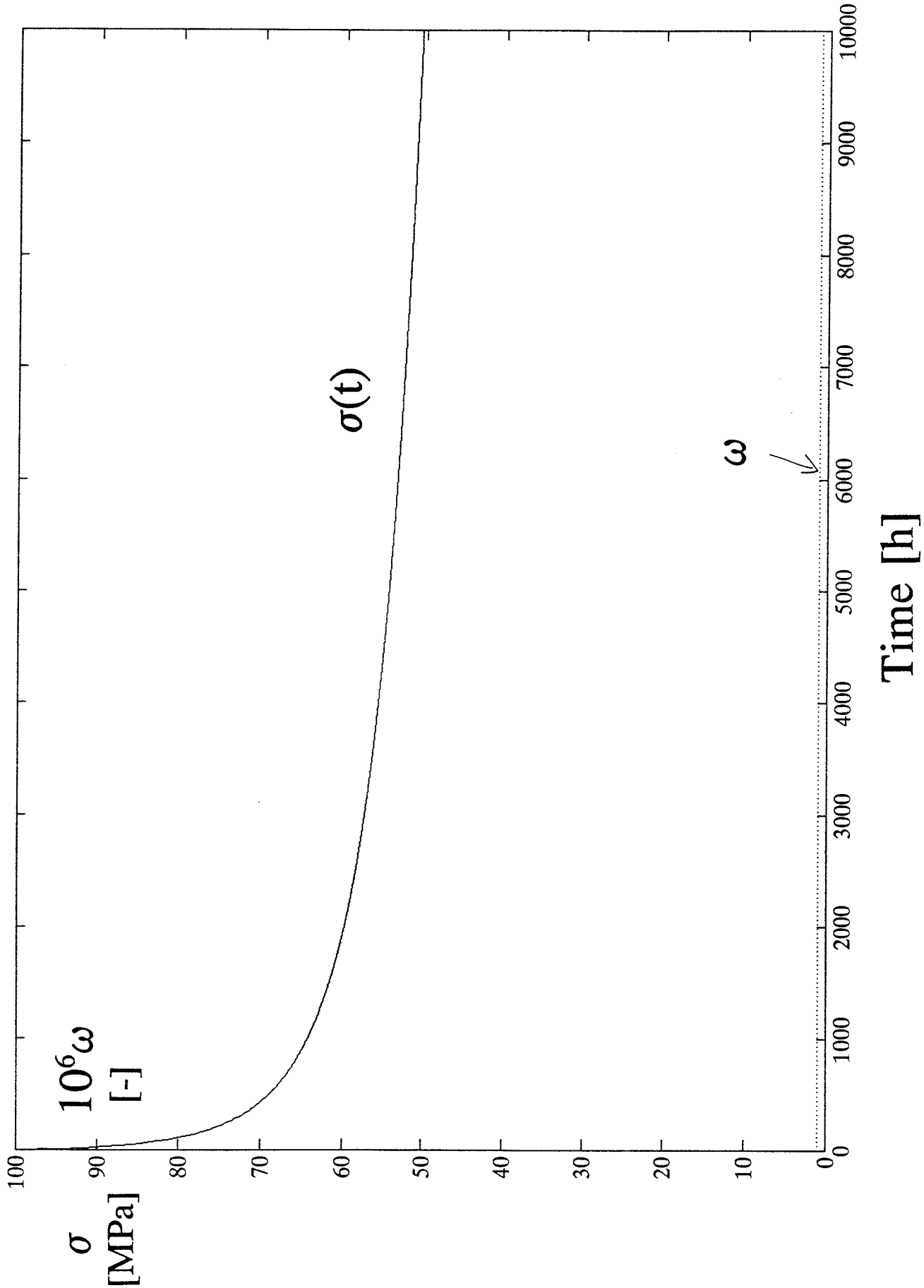
σ(t)
ω
$10^6\omega$ [-]
σ [MPa]
Time [h]
0
1000
2000
3000
4000
5000
6000
7000
8000
9000
10000
10
20
30
40
50
60
70
80
90
100

List of SKB reports

Annual Reports

1977-78
TR 121
KBS Technical Reports 1 – 120
Summaries
Stockholm, May 1979

1979
TR 79-28
The KBS Annual Report 1979
KBS Technical Reports 79-01 – 79-27
Summaries
Stockholm, March 1980

1980
TR 80-26
The KBS Annual Report 1980
KBS Technical Reports 80-01 – 80-25
Summaries
Stockholm, March 1981

1981
TR 81-17
The KBS Annual Report 1981
KBS Technical Reports 81-01 – 81-16
Summaries
Stockholm, April 1982

1982
TR 82-28
The KBS Annual Report 1982
KBS Technical Reports 82-01 – 82-27
Summaries
Stockholm, July 1983

1983
TR 83-77
The KBS Annual Report 1983
KBS Technical Reports 83-01 – 83-76
Summaries
Stockholm, June 1984

1984
TR 85-01
Annual Research and Development Report 1984
Including Summaries of Technical Reports Issued during 1984. (Technical Reports 84-01 – 84-19)
Stockholm, June 1985

1985
TR 85-20
Annual Research and Development Report 1985
Including Summaries of Technical Reports Issued during 1985. (Technical Reports 85-01 – 85-19)
Stockholm, May 1986

1986
TR 86-31
SKB Annual Report 1986
Including Summaries of Technical Reports Issued during 1986
Stockholm, May 1987

1987
TR 87-33
SKB Annual Report 1987
Including Summaries of Technical Reports Issued during 1987
Stockholm, May 1988

1988
TR 88-32
SKB Annual Report 1988
Including Summaries of Technical Reports Issued during 1988
Stockholm, May 1989

1989
TR 89-40
SKB Annual Report 1989
Including Summaries of Technical Reports Issued during 1989
Stockholm, May 1990

1990
TR 90-46
SKB Annual Report 1990
Including Summaries of Technical Reports Issued during 1990
Stockholm, May 1991

1991
TR 91-64
SKB Annual Report 1991
Including Summaries of Technical Reports Issued during 1991
Stockholm, April 1992

Technical Reports
List of SKB Technical Reports 1992

TR 92-01
GEOTAB. Overview
Ebbe Eriksson[1], Bertil Johansson[2], Margareta Gerlach[3], Stefan Magnusson[2], Ann-Chatrin Nilsson[4], Stefan Sehlstedt[3], Tomas Stark[1]
[1]SGAB, [2]ERGODATA AB, [3]MRM Konsult AB
[4]KTH
January 1992

TR 92-02
Sternö study site. Scope of activities and main results
Kaj Ahlbom[1], Jan-Erik Andersson[2], Rune Nordqvist[2], Christer Ljunggren[3], Sven Tirén[2], Clifford Voss[4]
[1]Conterra AB, [2]Geosigma AB, [3]Renco AB, [4]U.S. Geological Survey
January 1992

TR 92-03
Numerical groundwater flow calculations at the Finnsjön study site – extended regional area
Björn Lindbom, Anders Boghammar
Kemakta Consultants Co, Stockholm
March 1992

TR 92-04
Low temperature creep of copper intended for nuclear waste containers
P J Henderson, J-O Österberg, B Ivarsson
Swedish Institute for Metals Research, Stockholm
March 1992

TR 92-05
Boyancy flow in fractured rock with a salt gradient in the groundwater – An initital study
Johan Claesson
Department of Building Physics, Lund University, Sweden
February 1992

TR 92-06
Characterization of nearfield rock – A basis for comparison of repository concepts
Roland Pusch, Harald Hökmark
Clay Technology AB and Lund University of Technology
December 1991

TR 92-07
Discrete fracture modelling of the Finnsjön rock mass: Phase 2
J E Geier, C-L Axelsson, L Hässler, A Benabderrahmane
Golden Geosystem AB, Uppsala, Sweden
April 1992

TR 92-08
Statistical inference and comparison of stochastic models for the hydraulic conductivity at the Finnsjön site
Sven Norman
Starprog AB
April 1992

TR 92-09
Description of the transport mechanisms and pathways in the far field of a KBS-3 type repository
Mark Elert[1], Ivars Neretnieks[2], Nils Kjellbert[3], Anders Ström[3]
[1]Kemakta Konsult AB
[2]Royal Institute of Technology
[3]Swedish Nuclear Fuel and Waste Management Co
April 1992

TR 92-10
Description of groundwater chemical data in the SKB database GEOTAB prior to 1990
Sif Laurent[1], Stefan Magnusson[2], Ann-Chatrin Nilsson[3]
[1]IVL, Stockholm
[2]Ergodata AB, Göteborg
[3]Dept. of Inorg. Chemistry, KTH, Stockholm
April 1992

TR 92-11
Numerical groundwter flow calculations at the Finnsjön study site – the influence of the regional gradient
Björn Lindbom, Anders Boghammar
Kemakta Consultants Co., Stockholm, Sweden
April 1992

TR 92-12
HYDRASTAR – a code for stochastic simulation of groundwater flow
Sven Norman
Abraxas Konsult
May 1992

TR 92-13
Radionuclide solubilities to be used in SKB 91
Jordi Bruno[1], Patrik Sellin[2]
[1]MBT, Barcelona Spain
[2]SKB, Stockholm, Sweden
June 1992

TR 92-14
Numerical calculations on heterogeneity of groundwater flow
Sven Follin
Department of Land and Water Resources, Royal Institute of Technology
June 1992

TR 92-15
Kamlunge study site.
Scope of activities and main results
Kaj Ahlbom[1], Jan-Erik Andersson[2],
Peter Andersson[2], Thomas Ittner[2],
Christer Ljunggren[3], Sven Tirén[2]
[1]Conterra AB
[2]Geosigma AB
[3]Renco AB
May 1992

TR 92-16
Equipment for deployment of canisters with spent nuclear fuel and bentonite buffer in horisontal holes
Vesa Henttonen, Miko Suikki
JP-Engineering Oy, Raisio, Finland
June 1992

TR 92-17
The implication of fractal dimension in hydrogeology and rock mechanics Version 1.1
W Dershowitz[1], K Redus[1], P Wallmann[1],
P LaPointe[1], C-L Axelsson[2]
[1]Golder Associates Inc., Seattle, Washington, USA
[2]Golder Associates Geosystem AB, Uppsala, Sweden
February 1992

TR 92-18
Stochastic continuum simulation of mass arrival using a synthetic data set. The effect of hard and soft conditioning
Kung Chen Shan[1], Wen Xian Huan[1], Vladimir Cvetkovic[1], Anders Winberg[2]
[1] Royal Institute of Technology, Stockholm
[2] Conterra AB, Gothenburg
June 1992

TR 92-19
Partitioning and transmutation.
A review of the current state of the art
Mats Skålberg, Jan-Olov Liljenzin
Department of Nuclear Chemistry,
Chalmers University of Technology
October 1992

TR 92-20
SKB 91
Final disposal of spent nuclear fuel. Importance of the bedrock for safety
SKB
May 1992

TR 92-21
The Protogine Zone.
Geology and mobility during the last 1.5 Ga
Per-Gunnar Andréasson, Agnes Rodhe
September 1992

TR 92-22
Klipperås study site.
Scope of activities and main results
Kaj Ahlbom[1], Jan-Erik Andersson[2],
Peter Andersson[2], Tomas Ittner[2],
Christer Ljunggren[3], Sven Tirén[2]
[1]Conterra AB
[2]Geosigma AB
[3]Renco AB
September 1992

TR 92-23
Bedrock stability in Southeastern Sweden. Evidence from fracturing in the Ordovician limestones of Northern Öland
Alan Geoffrey Milnes[1], David G Gee[2]
[1]Geological and Environmental Assessments (GEA), Zürich, Switzerland
[2]Geologiska Institutionen, Lund, Sweden
September 1992

TR 92-24
Plan 92
Costs for management of the radioactive waste from nuclear power production
Swedish Nuclear Fuel and Waste Management Co
June 1992

TR 92-25
Gabbro as a host rock for a nuclear waste repository
Kaj Ahlbom[1], Bengt Leijon[1], Magnus Liedholm[2],
John Smellie[1]
[1]Conterra AB
[2]VBB VIAK
September 1992

TR 92-26
Copper canisters for nuclear high level waste disposal. Corrosion aspects
Lars Werme, Patrik Sellin, Nils Kjellbert
Swedish Nuclear Fuel and Waste Management Co, Stockholm, Sweden
October 1992

TR 92-27

Thermo-mechanical FE-analysis of butt-welding of a Cu-Fe canister for spent nuclear fuel

B L Josefson[1], L Karlsson[2], L-E Lindgren[2], M Jonsson[2]
[1]Chalmers University of Technology, Göteborg, Sweden
[2]Division of Computer Aided Design, Luleå University of Technology, Luleå, Sweden
October 1992

TR 92-28

A rock mechanics study of Fracture Zone 2 at the Finnsjön site

Bengt Leijon[1], Christer Ljunggren[2]
[1]Conterra AB
[2]Renco AB
January 1992

TR 92-29

Release calculations in a repository of the very long tunnel type

L Romero, L Moreno, I Neretnieks
Department of Chemical Engineering,
Royal Institute of Technology, Stockholm, Sweden
November 1992

TR 92-30

Interaction between rock, bentonite buffer and canister. FEM calculations of some mechanical effects on the canister in different disposal concepts

Lennart Börgesson
Clay Technology AB, Lund Sweden
July 1992

TR 92-31

The Äspö Hard Rock Laboratory: Final evaluation of the hydro-geochemical pre-investigations in relation to existing geologic and hydraulic conditions

John Smellie[1], Marcus Laaksoharju[2]
[1]Conterra AB, Uppsala, Sweden
[2]GeoPoint AB, Stockholm, Sweden
November 1992

TR 92-32

Äspö Hard Rock Laboratory: Evaluation of the combined longterm pumping and tracer test (LPT2) in borehole KAS06

Ingvar Rhén[1] (ed.), Urban Svensson[2] (ed.), Jan-Erik Andersson[3], Peter Andersson[3], Carl-Olof Eriksson[3], Erik Gustafsson[3], Thomas Ittner[3], Rune Nordqvist[3]
[1]VBB VIAK AB
[2]Computer-aided Fluid Engineering
[3]Geosigma AB
November 1992

TR 92-33

Finnsjö Study site. Scope of activities and main results

Kaj Ahlbom[1], Jan-Erik Andersson[2], Peter Andersson[2], Thomas Ittner[2], Christer Ljunggren[3], Sven Tirén[2]
[1]Conterra AB
[2]Geosigma AB
[3]Renco AB
December 1992

TR 92-34

Sensitivity study of rock mass response to glaciation at Finnsjön, Central Sweden

Jan Israelsson[1], Lars Rosengren[1], Ove Stephansson[2]
[1]Itasca Geomekanik AB, Falun, Sweden
[2]Royal Institute of Technology,
Dept. of Engineering Geology, Stockholm, Sweden
November 1992

TR 92-35

Calibration and validation of a stochastic continuum model using the Finnsjön Dipole Tracer Test. A contribution to INTRAVAL Phase 2

Kung Chen Shan[1], Vladimir Cvetkovic[1], Anders Winberg[2]
[1]Royal Institute of Technology, Stockholm
[2]Conterra AB, Göteborg
December 1992

TR 92-36

Numerical simulation of double-packer tests in heterogeneous media

Sven Follin
Department of Engineering Geology, Lund University, Lund, Sweden
December 1992

TR 92-37
Thermodynamic modelling of bentonite-groundwater interaction and implications for near field chemistry in a repository for spent fuel
Hans Wanner, Paul Wersin, Nicolas Sierro
MBT Umwelttechnik AG, Zürich, Switzerland
November 1992

TR 92-38
Climatic changes and uplift patterns – past, present and future
S Björck, N-O Svensson
Department of Quaternary Geology,
University of Lund
November 1992

TR 92-39
Characterization of crystalline rocks in deep boreholes. The Kola, Krivoy Rog and Tyrnauz boreholes
NEDRA
December 1992

TR 92-40
PASS – Project on Alternative Systems Study. Performance assessment of bentonite clay barrier in three repository concepts: VDH, KBS-3 and VLH
Roland Pusch, Lennart Börgesson
Clay Technology AB, Lund
December 1992

TR 92-41
Buoyancy flow in fractured rock with a salt gradient in the groundwater. A second study of coupled salt and thermal buoyancy
Johan Claesson, Göran Hellström,
Thomas Probert
Depts. of Building Physics and Mathematical Physics, Lund University, Sweden
November 1992

TR 92-42
Project on Alternative Systems Study – PASS. Comparison of technology of KBS-3, MLH, VLH and VDH concepts by using an expert group
Lars Olsson[1], Håkan Sandstedt[2]
[1]Geostatistik Lars Olsson AB
[2]Bergsäker Öst AB
September 1992

TR 92-43
Project Alternative Systems Study – PASS. Analysis of performance and long-term safety of repository concepts
Lars Birgersson, Kristina Skagius, Marie Wiborgh, Hans Widén
Kemakta Konsult AB
September 1992

TR 92-44
Project on Alternative Systems Study – PASS. Cost comparison of repository systems
Lars Ageskog, Thomas Högbom
VBB VIAK AB
September 1992